UNIVERSITÀ DEGLI STUDI DI TRIESTE

XXXIV CICLO DEL DOTTORATO DI RICERCA IN AMBIENTE E VITA

BIOLOGICAL AND ECOLOGICAL LINKS BETWEEN JELLYFISH AND THEIR PARASITES IN THE GULF OF TRIESTE (ITALY)

Settore scientifico-disciplinare: BIO/05 ZOOLOGIA

DOTTORANDO
GREGORIO MOTTA

COORDINATORE
PROF. GIORGIO ALBERTI

SUPERVISORE DI TESI
PROF. ANTONIO TERLIZZI

CO-SUPERVISORE DI TESI
DOTT. MASSIMILIANO BOTTARO

ANNO ACCADEMICO 2020/2021

Biological and ecological links between jellyfish and their parasites in the Gulf of Trieste (Italy).

Lebour, M. U. (1908). Fish trematodes of the Northumberland coast.

Gregorio Motta

UNIVERSITÀ DEGLI STUDI DI TRIESTE

Stazione Zoologica Anton Dohrn Napoli

University of Trieste – Stazione Zoologica Anton Dohrn

Supervised by:

Professor **Antonio Terlizzi**

Dipartimento di Ecologia Marina Integrata, Stazione Zoologica Anton Dohrn (SZN), Italy.
Dipartimento di Scienze della Vita, Università degli studi di Trieste (UNITS), Italy.

Co-Supervised by:

Dr. **Massimiliano Bottaro**

Dipartimento di Ecologia Marina Integrata, Stazione Zoologica Anton Dohrn (SZN), Italy.

INDEX

Riassunto

Al giorno d'oggi le meduse, e il plancton gelatinoso in generale, non possono più essere considerati personaggi secondari come accaduto in passato, è sempre più evidente che questi organismi giocano un ruolo chiave negli ecosistemi con numerosi collegamenti nella rete trofica.

Con questo dottorato, l'obiettivo è stato investigare le dinamiche tra il plancton gelatinoso e una particolare sottoclasse di parassiti, i Digenea, per determinare il ruolo delle meduse (ospite intermedio) come link o trasmettitore di questi parassiti dal comparto bentonico (gasteropode, primo ospite) a quello pelagico (pesci, ospiti definitivi). Ancora più cruciale se consideriamo il notevole aumento di bloom negli ultimi decenni. L'aumento di numero e biomassa di meduse potrebbe andare a favorire la trasmissione di questi parassiti ai livelli più alti delle reti trofiche. Questo potrebbe portare a un aumento del numero di parassiti nei pesci e nei gasteropodi, con imprevedibili effetti sul loro metabolismo, ed a un generale aumento di questi parassiti negli ecosistemi. Questa tesi mira anche a sfruttare questi nuovi dati parassitologici come uno strumento per meglio determinare la posizione delle meduse negli ecosistemi e le interazioni tra pesci e plancton gelatinoso (la predazione pesce-medusa è fondamentale per i digenei per chiudere il proprio ciclo vitale), integrando altri studi basati sui metodi tradizionali di ecologia trofica.

La parte centrale del PhD, incentrata sull'investigare per la prima volta le dinamiche di questi parassiti nel plancton gelatinoso del golfo di Trieste, ha mostrato che ogni specie del plancton gelatinoso è risultata essere ospite di parassiti digenei, a prescindere dal luogo e periodo di campionamento. La maggioranza di parassiti è risultata appartenere al genere *Clavogalea*, una prima descrizione per questo genere nelle meduse e prima osservazione di questo parassita nel mar Mediterraneo. Il secondo genere trovato, *Opechona*, è già stato descritto in meduse ma mai nel Mediterraneo.

L'alta prevalenza di parassiti registrata in ogni specie (>80%) nel golfo di Trieste suggerisce che il plancton gelatinoso è un importante secondo ospite intermedio per digenei lepocreadidi e gioca quindi un ruolo importante per i loro cicli vitali nell'area investigata. I nostri risultati supportano anche l'ipotesi che queste specie gelatinose siano una parte importante della dieta dei pesci, ospiti definitivi

dei lepocreadidi, in quanto il trasferimento trofico è necessario per questi parassiti per chiudere il loro ciclo vitale.

Il progetto sui parassiti di pesci, finalizzato a identificare gli ospiti definitivi di queste due specie di digenei, ha per ora dato esito negativo per quanto riguarda *Clavogalea*, lasciando il ciclo vitale di questi organismi ancora indefinito. Individui del genere *Opechona* sono invece stati trovati in S*comber scombrus* ma le basse intensità riscontrate in *Aequorea forskalea* rendono difficile teorizzare una relazione trofica stabile tra queste due specie. Allo stesso tempo, l'assenza di esemplari adulti di *Clavogalea* sp. (molto più abbondanti di *Opechona* sp. in *Aequorea forskalea*) negli sgombri suggeriscono che questo pesce ha ottenuto tali digenei da un altro secondo ospite intermedio.

In ultimo, durante questo PhD, l'anatomia morfologica e funzionale del sistema gastrovascolare di *Rhizostoma pulmo* (Macri 1778) è stata investigata tramite la creazione e l'utilizzo di un inedito protocollo con tecniche innovative mai adottate nella ricerca su meduse: endocast in resina e analisi microtomografica 3D a raggi X.

Concludendo, questo lavoro è stato un primo passo verso il completare il quadro riguardante i parassiti di meduse e l'ecologia di queste ultime nel nord Adriatico, investigando e facendo luce sul grande buco di conoscenza riguardo questi argomenti e, al tempo stesso, aprendo numerosi punti interrogativi che necessitano di essere affrontati.

Abstract

Nowadays, jellyfish can not be considered secondary characters as happened in the past. It is more and more evident that gelatinous zooplankton play a major role in the ecosystems with numerous links in the food webs.

With this thesis, we aimed at addressing the dynamics between gelatinous zooplankton and a peculiar subclass of parasites, the Digenea, crucial to determine the role of jellyfish (intermediate host) as a link or transmitter of these parasites from the benthic compartment (gastropods, first host) to the pelagic compartment (fish, definitive hosts). Even more crucial if we consider the noticeable increase of blooms in the last decades. The increase in number and biomass of jellyfish could favor the transmission of these parasites to the upper levels of the trophic webs. Potentially, this could lead to a higher number of digenean parasites in fish and gastropods, with still uncharted effects on their physiology, and an overall increase of these parasites in the ecosystems.

Simultaneously, few information on fish-jellyfish feeding interactions is available at the current state of the art. This thesis aimed at exploiting its brand-new parasitological data about jellyfish digeneans as a useful tool to better estimate the trophic position of jellyfish in the ecosystems and the interactions between fish and gelatinous organisms in the area (feeding on jellyfish is needed for Digenea to close their life cycle), potentially providing new hints and integrating other studies based on trophic ecology traditional methods (gut contents and stable isotopes analysis of fish).

The core part of the PhD, focusing on investigating for the first time the dynamics of these parasites in the gelatinous zooplankton of the Gulf of Trieste, showed that every gelatinous zooplankton species resulted to be host to digenean parasites despite sampling location and month. The majority of parasites belonged to the genus *Clavogalea*, a first record for this genus in jellyfish, and a first record in the Mediterranean Sea. The second genus found, *Opechona*, has already been observed in jellyfish, but never in the Mediterranean Sea.

The high prevalence of parasites recorded in every species (>80%) in the Gulf of Trieste, suggests that the gelatinous zooplankton is an important second intermediate host for lepocreadiid digeneans and therefore plays a key role in their life cycle in the investigated area. Our findings also support the

hypothesis that these gelatinous species are an important part in the diet of teleost fish, which are reported as definitive hosts of lepocreadiids, since trophic transmission is necessary for these parasites to complete their life cycles.

The project on fish parasites, aimed to find the definitive hosts of these two digenean species, did not record any *Clavogalea,* leaving the life cycle of this organisms still unclear. *Opechona* sp. individuals have been found in *Scomber scombrus* but the intensities recorded in *Aequorea forskalea* were so low that it would be hard to theorize a stable trophic relation between S*comber scombrus* and the hydromedusa. At the same time, the absence of *Clavogalea* sp. (much more abundant in *Aequorea forskalea.* compared to *Opechona* sp.) in S*comber scombrus* would suggest that the fish got the parasites from another intermediate host.

Last, during this PhD, morphological and functional anatomy of the gastrovascular system of *Rhizostoma pulmo* (Macri 1778) was investigated in detail by using a brand-new protocol (created by us), involving innovative techniques never adopted in jellyfish science: resin endocasts and 3D X-ray computed microtomography.

Concluding, this work has been a first step in jellyfish parasitology and jellyfish ecology in the north Adriatic since it started investigating and shedding light on the huge hole of knowledge about this topic and opened numerous questions that still need to be addressed.

Glossary

Term	Definition
Abundance	"The number of individuals of a particular parasite in/on a single host regardless of whether or not the host is infected" [1]
Accidental host	a host which is erroneously infected by a parasite. Dead end for the life cycle
Cercaria	Free swimming stage of a digenean
Definitive host	Last host of the life cycle in which the adult parasite stage matures and reproduces sexually
Digenea	Subclass of parasitic flatworms (Platyhelminthes – Trematoda)
Forebody	Distance between oral and ventral sucker on adult digeneans
Hindbody	Distance between ventral sucker and the end of the adult Digenea body
Intensity	"the number of individuals of a particular parasite species in a single infected host" [1]
Intermediate host	True host for the life cycle of a parasites. i.e., first host: cercaria stage. Second host: metacercaria stage.
Jellyfish parasite	parasites which use jellyfish as hosts
Manubrium	Part of the jellyfish body hanging from the subumbrellar cavity
Metacercaria	Digenean intermediate stage between cercaria and sexual adult
Miracidium	digenean motile ciliated larva
Oral/Ventral sucker	Digenea structures for attachment, locomotion, and feeding on the host tissue
Parasite	"an organism that lives in or on an organism of another species (its host) and benefits by deriving nutrients at the other's expense." Oxford English Dictionary
Planula	cnidarian free-swimming larval form
Polyp	cnidarian asexual reproducing generation

Prevalence	"The number of hosts infected with 1 or more individuals of a particular parasite species (or taxonomic group) divided by the number of hosts examined for that parasite species" (Bush et al 1997)

Introduction

Gelatinous Zooplankton

Gelatinous zooplankton is one of the most varied, numerous and widespread group in our oceans [2,3]. They may be found in different ecosystems, from shallow waters to deep seas as well from tropical areas to the poles [4,5]. Taxonomically speaking, gelatinous zooplankton include organisms from different phyla: Cnidaria (hydromedusae, scyphomedusae, cubomedusae, siphonophores), Ctenophora, Tunicata and Chaetognatha [6,7] (Fig. 1).
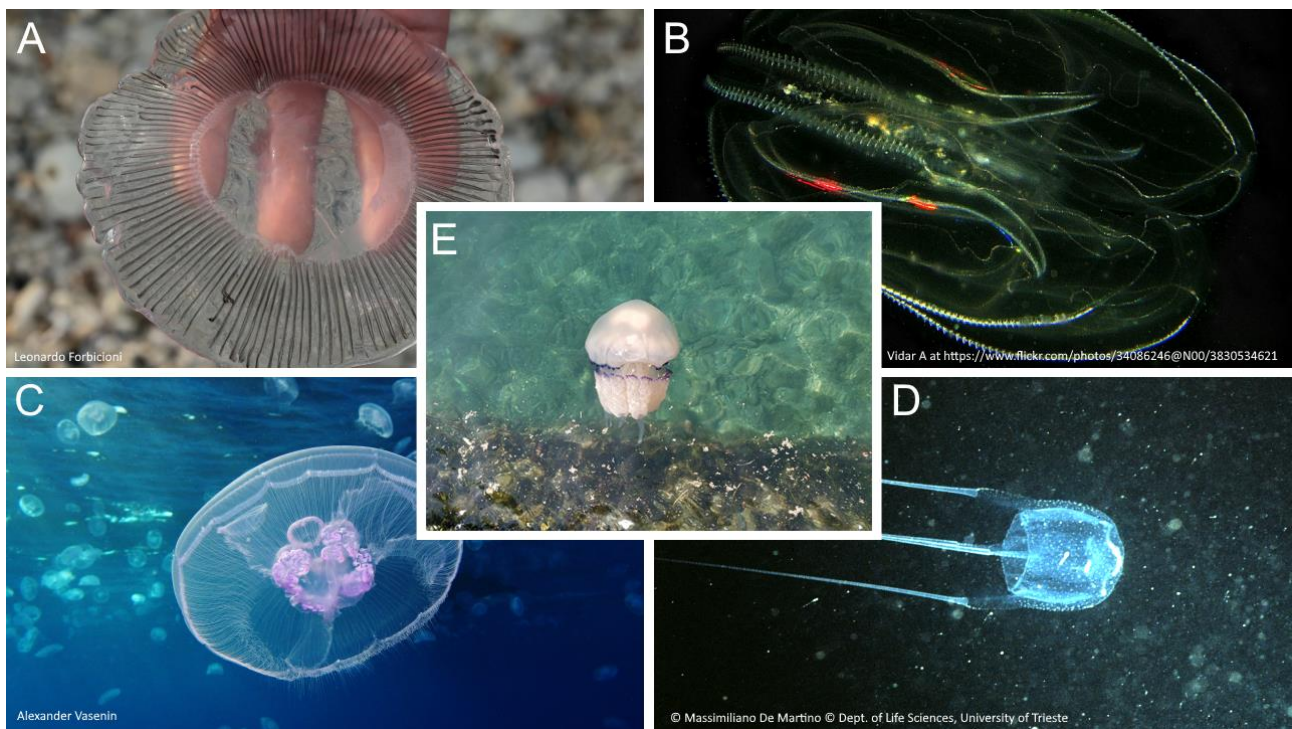

Figure 1. Gelatinous zooplankton organisms from different phyla and classes: **(a)** Cnidaria: Hydrozoa; **(b)** Ctenophora: Lobata; **(c)** Cnidaria: Scyphozoa; **(d)** Cnidaria: Cubozoa; **(e)** Cnidaria: Scyphozoa.

In recent times, gelatinous zooplankton and its blooms have become a discussed topic by marine biologists since they may directly and indirectly interact and interfere with human economic and recreational activities, ecosystem services, public health, local wildlife and ecosystem functioning [8,9]. Gelatinous zooplankton blooms always occurred in history, nowadays we are observing a marked change in frequency and magnitude, probably related to climate change and anthropic activities [3,10].

In the ecosystems, blooms may cause shifts in the structure of planktonic communities and they can modify the flow of energy trough the food webs [11].

It is evident that having a complete picture of their biology, physiology, anatomy, the ecological role and relationships with other species, and the position of the different organisms belonging to the gelatinous zooplankton in marine ecosystems is fundamental to better understand and predict their occurrence, potential impacts, and address the issues related with their presence, in particular during blooming events.

Cnidaria

Cnidaria (Hatschek, 1888) is a Precambrian phylum comprising about 10.000 known living species [12]. This phylum is characterized by radial symmetry, and they include both sessile and free-swimming organisms, solitary and colonially forms [13]. The main remarkable character of Cnidaria is the body composition made of only two layers of tissues: the ectoderm (or epiderm) and the gastroderm (or endoderm), connected by a middle acellular level called mesoglea made of collagen [14]. Even if cnidarians have a low-level body organization, it is possible to detect a large number of morphological structures and a complex diversity in this clade [15].

Despite the absence of a true nervous system, Cnidaria possess nerve cells linked in a nerve net, connected to the sense organs, receiving stimuli from light receptors, mechanoreceptors, gravity receptors and hydrostatic pressure receptors [14,16]. Predation and defense are performed by cnidocytes (or nematocytes), also called stinging cells, which act in response to tactile or chemical stimuli. Most of cnidarians are carnivore, feeding through the central mouth; others, like those of the family Rhizostomatidae, have many mouth openings on their oral arms [16].

The life cycle of cnidarians is composed by two main structural body plans which are the polyp and the medusa (or jellyfish), even if some species may miss one of the two life stages [14]. Polyps are benthonic, colonial or solitary. Generally, the polyp releases free-swimming medusa juveniles or, in Scyphozoa, larval stages called ephyrae, which will later metamorphose in the medusa [13]. In some classes, i.e. Anthozoa, the medusa stage is missing and the polyp directly release male and female gametes, and the embryo attach on the substrate and develop in a new polyp [17]. Differently from polyps, medusae are solitary, pelagic and usually gonochoric with separate sexes. To reproduce, the medusa release gametes through internal or external fertilization which generates a larval stage called planula, which will settle on the bottom and metamorphose into the polyp. Other species, such as *Pelagia noctiluca* miss the polyp stage [18]. Here, the swimming planula directly develops into the ephyra. Summarizing, the asexual polypoid stage alternates with the sexual medusoid stage [16].
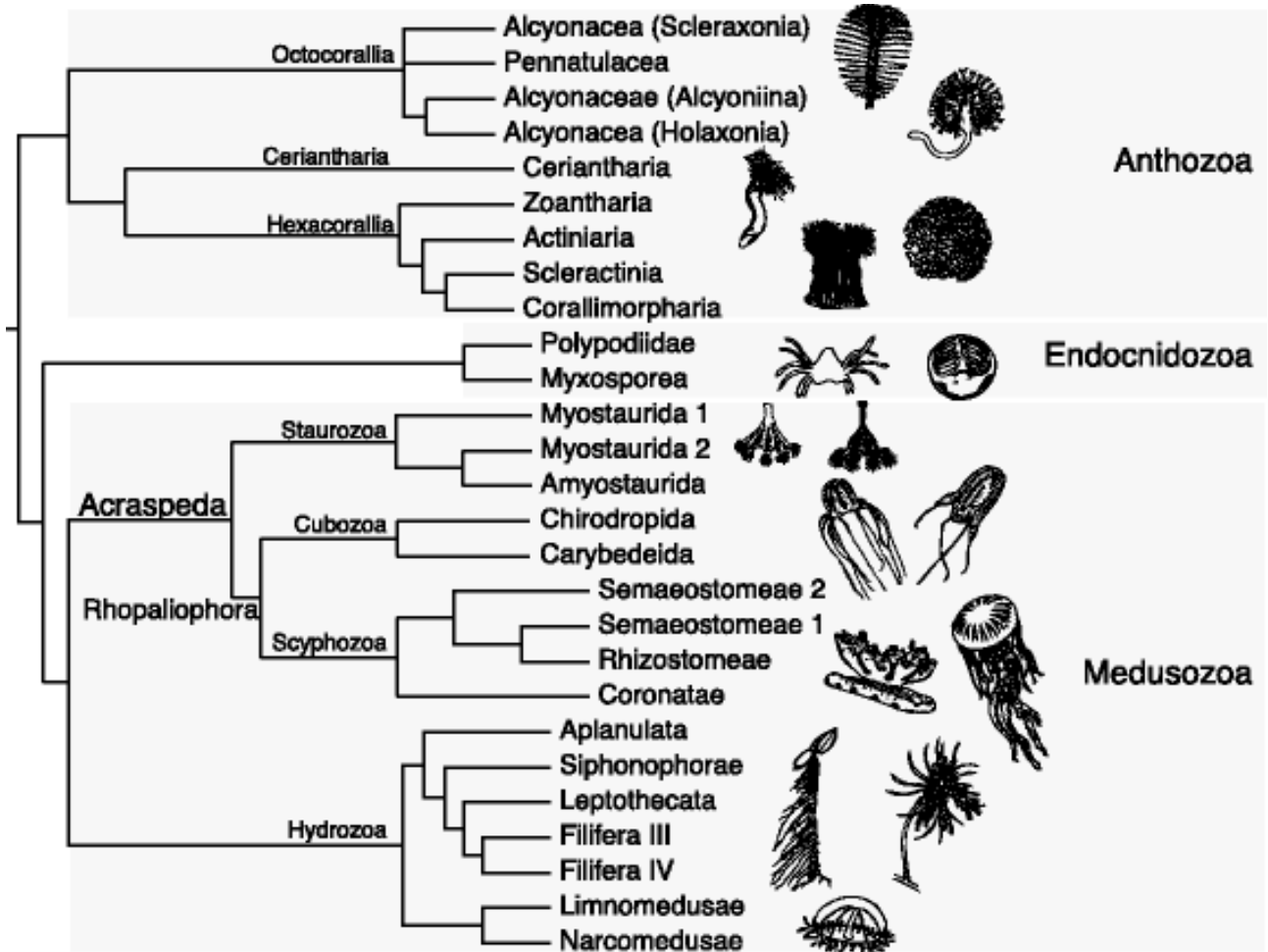
Figure 2. Cnidarian phylogeny using genomic and transcriptomic data from representatives of all classes, summarized. (taken from [13,19])

Cnidaria systematics division was recently revised (Fig. 2) and includes Anthozoa, Cubozoa, Hydrozoa Myxozoa, Scyphozoa and Staurozoa [12]. Even if Cnidaria is one the "oldest" phyla, some phylogenetic relationships between taxa are currently unclear.

Schyphozoa (Goette, 1887)

Scyphozoa, or "true jellyfish", presence on Earth is estimated from the Cambrian [20]. They are one of the six classes actually accepted of the phylum Cnidaria, including about 250 known species in the subclasses Coronamedusae and Discomedusae [12] (Fig. 3).
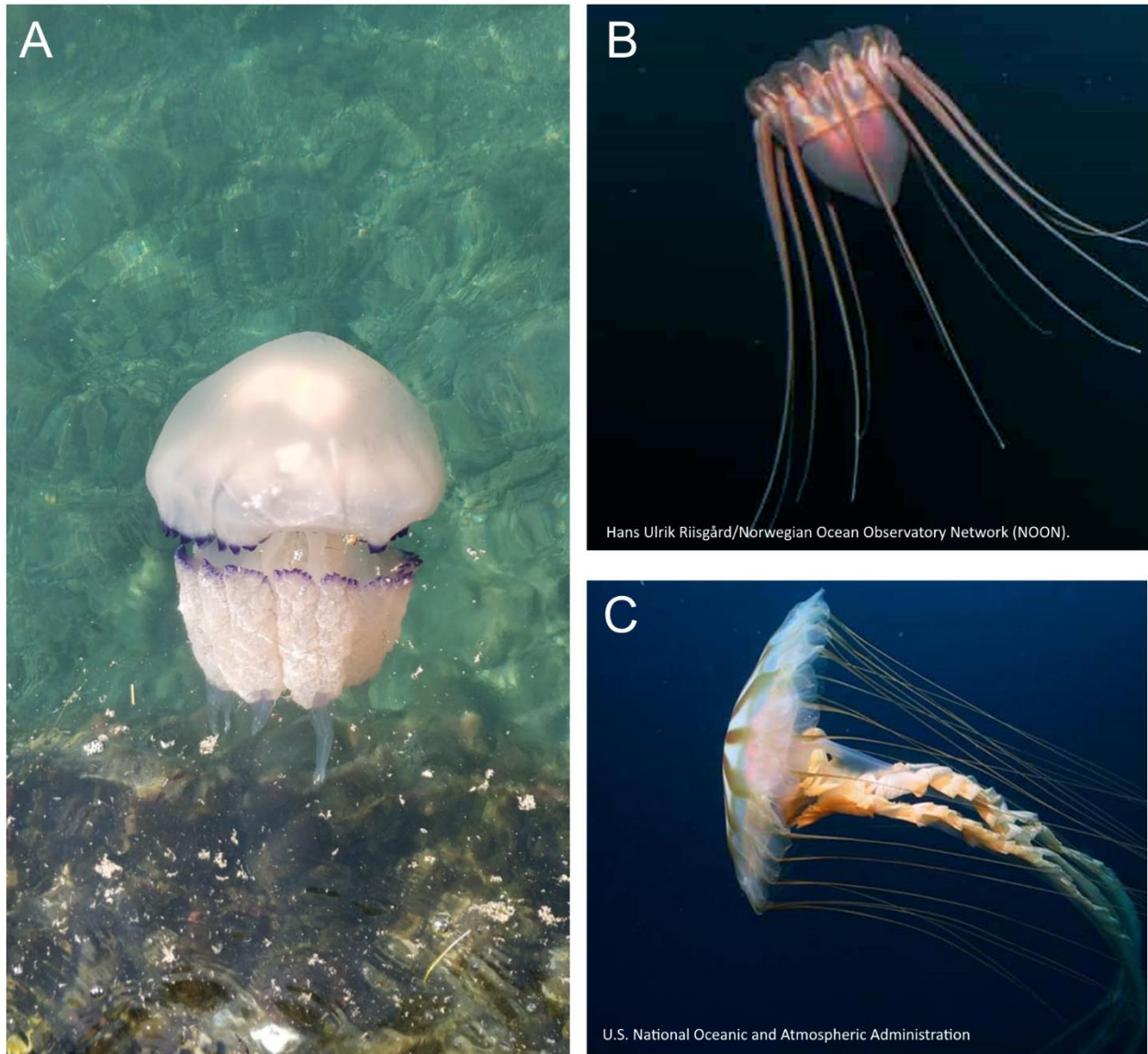

Figure 3. Scyphomedusae. **(a)** *Rhizostoma pulmo* (Rhizostomeae); **(b)** *Periphylla periphylla* (Coronatae); **(c)** *Chrysaora hysoscella* (Semaeostomeae).

The medusa stage is characterized by a typical bell-shape called umbrella with a tetramerous symmetry: the bell is separated into quadrants through the two orthogonal perradial axes, then separated again in four sections through the interradial axed obtaining eight sections [16]. The bell margin is mainly octamerous with marginal lappets divided into clefts. The central part of the

subumbrella is connected to the manubrium, a tubular structure which hang the oral arms to the umbrella [16].

Scyphozoans have a cosmopolite distribution and are present at all depths and latitude [16]. They could be pelagic, or they could be found in shallow coastal waters, causing implications on ecosystems and some human activities due to their venom, even if it usually is scarcely dangerous [21]. The number of species living in the Mediterranean Sea is about 20, of which 13 of them are common and widespread [21,22].

Coronatae include about 30 species, mainly inhabiting deep-waters. The umbrella presents a horizontal coronal groove and a lapped margin of the bell, as seen in *Periphylla periphylla* [23].

Semaeostomeae include the most famous and abundant large jellyfish species (i.e., genera *Aurelia*, *Pelagia*, *Chrysaora* in the Mediterranean Sea). The umbrella margin is divided into lappets where sense organs and tentacles are located. The mouth opening is surrounded by four long oral arms and gonads are in folds of the subumbrella [16].

Rhizostomeae include 80 described species, mainly present in coastal ecosystems (the only species in the Mediterranean Sea are *Rhizostoma pulmo* and, rarer, *Rhizostoma luteum* [24,25]). This order lacks tentacles for prey capture, and instead ingest small particles carried into numerous small mouth openings by water currents. Some species in tropical waters, the upside-down jellyfish like *Cassiopea andromeda*, host intracellular symbiotic algae [16].

Hydrozoa

Hydromedusae are a broad group (> 800 species) [12]. The majority of them do not measure more than 1 cm in diameter and their bodies are generally transparent [26]. They include several orders (Anthomedusae, Leptomedusae, Limnomedusae, Trachymedusae, Narcomedusae) with peculiar body shapes and life cycles (Fig. 4).
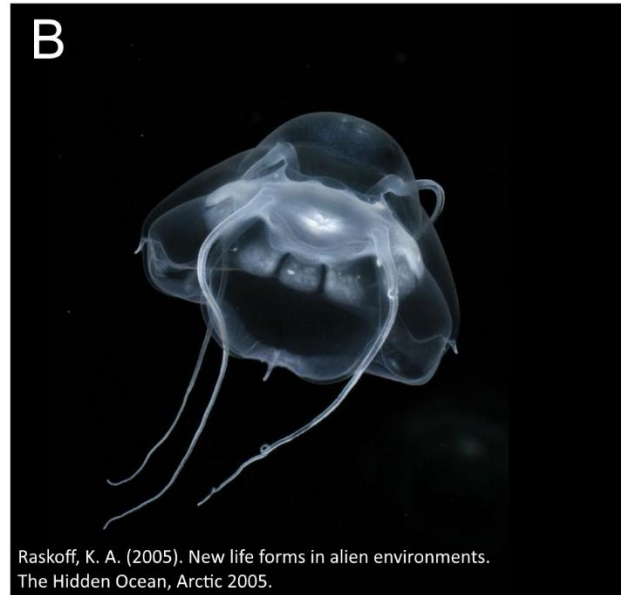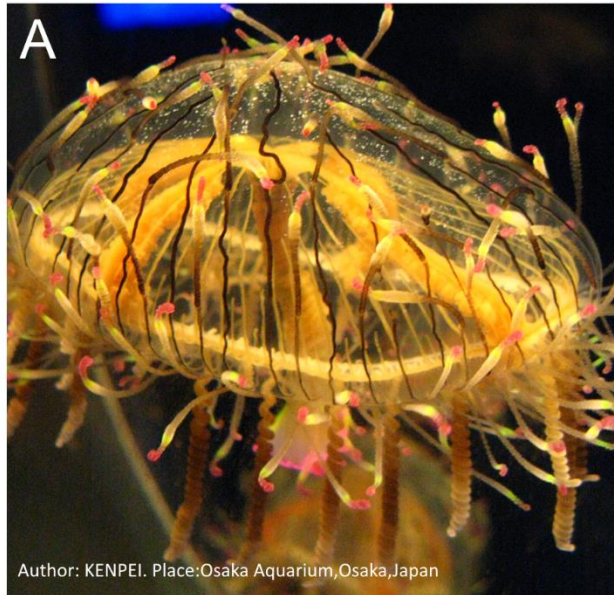
Figure 4. Hydromedusae. **(a)** *Olindias formosa* (Limnomedusae); **(b)** *Bathykorus bouilloni* (Narcomedusae); **(c)** *Velella velella* (Anthomedusae); **(d)** *Crossota* sp. (Trachymedusae).

Anthomedusae range from less than 1 mm to several cm, their umbrella is bell shaped with gonads located on the sides of the central mouth. They do not show a defined number of tentacles. Anthomedusae may alternate with polyp stage or some species bud medusae directly [23].

Leptomedusae possess flatter umbrellas, 4 or more radial canals with associated gonads and tentacles on the margin of the umbrella. Leptomedusae also alternate with polyps, but some species produce new medusae by budding or fission [23]. In the north Adriatic *Aequorea forskalea* represent this group.

Limnomedusae may possess different umbrella shapes and gonad placement. Their life cycles involve both polyp and medusa stages. Peculiar of this order are the 20 species of freshwater jellyfish known (Class Hydrozoa, family Olindiidae) [23,27].

Trachymedusae umbrella are high with a stiff mesogleal layer. They live in deep waters and they present marked pigmentation. This order have reduced polyp stage or totally lacks the polyp, young medusae develop directly from planula larvae, or by asexual budding [13,14,23].

Narcomedusae are characterized by the lack of polyp stage and the parasitic behavior of its larval stage on other jellyfish. Their gastric cavity is wide and they do not possess radial canals [23].

Cubozoa

Box jellyfish, or Cubozoa, were named after their cube-shaped body. They represent the smallest cnidarian class with 48 species (updated in 2021) [12], of which only one is found in Italian waters, namely *Carybdea marsupialis*.

The squared body presents, from each of its lower corners, four short pedaliums each one with a single tentacle [16]. The border of the umbrella is folded inward, creating a Cubozoa peculiar structure which is the velarium, dedicated to the propulsion of the animal. Thanks to the velarium, Cubozoa are the fastest jellyfish in the oceans, reaching top speeds up to 1 m/s [28] in the wild current-assisted (in laboratory the highest speed ever recorded is 115 mm/s [29]).

Another great evolutionary achievement in Cubozoa is their sight ability (Fig. 5). Cubozoa rhopalia and their ocelli are the most complex within Cnidarian [15,16]. Each rhopalium carries a similar set of six eyes, two large complex medial eyes, a lateral pair of pigment pit eyes, and a lateral pair of pit-shaped ocelli (pit eyes), and an identical pair of slit-shaped ocelli (slit eyes). The medial eyes possess a cornea, cellular lens, and a retina with pigmented cells [30] showing similar features to the eyes of vertebrates and cephalopods, even if their function is not totally defined yet.
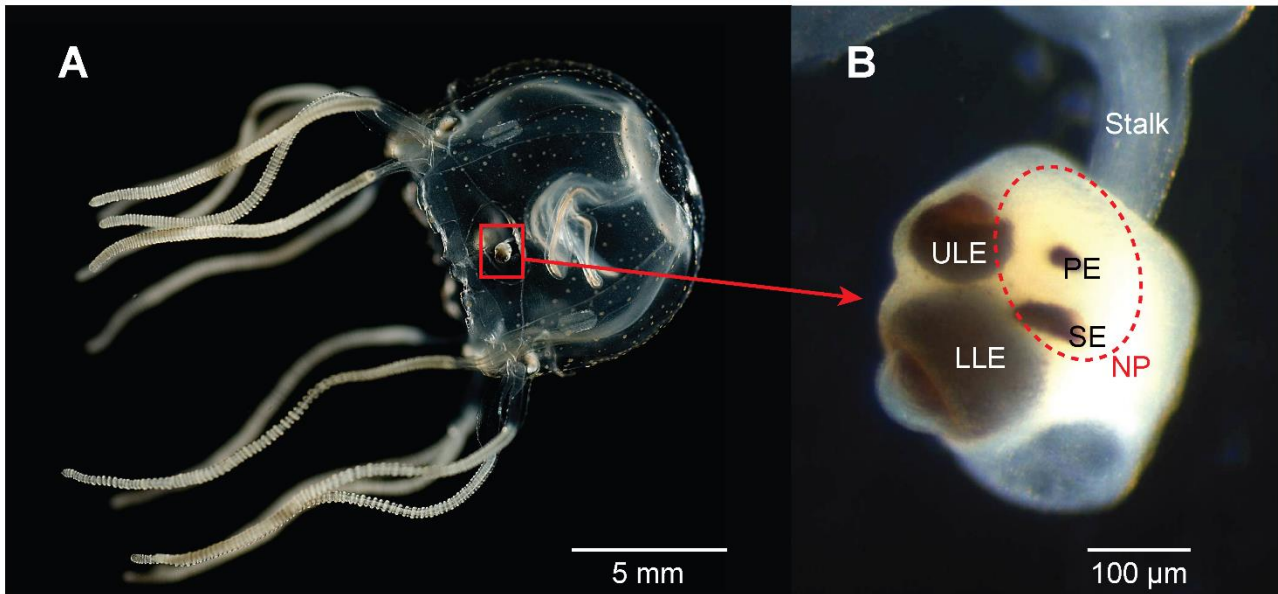
Figure 5. Visual system of *Tripedalia cystophora* (**a**) in the red box the sensory structures called rhopalia (**b**). Each rhopalium carries six eyes of four morphological types (lower lens eye LLE, upper lens eye ULE, pit eye PE and slit eye SE) and a light sensitive neuropil (NP, red broken line). The eyes are responsible for the image formation in the animal and the light sensitive neuropil is thought to be involved in diurnal activity. Taken from [31]

Last, Cubozoa include some of the most venomous organisms in the world and the most dangerous jellyfish, *Chironex fleckeri*, belongs to this class.

Ctenophora

The phylum Ctenophora (commonly called comb jellies, Sea walnuts, Sea gooseberries) include about 180 exclusively marine species [12]. Their areal of distribution is wide, with broad ranges of latitudes (from polar to tropical waters) and depth (from shallow waters down to 3000 m) [32]. The name Ctenophora derives from the ancient Greek "κτείς" or "comb," and "φέρω" or "to carry", due to their peculiar rows of cilia called "cteni"[33]. The body anatomy differs from Cnidaria radial symmetry, Ctenophora possess a peculiar rotational symmetry. They can range from few millimeters long organisms, such as *Pleurobrachia*, to huge organisms (if compared to gelatinous zooplankton mean size) like Cestum veneris, also called Venus' girdle, measuring over 1 meter [14]. As mentioned, they swim using their eight rows of ciliary combs that while moving, they refract light producing the typical prims-like effect [13](Fig. 6).
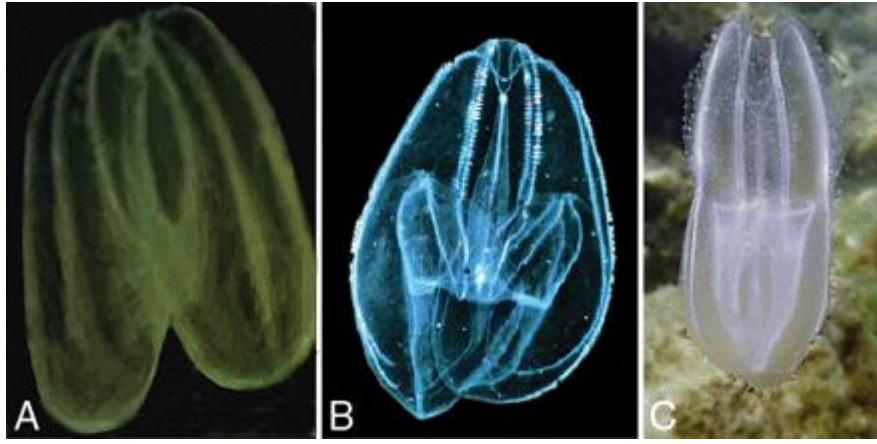
Figure 6. **(a)** *Mnemiopsis leidyi* (photo of Janez Forte); **(b)** *Bolinopsis vitrea*, **(c)** *Leucothea multicornis* (photo of Marjan Richter). Taken from [34]

Ctenophora are voracious predators of zooplankton (sadly famous the collapse of fisheries in the black Sea due to the invasive *Mnemiopsis leidyi* eating on ichthyoplankton [35]), captured using specific cells called colloblasts, which release an adhesive compound [13,14,33]. Colloblasts are one of the features that anatomically distanced Cnidaria (which possess nematocysts filled with venom) from Ctenophora. Their gelatinous bodies, in the first observations in the past, wrongly suggested similarities between these two phyla, which, actually, are evolutionarily speaking significantly separated.

The most common Ctenophora classes in the Mediterranean Sea are Lobata, Cydippida, Cestida and Beroidea.

Cydippida include species with paired tentacles that exit the body from tentacle sheaths. This class may prey small crustaceans, salps, jellyfish and fish. In particular, *Haeckelia rubra*, after eating jellyfish, is able to steal nematocysts from its prey to enhance its defensive capacity [36,37]. In the past, the presence of nematocyst in Ctenophora erroneously brought to the idea of a close relationship between Cnidarians and Ctenophores. In the Mediterranean Sea the most famous genera are *Pleurobrachia and Haeckelia*.

Lobata lack the pair of tentacles and its predatory activities are carried out by oral lobes and auricles, spread out during swimming to form a "trap" for preys, which remain attached to them due to the presence of adhesive mucus released by colloblasts [13,23]. *Mnemiopsis leidyi* is the most famous

ctenophore of this class, due to its worldwide spreading (it is one of the "best" invasive species, north Adriatic included) and impact on human activities and ecosystems (the infamous case of the collapse of fisheries in the Black Sea in the 90's [35,38]). besides *Mnemiopsis leidyi*, other common species are *Leuchothea multicornis* and *Bolinopsis vitrea*.

Beroida are predators of other ctenophores, and occasionally salps. They lack tentacles and capture prey by engulfing them and dismembering pieces with macrocilia located behind the mouth [23]. Three species are present in the Mediterranean Sea, namely *Beroe ovata sensu Chun*, *Beroe ovata sensu Mayer*, *Beroe cucumis* and *Beroe forskalii* [34].

Table 1. Summary of features highlighting similarities and differences between cnidarians and ctenophores. Modified from [33]

FEATURES	CNIDARIA	CTENOPHORA
Habitat	Fresh water and marine water	Exclusively marine
Colonial, solitary	Both solitary and colonial	Always solitary
Polymorphism	exhibited by class Hydrozoa	Completely absent
Resemblance	Polyp/Medusa	Like Medusa
Tentacles	Hollow, many, surrounding mouth, cannot be retracted within.	Solid, two, present away from mouth, can be retracted within the tentacular sheath.
Body wall	Diploblastic i.e. ectoderm and gastroderm with gelatinous mesogloea in between	Diploblastic, with gelatinous mesogloea having amoebocyte cells.
Statocyst	Commonly 8 present at the margins of medusa	Only one is present at the aboral end. Also called apical organ.
Nematocyst (Stinging cell)	Present in ectoderm and on tentacles. Paralyze the prey	Absent, if present, borrowed from cnidarians
Colloblasts (Adhesive prey capturing cells)	Absent	Colloblasts are present in the ectoderm and on tentacles. Release mucous and sticks the prey.
Muscles	Present in mesogloea	Present in gastrodermis
Ciliary cells	Monociliated	Multiciliated
Digestive System	Gastrovascular canals, opens only by mouth, no anus.	Gastrovascular canals open by mouth and anus.

Comb plates	Completely absent	8 comb rows of partially fused ciliary comb plates present.
Swimming	By jet propulsion	By coordinated activities of partially fused cilia in various comb rows.
Sex organs	Commonly Hermaphrodite (some gonochoristic)	Dioecious/Gonochoristic (having separate sexes)
Cleavage	Inderminate (cell fates are not decided)	Determinate (cell fates are fixed at the 1st cell division.
Gastrulation	Delamination, epiboly or invagination	Epiboly or invagination
Common larval stage	Planula larva (a free swimming, double layered, ciliated larva)	Cydippid larva (8 comb rows, a statocyst, and 2 tentacles) resembles adult.

Gelatinous zooplankton and their parasites

Gelatinous zooplankton have been historically considered as secondary characters in the ecosystems. In the last decades, the huge increase in frequency of jellyfish blooms [39], the consequent issues on human activities [40], and the growing importance of jellyfish as human food [41,42] pulled the attention of the scientific community on the gelatinous zooplankton. Most of the studies focused on their biology, life cycles and role in the ecosystems. Other aspects, such as symbiosis and parasitism have been often neglected [43].

Gelatinous zooplankton may host a wide range of parasites, the better studied are Ciliphora, Hydrozoa, Anthozoa, Amphipoda, Cestoda [44,45], Trematoda [46,47], Pycnogonida [48], and Lepadomorpha [49] (Table 2).

Table 2. Examples of different gelatinous zooplankton parasites.

Parasite		Jellyfish	Description	Author
Group	Species	Species		
Ciliophora	*Vampyrophrya pelagica; Trichodina ctenophorii; Flabellula-like gymnamoebae*	Numerous species	After the copepod (the first host) is ingested by jellyfish, it metamorphoses into the feeding-stage trophont, able to consume the copepod tissues more quickly than jellyfish do.	Moss et al. [50] Ohtsuka et al. [43]
Hydrozoans	*Genus: Cunina; Pegantha*	Anthomedusae, Leptomedusae, Trachymedusae, Narcomedusae, Scyphomedusae	Polypoid stages develop in the gastric cavities and the subumbrella of the jellyfish.	Bouillon, [51]
Anthozoans	*Edwardsiella lineata*	*Mnemiopsis leidyi*	This species selectively parasitizes the digestive cavity of	Bumann & Puls [52]

			the ctenophore before metamorphosing into a vermiform body. It may lead to starvation and a reduction in fecundity	
Trematoda	Numerous species	Numerous species	Gelatinous zooplankton is used as second intermediate or paratenic hosts	
Pycnogonida	*Pallenopsis scoparia*	*Periphylla periphylla*	Juveniles and adults attach to the subumbrella and feed on tentacles and other tissues	Child & Harbison [48]

Digenea (Trematoda)

Digeneans (Platyhelminthes: Trematoda: Digenea) include the majority of Trematoda, a class exclusively composed by parasitic species [53]. Their life cycles separate them from others platyhelminths. They are heteroxenous, this peculiar life cycle involves (with exceptions) three stages, two intermediate and one definitive host, usually a vertebrate [54,55] (Fig. 7).

Digenea life cycle and transmission

Adults, hosted in fish, release eggs that will be expelled by the host digestive system. The egg will hatch into a motile larva called miracidium, which will "swim" until it finds the first hosts, commonly a molluscan gastropod [56]. At this stage, the miracidium develops into a new body conformation, called sporocists, characterized by asexual reproduction inside the host, releasing other daughter sporocysts and rediae [57]. Within the rediae, cercariae are produced. The cercaria is another ciliated free-swimming stage that will be released from the gastropod and will move until the physical contact with the second intermediate host (for example jellyfish) [56,57]. Here, the cercaria actively penetrate the host body and during this the tail is lost and it transform into a metacercaria, a resting stage waiting the transfer to the definitive host to fully mature into an adult [58].
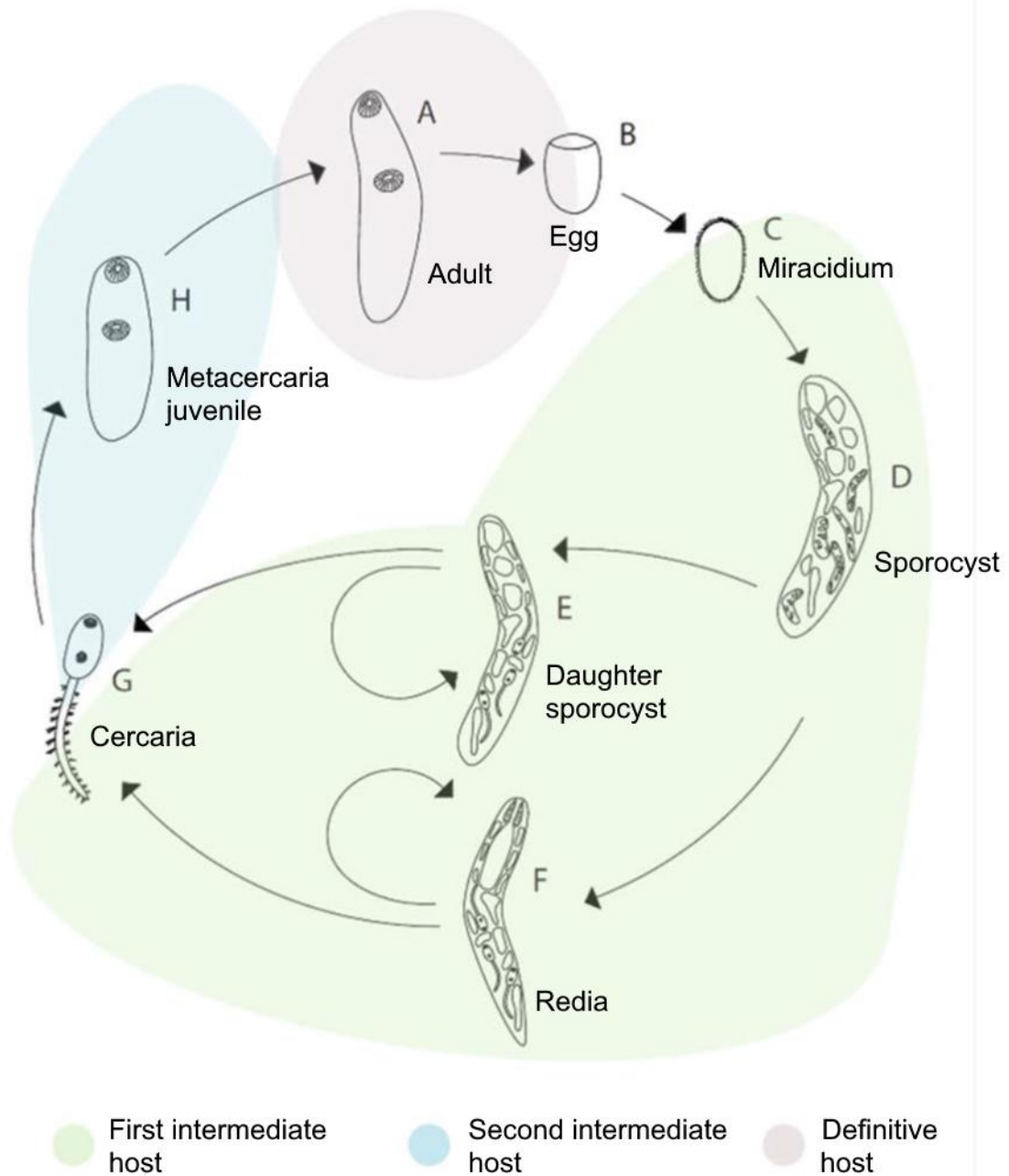
Figure 7. Diagrammatic representation of a digenean three host life cycle. Modified from [59]

Digenea – Jellyfish host. State of the art

To date, most of the research done on jellyfish digeneans is restricted to South America, Japan and Australia [43,46,47,59–67]. As shown in Table 3 made by Nogueira Júnior et al. [60], there is a huge hole about the knowledge on digeneans dynamics in the gelatinous zooplankton, both in terms of prevalence and intensity, digenean and jellyfish species involved, temporal and spatial variations, and transmission from the first unknown hosts to the unknown definitive hosts.

Table 3. Review of scyphomedusae hosting larval digeneans worldwide. Modified from [60]

Scyphomedusae	Parasite	Observations	Location	Data source
Semaeostomeae				
Aurelia aurita	*Neopechona* sp.	$P = 100$; $I > 90$ ($n = 20$)	Seto Inland Sea, Japan	Ohtsuka et al. [43]
Aurelia sp.	*Lepocreadium clavatum*, *Cephalolepidapedon saba*, *Opechona olssoni*	$P = 92$; $I = 1–352$ ($n = 12$), both P and I show a remarkable seasonality	Seto Inland Sea, Japan	Ohtsuka et al. [68], Kondo et al. (2013)
Aurelia sp. (ephyrae)	Lepocreadiidae	Only 3 out of several ephyrae were infected	Tuticorin (South India)	Thapar apud Lauckner [62]
Cassiopea borbonica (= *Cotyorhiza tuberculata*?)	*Distoma carinariae*			Della Valle (1830) apud Thiel [61]
Cassiopea sp.	*Pseudopisthogoporus vitellosus* and more 20 morphotypes		Queensland, Australia	Browne et al. (2013) [59]
Pelagia noctiluca	*Distoma pelagiae*		Naples, Italy	Kölliker (1849) apud Thiel [61]
Pelagia noctiluca	Inadequately described larval trematodes		Mediterranean	Lauckner [62]
Cyanea muellerianthe	Metacercariae			Haacke (1886) apud Thiel [61]
Cyanea nozakii	*Lepocreadium clavatum*, *Cephalolepidapedon saba*, *Opechona olssoni*	$P = 100$ throughout the year	Seto Inland Sea, Japan	Kondo et al. (2013)
Chrysaora quinquecirrha	*Opechona pyriforme*	massive parasitism in experimental infections	Woods Hole, USA	Stunkard [64,66,69]
Chrysaora quinquecirrha	*Lepocreadium setiferoides*	experimental infections	Woods Hole, USA	Stunkard [65]
Chrysaora quinquecirrha	*Bacciger brevoortii*		Gulf of Mexico	Martorelli et al. (2010)
"scyphozoans" (*C. quinquecirrha*?)	*Neopechona cablei*		Woods Hole, USA	Stunkard [47]

C. lactea	*Opechona* sp.	$P = 10.5; I = 2$ -16 ($n = 285$)	São Paulo, Brazil	Morandini et al. [70]
C. lactea	*Opechona* sp.	$P = 55$ ($n = 96$)	Argentina	Diaz-Briz et al. [67]
C. lactea	*Opechona* sp.	$P = 40.8; I = 1$ -35 ($n = 817$)	Paraná, Brazil	Present study
C. melanaster	*Neopechona* sp.	$P = 100$ ($n = 1$)	Seto Inland Sea, Japan	Ohtsuka et al. [43]
C. pacifica	*Lepocreadium clavatum, Cephalolepidaped on saba, Opechona olssoni*		Seto Inland Sea, Japan	Kondo et al. (2013)
Rhizostomeae				
Cotylorhiza tuberculata	Inadequately described larval trematodes		Mediterranean	Lauckner [62]
Lobonemoides sewelli	*Distoma*			Rao (1931) apud Thiel [61]
Lyhcnorhiza malayensis	Metacercariae			Menon (1930) apud Thiel [61]
L. lucerna	*Opechona* sp.	$P = 0.35; I = 1$ ($n = 38$)	São Paulo, Brazil	Morandini et al. [70]
L. lucerna	*Opechona* sp.	$P = 2.7; I = 1-$ 3 ($n = 968$)	Paraná, Brazil	Present study
Rhizostoma octopus (as *R. cuvieri*)	Metacercariae (Lepocreadiid?)		Camaret sur mer, France	Bavay [71]
R. octopus (as *R. cuvieri*)	Inadequately described larval trematodes		Mediterranean	Lauckner [62]

In the Mediterranean Sea, no studies about intensity and prevalence are available. The few data available for this region are old zoological studies which focused exclusively on the morphological description of trematode species [60–62].

Thesis Objectives

With this thesis, we aimed at investigating the potential dynamics between gelatinous zooplankton species from the Gulf of Trieste and their parasites, a fundamental aspect to determine the role of gelatinous zooplankton as a link or transmitter of parasites from the benthic compartment (the gastropod, first host) to the pelagic compartment (fish, definitive hosts) and back.

At the same time, most of the trophic relationships between fish and jellyfish are still unknown at the current state of the art. In this context, this thesis aimed at providing brand-new parasitological data about jellyfish digeneans to be used as a useful indicator to better estimate the trophic position of jellyfish and fish in the ecosystems and the possible interactions between them in the area (feeding on jellyfish is needed for Digenea to close their life cycle). Data from this study could complement other studies based on trophic ecology traditional methods such as gut contents and stable isotopes analysis.

The main aims and activities of this PhD were divided into three parts.

The first and core part, focusing on the dynamics of parasites in the gelatinous zooplankton of the Gulf of Trieste, in which we attempted to investigate jellyfish digeneans with a modern, and more complete, approach compared to literature made by a combination of traditional morphological analysis, molecular analysis (fundamental to overcome the issues related with the "age" and holes of bibliography about these organisms and "double check" the morphological identification), and statistical analysis (to better describe prevalence and intensity dynamics in relation with different factors).

The second block is focused on shedding light on the multi-host life cycle of digeneans parasites infecting North Adriatic jellyfish. In this part, we investigated several fish species from the area looking for the potential definitive host. Due to logistic issues, we could not arrange a proper sampling for the first potential host, so the part about gastropod is still under development.

Last, the third part, in collaboration with Professor Massimo Avian of the University of Trieste, in which we focused on filling the gap about *Rhizostoma pulmo* anatomy and physiology. This species

is one on the first described jellyfish (Macri, 1778) and the most common jellyfish in the Gulf of Trieste, protagonist of recent massive blooms. Despite its fame, a proper anatomical and functional description for this species is not available.

Chapter 1

Parasitic infections in mediterranean scyphomedusae: the case of *Rhizostoma pulmo* (Macri, 1778) from the Gulf of Trieste

Gregorio Motta [1,2,4], Monica Caffara [3], Maria Letizia Fioravanti [3], Massimiliano Bottaro [2], Massimo Avian [1], Antonio Terlizzi [1,2], Perla Tedesco [3,4,*]

[1]Department of Life Science, University of Trieste, 34127 Trieste, Italy. [2]Department of Integrative Marine Ecology (EMI), Stazione Zoologica Anton Dohrn – Italian National Institute for Marine Biology, Ecology and Biotechnology, 80121 Napoli, Italy. [3]Department of Veterinary Medical Sciences, Alma Mater Studiorum University of Bologna, Ozzano dell'Emilia, 40064 Bologna, Italy.

***Correspondence: perla.tedesco@unibo.it

[4]These authors contributed equally to this work.

Abstract. Very little information is reported for parasites of cnidarians, therefore, the present work aimed to investigate parasitic infections in one of the most widespread jellyfish in the Mediterranean Sea, *Rhizostoma pulmo*. The goals were to determine prevalence and intensity of parasites in *Rhizostoma pulmo*, identify the species involved through morphological and molecular analysis, test whether infection parameters differ in different body parts and in relation to jellyfish size. 58 individuals were collected, 100% of them infected with digenean metacercariae. Intensity varied between 18.7 ± 6.7 per individual in 0-2 cm diameter jellyfish up to 505 ± 50.6 in 14 cm ones. Morphological and molecular analyses suggest that the metacercariae belonged to the family Lepocreadidae and could be possibly assigned to the genus *Clavogalea*.

100% of infected individuals suggests that *Rhizostoma pulmo* is an important intermediate host in the life cycle of lepocreadiids in the region. Our findings also support the hypothesis that *Rhizostoma pulmo* is an important part in the diet of teleost fish, which are reported as definitive hosts of lepocreadiids, since trophic transmission is necessary for these parasites to complete their life cycles.

Parasitological data may therefore be useful to investigate fish-jellyfish predation, integrating traditional methods such as gut contents analysis.

Keywords: Jellyfish, *Rhizostoma pulmo*, Parasites, Digenea, Lepocreadiidae, Grado Lagoon, Gulf of Trieste, Metacercariae

1. Introduction

In recent times, jellyfish and their blooms have become a discussed topic by marine biologists due to their potential impacts on human activities and ecosystem functioning [8,9]. It is widely recognized that these blooming events always occurred in history, nevertheless, although debates exist concerning changes in frequency and magnitude of jellyfish blooms in relation to climate change and anthropic activities [3,10], historical data show that jellyfish populations are increasing [72,73].

Most of jellyfish research focused on their trophic interactions both as predators and preys, while their role as intermediate hosts for a wide variety of parasitic organisms is less known [74–77]. Parasites have been indicated as an important but often neglected component of ecosystems [78]. In this already neglected context, there is a lack of knowledge on parasites of cnidarians: these include Cestoda [44,45], Trematoda [46,47], Pycnogonida [48], other Cnidaria [51], and Lepadomorpha [49].

In particular, digenetic trematodes have been shown to use cnidarians as second intermediate or paratenic host during their life cycle [58,70,79]. The life cycles of these parasites are poorly known [70] and very few evidence of trophic transmission of trematodes from jellyfish to fish has been reported [63]. Equally, few studies addressed the inter-annual presence of digeneans in jellyfish hosts [60,63]. Moreover, recent research mainly focused on hydromedusae and ctenophores as hosts, while data on scyphomedusae are lacking [60]. Up to now, most of the data are spatially limited to South America, Japan and Australia [60]. In the Mediterranean Sea, few zoological studies are available [60–62], which focused exclusively on the morphological description of trematode species. The knowledge of Scyphozoa – parasite relationships is crucial to determine the role of gelatinous zooplankton as transmitter of parasites to the fish compartment and, in addition, parasitological data could shed light on fish-jellyfish feeding interactions [60].

This study is aimed at investigating the occurrence of digenean parasites in one of the most complex and widespread jellyfish species in the Mediterranean Sea, namely the barrel jellyfish *Rhizostoma pulmo* (Macri, 1778) [80]. The species is endemic from Mediterranean Sea and among the biggest jellyfish of this basin (over 40 cm in diameter) [81]. In recent years, *Rhizostoma pulmo* has been recorded blooming all over the Mediterranean Sea from the Northern to Southern Adriatic Sea, the

Ionian Sea, the Eastern and Western Mediterranean, and the Black Sea [22]. In the Gulf of Trieste (North Adriatic Sea), it is present year-round with the highest densities observed from late summer to winter [82].

Particularly, our goals were to: 1) determine prevalence (P) and intensity (I) of infection of metacercariae in *Rhizostoma pulmo*; 2) identify the parasite species involved through morphological and molecular analysis, 3) test whether infection parameters change in different body parts and in relation to jellyfish size. To the authors knowledge, this work is the first attempt to study these parasites dynamics in Mediterranean scyphomedusae.

2. Results

2.1 Parasite Count.

Rhizostoma pulmo umbrella diameter ranged from 1 to 14.8 cm (5.82±4.18 cm). All specimens analyzed were parasitized by trematode metacercariae (prevalence 100%). Intensity values ranged between 10 (recorded in a 1 cm juvenile *Rhizostoma pulmo*) and 556 (recorded in a 13.2 cm specimen). Mean, min and max intensity for each class interval are reported in Table 1.

Table 1. Comparison of mean, standard deviation, min and max intensity for each size class of *Rhizostoma pulmo* from the Gulf of Trieste.

Diameter (cm)	Mean Intensity	Sd Intensity	Min Intensity	Max Intensity
1-2	18.7	6.68	10	30
2-4	92.2	61	12	200
4-6	238	86.2	128	400
6-8	311	55.6	243	377
8-10	316	26.2	292	351
10-12	418	55.1	350	470
12-14	505	50.6	443	556

14-16	411	17.2	399	431

Lower intensities were found in the smallest individuals (18.7 ± 6.68) and the number of parasites increased with size up to 505 ± 50.6 in 12-14 cm class size. Considering all the samples, 12,451 parasites have been counted, 6,144 in the umbrella and 6,307 in the whole manubrium (3,863 in the scapulae and 2,444 in the oral arms) (Fig. 1).
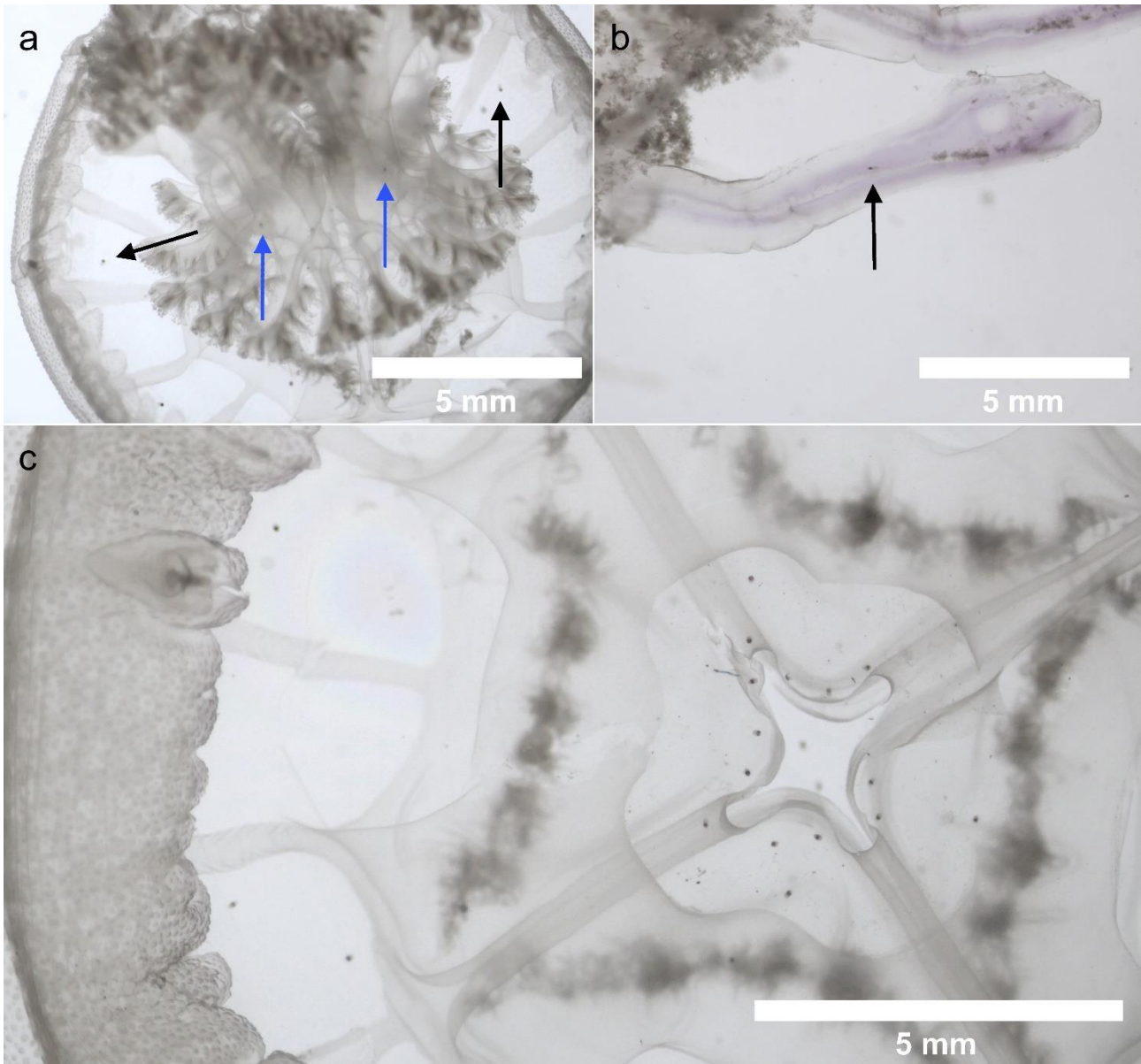

Figure 1. Lepocreadiid metacercariae in different body districts of *Rhizostoma pulmo*: **(a)** whole jellyfish. Umbrella (black arrow), manubrium (blue arrow), **(b)** oral arm terminal club, **(c)** subumbrellar view, manubrium excised.

Results of the LM provided positive and significant logarithmic regression relationships between the size and the number of parasites for both the whole body and the individual compartments (Fig. 2a-c). Formulas, coefficients, goodness of fit R2 and P values are reported in Fig. 2 and Supplementary Table S1.
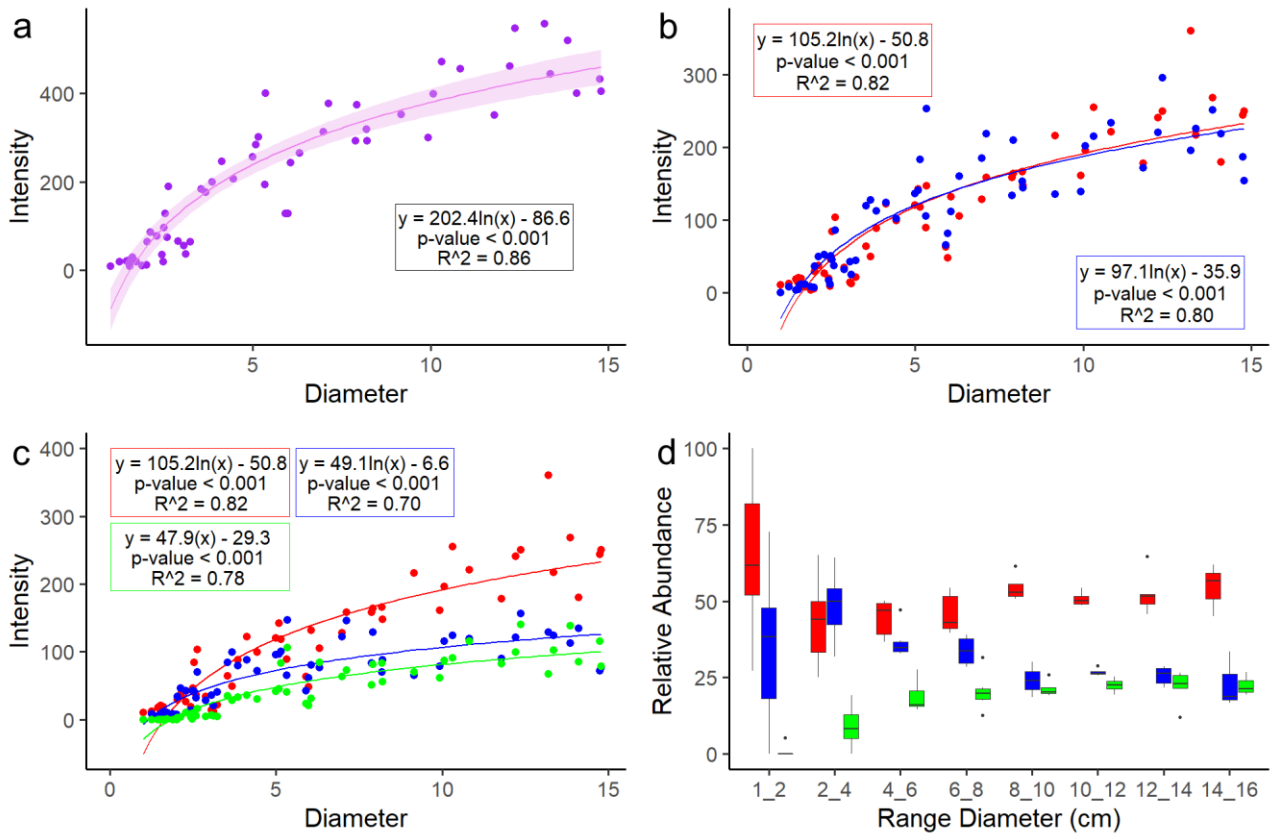

Figure 2. LM for size vs intensity **(a)** in whole body, **(b)** umbrella (red) and whole manubrium (blue), **(c)** umbrella (red), scapulae (blue) and oral arms (green). Coefficients, goodness of fit R2 and P values are reported in each relative box. **(d)** Relative abundance of parasites in umbrella (red), scapulae (blue) and oral arms (green) at different body size intervals (cm).

In juveniles (1-2 cm), high variability of infection was observed. The most infected compartment was the umbrella, followed by the manubrium (Fig. 2d). No parasites were found in the oral arms. In 2 to 4 cm individuals the umbrella and scapulae were equally parasitized, and parasites start to occur in the oral arms at low densities (8.66 ± 5.37 %). In jellyfish larger than 4 cm the oral arms become increasingly infected with increasing size of the host (up to 22.4 ± 3.81 %), while the oral arms

become less infected (23 ± 9.1 %). The relative abundance of parasites in the umbrella remains constant (slightly above 50 %) irrespective of host size.

2.2 Parasite identification.

The morphological analyses allowed to assign all the unencysted metacercariae analyzed to the family Lepocreadiidae; particularly, the presence of enlarged oral spines and general morphology (Fig. 3,4) would suggest a possible attribution to the genus *Clavogalea* Bray (1985), erected by Bray and Gibson[83] based on the examination of adult specimens, and whose larval stages have never been described.
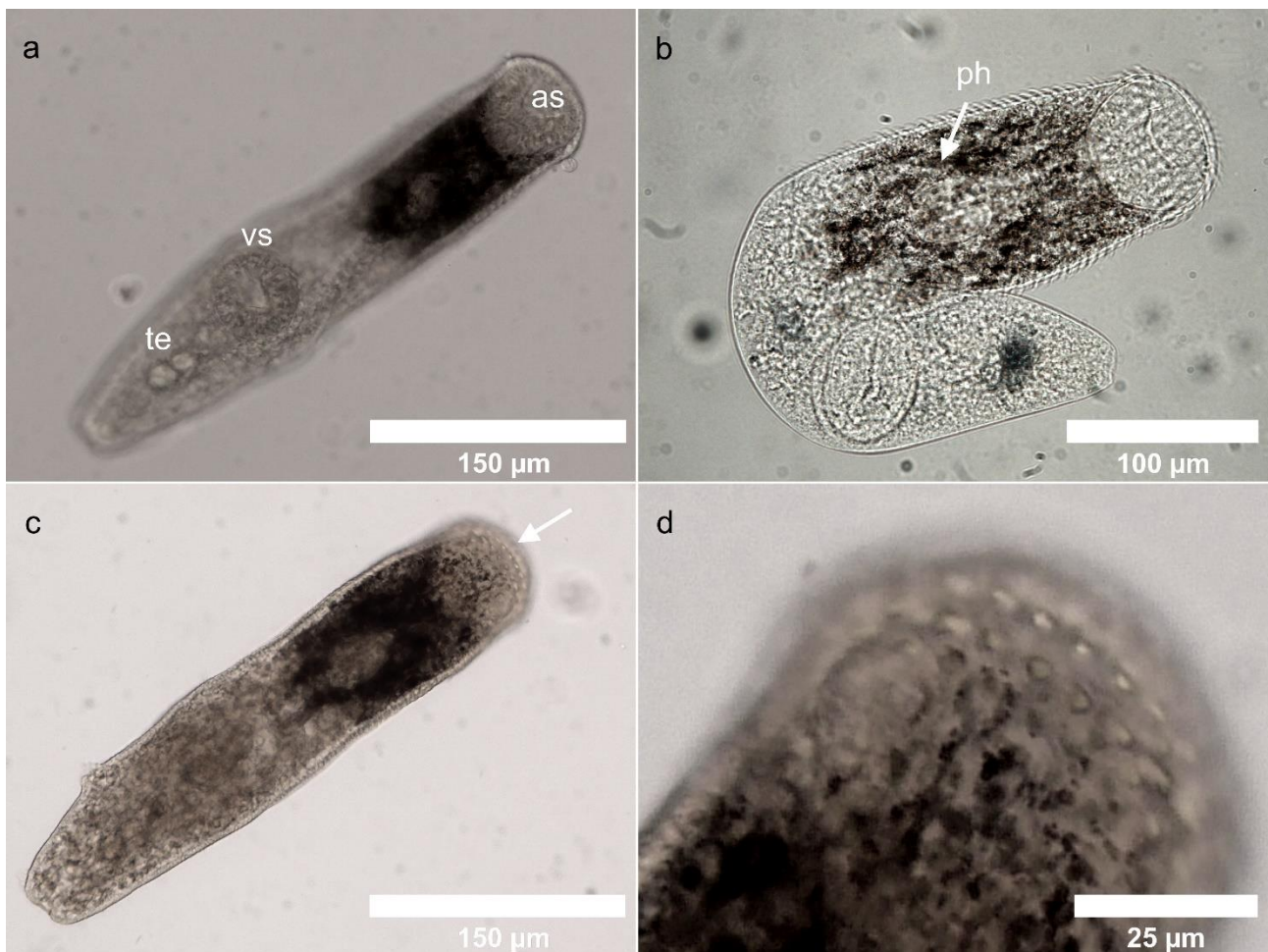

Figure 3. Lepocreadiid metacercariae from *Rhizostoma pulmo*, light microscopy: **(a)** ventral view, **(b)** cleared specimen, **(c)** dorsal view, **(d)** detail of anterior region showing double rows of oral spines characteristic of the genus *Clavogalea*. Abbreviations: anterior sucker (as), ventral sucker (vs), testes (te) and pharynx (ph).
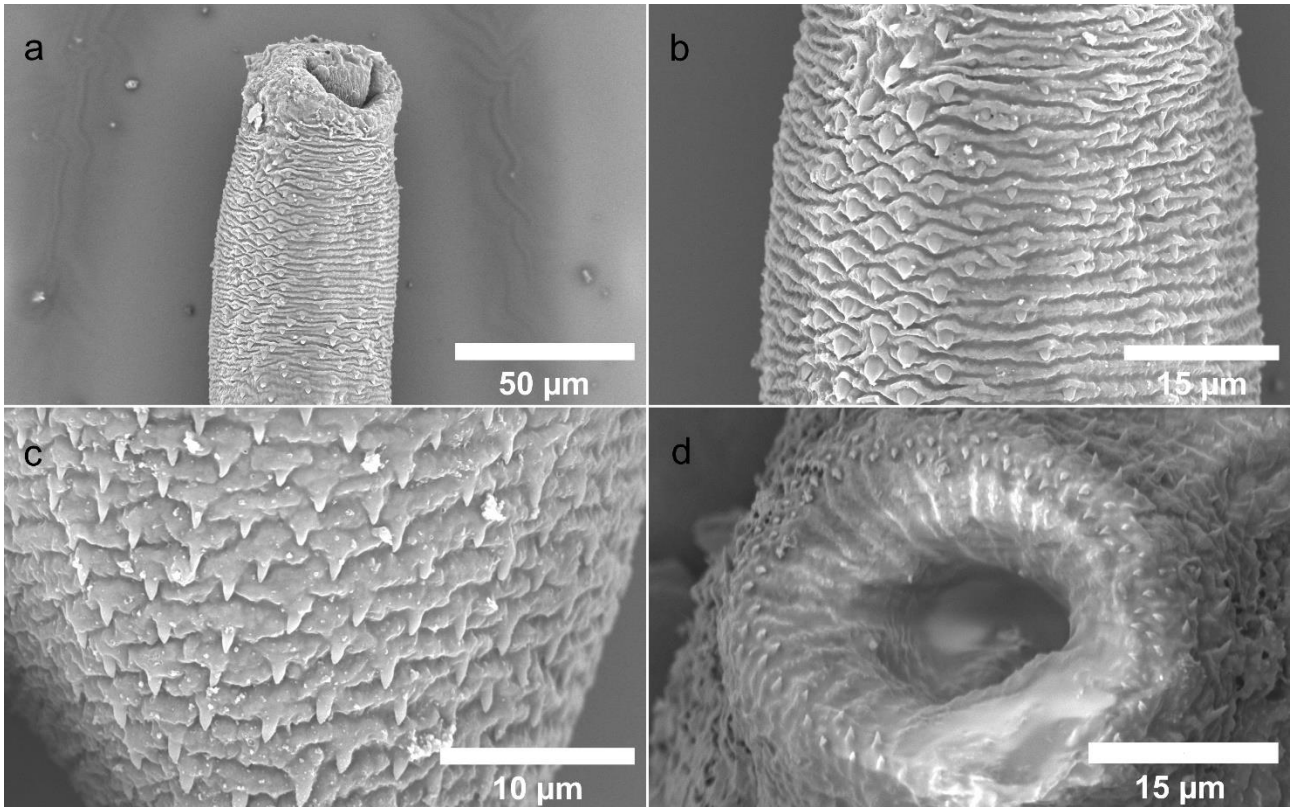
Figure 4. Lepocreadiid metacercariae from *Rhizostoma pulmo*, SEM micrographs: **(a)** anterior end showing the oral sucker and spiny tegument, **(b)** detail of spines in anterior region, **(c)** detail of spines in posterior region, **(d)** detail of ventral sucker.

Morphological description (based on 20 specimens), unit of measurement µm. Body elongate 215.43 - 461.61 (336.58 ± 56.13) long by 54.81 – 107.63 (81.63 ± 13.64) wide. Eye-spots pigment scattered in region of pharynx. Tegument spinous. Two rows of enlarged spines around aperture of oral sucker, with rounded base and triangular point, rows alternating. Oral sucker terminal, 45.61 – 71.58 (60.69 ± 8.76) long by 44.78 – 80.47 (55.99 ± 9.03) wide, infundibuliform. Ventral sucker rounded 40.99 – 63.04 (51.52 ± 7.79) long by 42.1 – 69.8 (54.05 ± 7.47) wide, smaller than oral sucker. Pharynx elongate, oval 36.55 – 40.54 (39.09 ± 1.59) long. Testes two, elongate, oval, oblique in posterior third of body, separated. Anterior testis 7.43 – 13.34 (10.30 ± 2.11) long by 12.01 – 18.19 (14.34 ± 2.35) wide, posterior testis 8.21 – 16.84 (12.35 ± 2.99) long by 13 – 17.9 (15.87 ± 1.69) wide. Distance between testes 3.57 – 7.89 (4.91 ± 1.54). Ovary rounded 6.12 – 10.77 (7.73 ± 1.84) long by 7.51 – 15.11 (9.97 ± 3) wide, entire, pre-testicular, separated from anterior testis. Excretory pore terminal.

Four subjects were successfully amplified giving a product of 1655 bp. BLAST search gave the highest identity (98%) with the Lepocreadiid group (*Opechona*, *Preptetos*, *Prodistomum* and *Clavogalea*) with a p-distance ranging from 0.020 to 0.031 (Fig. 5). The ML tree based on 28S rDNA showed our sequences included in the Lepocreadiid cluster, clearly separated and well supported. As already reported in other studies, the interrelationships among the Lepocreadiid group which include *Opechona*, *Preptetos*, *Prodistomum* and *Clavogalea* are unresolved and confirmed to be polyphyletic[84,85].
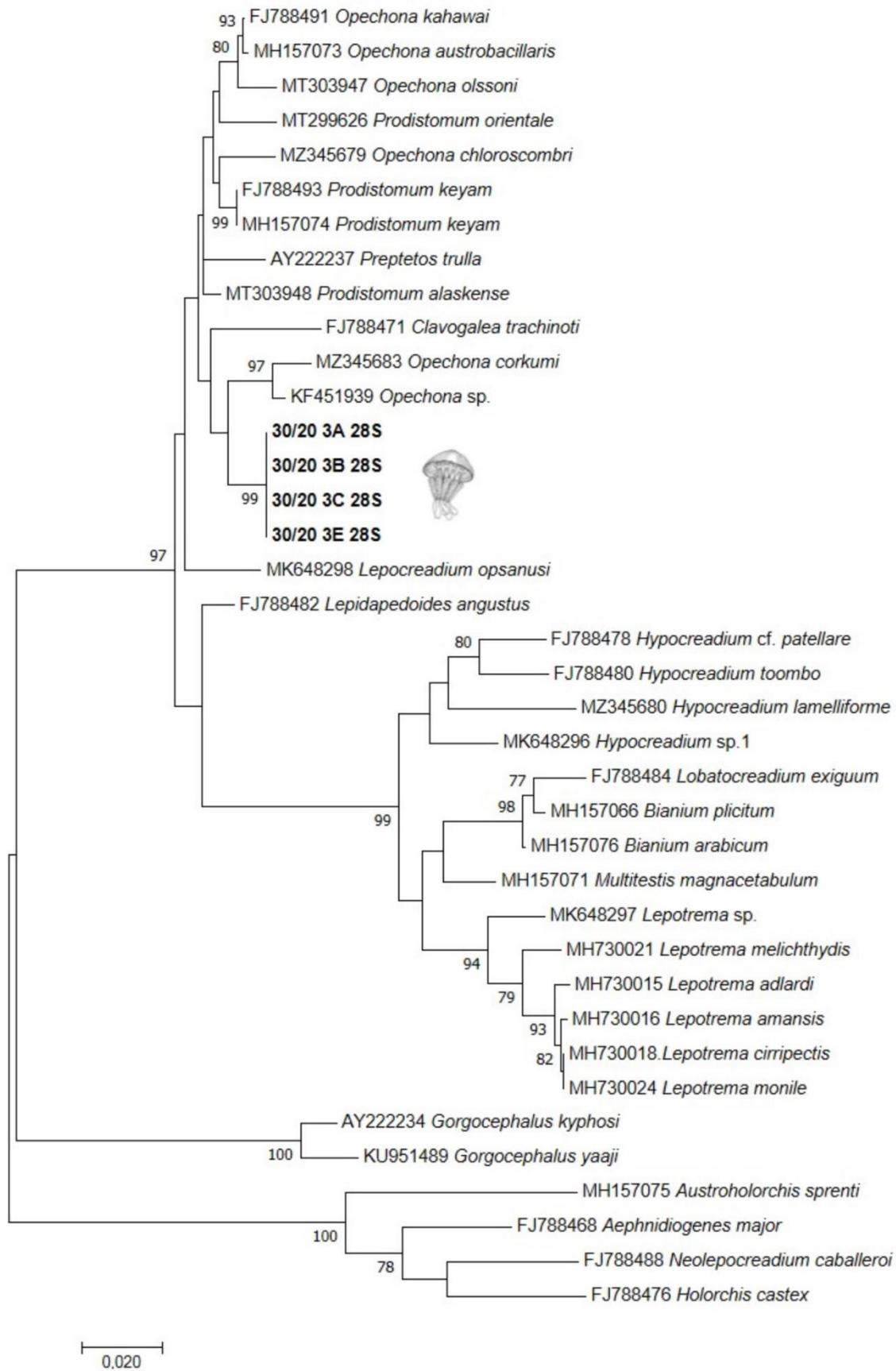
Figure 5. ML Tree of Lepocreadiid cluster based on 28S rDNA

3. Discussion

Data on the occurrence of metacercariae in Scyphozoa are limited [60,70]. To date, as regards the Mediterranean Sea, only few zoological studies aiming only at parasite morphology description are available [60–62]. This work is the first study focused on infection dynamics (in relation to body size and different body districts) in Mediterranean scyphomedusae as well as the first record of jellyfish as second intermediate hosts for digenetic trematodes in the Adriatic Sea.

The high (100%) prevalence found in the present study suggests that *Rhizostoma pulmo* is a key host in the life cycle of Lepocreadiid trematodes.

With respect to the fish host, records of Lepocreadiid parasites in the Mediterranean Sea include *Opechona bacillaris* (Molin 1859) [86] Looss, 1907, originally described infecting *Centrolophus niger* (Gmelin, 1789) from Adriatic Sea (Molin, 1859) and subsequently reported in *Pomatomus saltrix* and *Scomber scombrus* from different parts of the Mediterranean, Black Sea and Northern Atlantic Sea, and *Prodistomum polonii* in *Trachurus trachurus* from the same areas [83,87]. No *Clavogalea* spp. have been reported so far in either intermediate or definitive hosts from the Mediterranean Sea. This genus has been erected by Bray [88] to accommodate species that are very similar to *Opechona* spp. but with enlarged oral spines and short excretory vesicle as distinguishing features [89]. To date, only two species of *Clavogalea* have been described, namely *Clavogalea gaevskayae* infecting *Trachinotus botla* from South Africa, and *C. trachinoti* (synonymized with *Stephanostomum trachinoti* Fischthal & Thomas, 1968 and *Opechona pseudobacillaris* Fischthal & Thomas, 1970 [89] in *T. botla* and *T. coppingeri* from Australia; of these two species, morphological data are available only from adult stages. Therefore, in the present study it was not possible to confirm the specific identity of our metacercariae based on morphological data. Furthermore, life history and molecular data, which could support a correct species identification, are available only for a fraction of the currently recognized species. Our analysis of 28S rDNA sequences of metacercariae from *Rhizostoma pulmo* confirm the polyphyletic status among the Lepocreadiid group as reported by Bray et al. [84] and Sokolov et al. [85]. Recent phylogenetic analysis of Lepocreadiid based on 28S rDNA [90] confirmed that interrelationships among

members of the family, particularly *Opechona* spp. and other morphologically similar genera (including *Clavogalea*) are unresolved and probably all belong to the genus *Opechona*.

In our study, intensity values increase with *Rhizostoma pulmo* body size. This could be explained by the anatomy and life history of the individuals. Particularly, larger jellyfish may provide an extended contact surface for free-swimming cercariae and may have been exposed for longer time to acquisition and accumulation of parasites, as theorized by Yip [91]. Relative abundances in body districts indicate that colonization is not uniform during growth. Most of the studies providing quantitative data on digenean infection in jellyfish focused solely on the umbrella [70]. This is the first study that takes in consideration the entire body. Although no differences between the umbrella and the whole manubrium have been found in terms of intensity, we noticed a shift of parasite presence within the scapulae and oral arms during growth. It is interesting to notice that, regardless of the overall intensity in the whole organisms, the relative abundances in the different body compartment remain constant in a given size range.

It has been shown experimentally that lepocreadiid cercariae of the genus *Opechona* enter the second intermediate host through active penetration of body tissues [57]. However, our results concerning the relative abundance suggest the idea that parasitization/diffusion in *Rhizostoma pulmo* by lepocreadiid metacercariae do not take place randomly, but may be influenced by potential drivers, for example the anatomical changes occurring during jellyfish growth. *Rhizostoma pulmo* preys by active filtration of the water column, umbrella pulsations together with ciliary movement create an inward flux through its central oral pore in juveniles and, in adults, trough oral arms openings [92,93]. *Rhizostoma pulmo* juveniles (1-2cm diameter) have undeveloped oral arms and they still eat through a central oral pore under the umbrella [93,94]. This feeding habit and the related central flux could "pull" swimming cercariae that parasitize the nearest tissues around the stomach pouch and scapulae. Small *Rhizostoma pulmo* (2-4 cm) begin to possess developed oral arms filled with small mouths. From our observations, during this growth interval the juvenile oral pore slowly close up. These modifications suggest that parasites can now be drawn by both the oral pore (if still open) and oral arms currents. Umbrella and scapulae remain the most parasitized tissues at this stage. Parasites are now found in

the oral arms, but low intensity may be due to the fact that oral arms internal circulatory canals are still under development. In fully developed individuals, colonization increased in oral arms along with body size. The decrease of intensity observed in the scapulae may be related to its minor role in feeding from this life stage and to oral arms, which are now developed and filled with small channels. Thus, oral arms provide extended external and internal contact surfaces for parasites. At umbrellar level, its wide surface at every stage of jellyfish life, may offer a favorable environment for parasite encounter and penetration, thus justifying the almost constant parasite relative abundance.

As mentioned, this is the first study that investigates prevalence and intensity of digenean parasites in *Rhizostoma pulmo* and takes in consideration all the body in counting parasites in Rhizostomeae. From our results it is evident how counting parasites only in the umbrella brings to an important underestimation of real intensity, at least in *Rhizostoma pulmo*. At the same time, this study shows that the distribution of parasites in the organism changes during growth, a whole-body count is the proper way to assess intensity if no solid data about relative abundance in compartments at different sizes is available.

By comparing our data to other studies about jellyfish digeneans, it is evident the difference in prevalence and intensity observed in north Adriatic *Rhizostoma pulmo*. Morandini et al. [70] found a P < 10.5 and I < 16 in *Lychnorhiza lucerna* and *Chrysaora hysoscella lactea* scyphomedusae, Nogueira Junior et al. [60] found a P < 10 and I < 7 in several Hydrozoan species. In Kondo et al. [63] the mean intensities of the digenean *Lepotrema clavatum* in *Cyanea nozakii*, *Aurelia aurita* and *Chrysaora hysoscella pacifica* were 219.6, 46.5 and 8.8, respectively. *C. nozakii*, who showed similar intensity in Kondo et al. [63], ranged from 13.3 cm to 51.0 cm, up to 4 times the size of the specimens we analyzed.

The higher infection values observed in our study suggest that *Rhizostoma pulmo* could be a favorable host for this lepocreadiid and, at the same time, the characteristics of Grado Lagoon could provide a favorable spot for digeneans proliferation and transmission. Firstly, the order Rhizostomeae deviates from the traditional anatomy of Scyphozoa. The manubrium is thick and presents a complex canal system with branched lips forming eight oral arms presenting numerous mouth openings [15,92]. In

Rhizostoma pulmo, the thicker body and the presence of channels that run along all the manubrium up to the umbrella increase the surface of tissue available for colonization, if compared to other jellyfish genera as *Aurelia aurita*, *Aequorea forskalea*, *Pelagia* where most of the surfaces are limited to the umbrella and gastric pouch [13].

At the same time, marked P and I seasonality of jellyfish digeneans has been observed in temperate environments where water temperature changes drastically throughout the year [63,95]. Although no sampling was carried out during colder months, the high intensity observed during summer in our specimens reinforce Yip [91] hypothesis that metacercariae are favored in warmer conditions, as similarly showed in Kondo et al. [63], where highest P and I values of *L. clavatum*, *Cephalolepidapedon saba*, and *Opechona olssoni* in *Aurelia aurita and Chrysaora pacifica* have been recorded during spring and summer. The juvenile stages of *Rhizostoma pulmo* develop in Grado Lagoon, characterized by warmer water during summer compared to the open Sea. During winter and spring, only very large individuals (diameter > 30 cm) of *Rhizostoma pulmo* are available in the Gulf of Trieste. In contrast with small size specimens, characterized by transparent bodies, as *Rhizostoma pulmo* grows its tissues become thicker and remarkably opaque, thus affecting samples processing and drastically compromising the precision of parasite count and observation. For these reasons, at least for this area, it is impossible to properly assess the effect of seasonality and that is why sampling have been carried out only during summer.

Seasonal parasites fluctuation may be related to the release of free-swimming cercariae from the first hosts (usually benthic gastropods), which has been theorized to be positively related with water temperature [96]. No information regarding the first intermediate hosts of lepocreadiid digeneans in the area is available. In literature, digeneans free-swimming cercariae are released from a benthic gastropod in the water column. Køie [57] first described the presence of *Opechona* sp. cercariae in *Nassarius pygmaeus* from Scandinavia, Barnett et al. [97] reported the presence of *Stephanostomum*-like cercariae from Australian Nassaridae. Lepocreadiid digenean probably belonging to *Opechona* sp. were identified in gonads and digestive gland of *Buccinanops cochlidium* (Nassaridae) from San Jose´ Gulf, Argentina [95]. In the Gulf of Trieste, two species belonging to the family Nassaridae

(superfamily Buccinoidea), *Tritia mutabilis* and *Tritia varicosa* may be plausible candidates [98,99]. Both species inhabits fine sands and fine muddy sands at depths between 2 and 15 m [100]. Grado Lagoon with its sandy bottoms and depths <10 m provides a wide areal of distribution of these mollusks and the associated parasitic community, thus supporting the I and P measured in *Rhizostoma pulmo*. At the same time, lagoon shallow waters are likely to increase the chances of encounters among the parasite and the jellyfish. Plus, Grado Lagoon is subjected to a wide range of anthropic activities, from commercial suction dredge fishing and shellfish production to touristic maritime traffic, resulting in a potential increase in water turbulence. This mixing may promote the presence and dispersion of cercariae in the water column, thus favoring infection.

Focusing on the jellyfish-fish relationship, in the current scenario of climate change where the abundances of digenean parasites and jellyfish are likely both favored by warmer waters, along with the recent observations regarding active predation of fish on jellyfish [101], blooms may favor parasitic infection in the fish compartment. At the current state of the art, few studies focused on predatory interactions between fish and jellyfish that have yet to be fully clarified [75]. To the present day, *Rhizostoma pulmo* has been demonstrated to be part of the diet of *Trachurus mediterraneus* only, no information of other fish species is available [102,103]. Looking at our results, the 100% of infected individuals suggests that *Rhizostoma pulmo* is an important intermediate host of lepocreadiid digeneans and therefore plays a key role in their life cycle in the investigated area. This also supports the hypothesis that *Rhizostoma pulmo* is an important fish prey, since trophic interactions are necessary for these parasites to complete their cycles.

In conclusion, although it was not possible to identify the parasite at species level, due to the scarcity of literature information (at both morphological and molecular level) available for these organisms particularly in the considered area, our work provides important information on the role of *Rhizostoma pulmo* as intermediate host for lepocreadiids, and useful data as basis for future studies aimed to shed light on the life cycle of these parasites in the Mediterranean Sea. Furthermore, parasitological data may be a useful tool to evaluate trophic interactions between fish and gelatinous organisms, another underinvestigated aspect that needs to be fully clarified, integrating traditional

methods used in trophic ecology research (gut contents and stable isotopes analysis of fish). Further aspects should be investigated such as the full characterization of these parasites' life cycle (host species involved, mechanisms, effect on hosts physiology), the effect of seasonality and the possible differences in infection patterns between other Scyphozoan species in the gulf of Trieste.

4. Methods

Rhizostoma pulmo (Macri, 1778) individuals were collected in the Grado Lagoon (Gulf of Trieste, Northern Adriatic Sea, Italy) (Fig. 6) in July/August 2019 and August 2020.
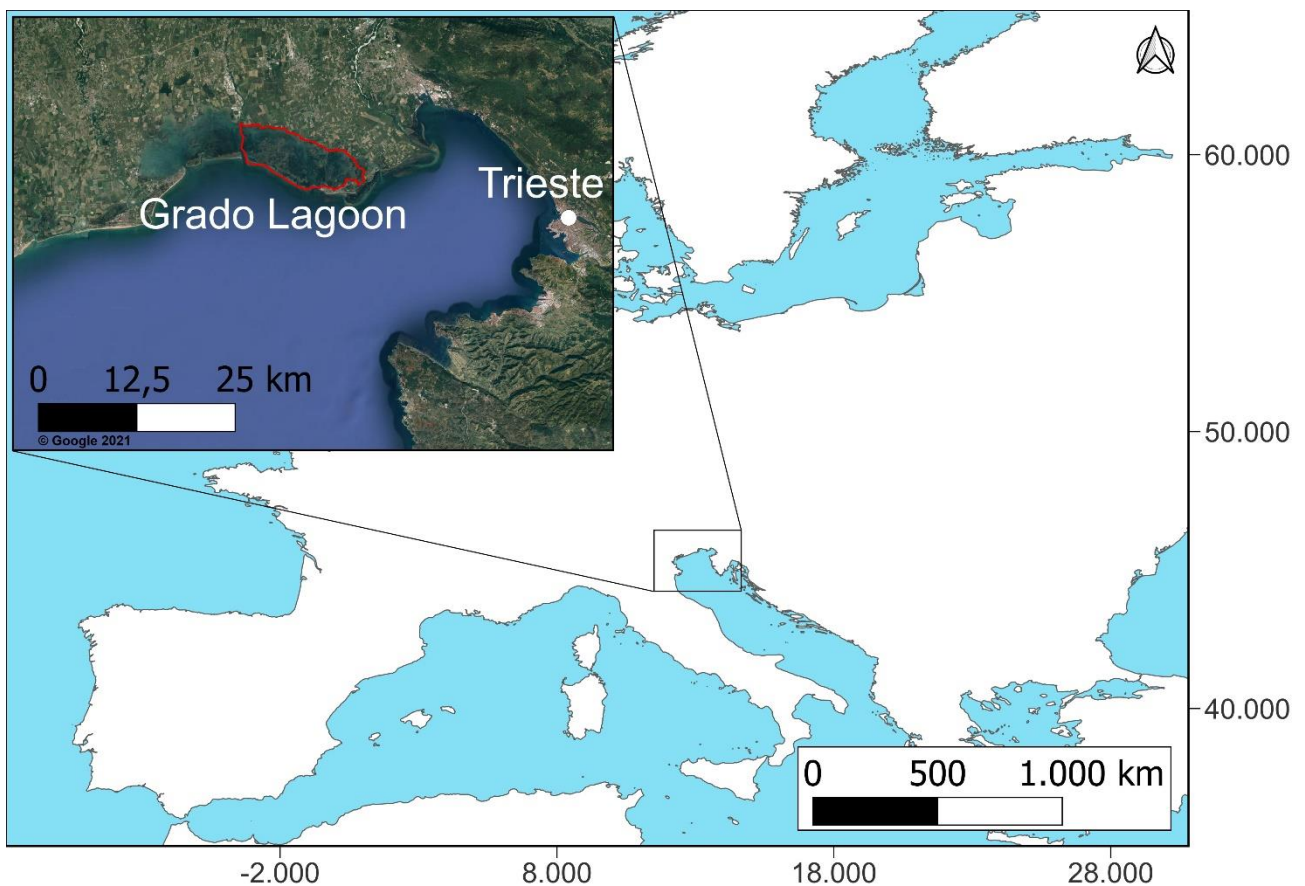

Figure 6. Sampling area of *Rhizostoma pulmo* (Grado Lagoon, Gulf of Trieste).

During summer (late July/early August), simultaneous blooms of young to large *Rhizostoma pulmo* medusae were observed in the Grado Lagoon, so, it was possible to collect specimens of different sizes at the same time. All the samples were collected through diving sessions using containers of adequate size to avoid damages to medusae. Samples were brought to the lab and umbrella diameters were measured with a precision caliper. A total of 70 jellyfish were collected.

4.1 Parasite Count.

Fifty-eight jellyfish (diameter 5.82 ± 4.18 cm) were preserved in 4% formalin-saltwater solution and then stored at room temperature. The umbrella, scapular area (just reported as "scapulae" in the manuscript) and oral arms were separated by a scalpel. Manubrium was divided as shown in Fig. 7.
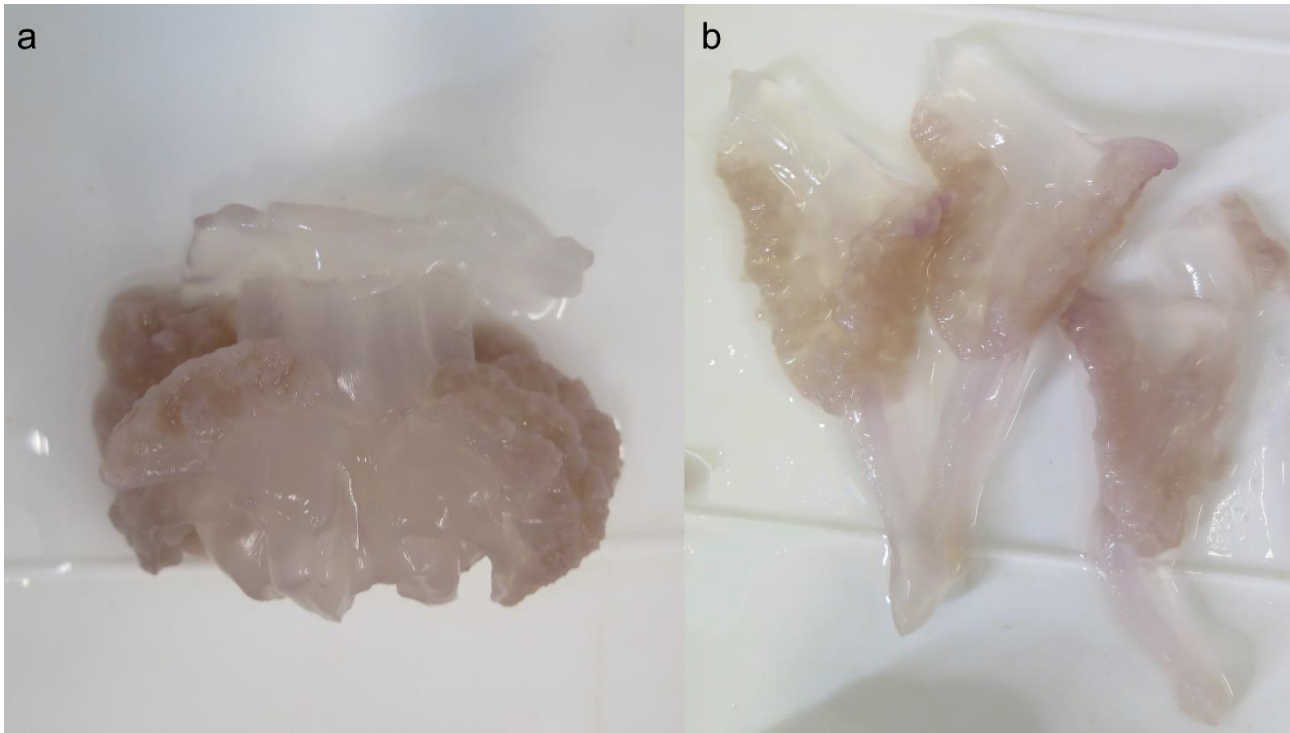

Figure 7. Whole manubrium dissection. Scapular area **(a)** and oral arms **(b)** divided right below scapular level.

Samples were dissected and the presence of parasites in the different body districts was evaluated under a stereomicroscope (Leica Mz-6). Prevalence (P) and intensity (I) values were defined following Bush et al. [1].

The relative abundance of parasites in the three different body compartments has been calculated as follows:

$$\text{Relative Abundance(Body district x)} = \frac{\text{Number of parasites in Body district x}}{\text{Total number of parasites in the sample}}$$

4.2 Parasite identification.

For identification, parasites were extracted from fresh tissues of 12 jellyfish and preserved in 70% ethanol for molecular analysis and 10% hot formalin for morphological analysis following Cribb & Bray [104].

For morphological analysis, 20 metacercariae were subjected to microscopical observation after clarification in Amman's lactophenol. All measurements were taken with the imaging software NIS-Elements expressed as ranges with mean values in parentheses.

For molecular analysis, genomic DNA was extracted from five metacercariae by PureLink® Genomic DNA Kit (Life Technologies, Carlsbad, CA, USA), following the manufacturer's instructions.

The amplification of the D1-D3 region of 28S rDNA was performed with primers U178_f (5′-GCACCCGCTGAAYTTAAG-3′) and L1642_r (5′-CCAGCGCCATCCATTTTCA-3′) [105], following Gustinelli et al. [106]. The PCR products were electrophoresed on 1% agarose gel stained with SYBR® Safe DNA Gel Stain (Thermo Fisher Scientific, Carlsbad, CA, USA) in 0.5X TBE. All amplicons were purified by NucleoSpin Gel and PCR Cleanup (Mackerey-Nagel, Düren, Germany, CA, USA) and sequenced with an ABI 3730 DNA analyzer (StarSEQ, Mainz, Germany). 28S rDNA amplicons were sequenced with the internal primers 900F (5′-CCGTCTTGAAACACGGACCAAG-3′) and EDC2 (5′-CCTTGGTCCGTGTTTCAAGACGGG-3′) of Lockyer et al. [105].

The DNA trace files were assembled with ContigExpress (VectorNTI Advance 11 software, Invitrogen, Carlsbad, California) and the consensus sequences were compared with previously published data by BLAST tools (https://blast.ncbi.nlm.nih.gov/Blast.cgi). Multiple sequence alignments of the newly generated sequences together with the all the sequences reported by Curran et al. [90], were built by BioEdit 7.2.5 [107]. Pairwise distance, using a Kimura 2-parameter model and maximum likelihood (ML) tree (BIC = GTR + G, bootstrap of 1000 replicates) were obtained by MEGA version X [108].

The sequences generated in this study were deposited in GenBank under the accession numbers OM910736-39.

4.3 Statistical analysis.

Five Linear Models (LM) were applied to assess the potential relationship between size and intensity in the whole body and in the different body compartments. The statistical models were developed under the R statistical environment v.3.6.2 [109]. Their specifications were as follows: for each body

compartment (whole body, umbrella, whole manubrium, scapulae and oral arms) the number of parasites has been selected as the response variable and the diameter of jellyfish has been set as the explanatory one. Normality of residuals for each LM was checked with Shapiro–Wilks test and by graphical diagnostics of residuals. In Supplementary Table S1, model formulas, model estimated coefficients and diagnostics are described in detail. Plots were performed using 'GGplot2' package [110]. To investigate statistical differences in intensity in the different body compartments, two one-way PERMANOVA were performed. In the first one intensity was compared between umbrella and whole manubrium (Supplementary Table S2), in the second intensity was compared between umbrella, scapulae and oral arms (Supplementary Table S3). Euclidean distances were calculated among intensities. The tests were performed using 9999 permutations. When significant, a posteriori pair-wise comparisons were performed among compartments via PERMANOVA t statistic with 9999 permutations (Supplementary Table S4). To investigate statistical differences in relative abundance in the different body compartments at different body size, a two-way PERMANOVA on the dataset was performed (Supplementary Table S5). The test was performed using 9999 permutations. When significant, a posteriori pair-wise comparisons were performed via PERMANOVA t statistic with 9999 permutations Supplementary (Supplementary Table S6).

Non-parametric analyses were performed using PRIMER-v7 [111] and the add-on package PERMANOVA+ [112].

Supplementary material

Supplementary materials for this chapter are over 10 pages long, if needed, they would be provided separately.

Chapter 2

Parasites (trematoda: Digenea) of ctenophore *Mnemiopsis leidyi* from the north Adriatic Sea

Gregorio Motta [1,2*], Perla Tedesco [3*], Monica Caffara [3], Maria Letizia Fioravanti [3], Massimo Avian [1], Antonio Terlizzi [1,2], Tjaša Kogovšek [4]

[1]Department of Life Science, University of Trieste, 34127 Trieste, Italy. [2]Department of Integrative Marine Ecology (EMI), Stazione Zoologica Anton Dohrn – Italian National Institute for Marine Biology, Ecology and Biotechnology, 80121 Napoli, Italy. [3]Department of Veterinary Medical Sciences, Alma Mater Studiorum University of Bologna, Ozzano dell'Emilia, 40064 Bologna, Italy.

[4] Independent Researcher, Strunjan 125, 6320 Portorož, Slovenia

*These authors contributed equally to this work.

1. Introduction

Ctenophores have been demonstrated to host a wide range of parasites: cestodes, nematodes, trematodes and amphipods [70,91,113–115].

Digenea (class Trematoda, phylum Platyhelminthes) are common parasites in the marine environment. They have been recorded to infest the gelatinous zooplankton, used as intermediate host during their life cycle, typically made of two intermediate invertebrate hosts and a definitive vertebrate host.

In jellyfish and ctenophores, Digenea act different compared to other hosts. Normally, when the free-swimming cercariae reach the second host, they actively penetrate its tissues, lose the tail and encysts, waiting to be eaten by the definitive host to excyst, mature as adults and reproduce. In gelatinous zooplankton, the cyst stage is missing, the metacercaria is observed already excysted [116].

This unique condition was subject of debate regarding the role of jellyfish and ctenophores for digeneans.

Dollfus [115] reviewed the metacercariae found in jellyfish, declaring unclear their role of true or accidental hosts for parasites. In the same period, Rebec [117] defined gelatinous zooplankton as potential facultative hosts for trematodes. Moreover, excysted conditions also questions the relationship between digeneans and jellyfish, it is unclear if parasites feed on the hosts tissues or they are just a temporary vehicle [118]. On the other hand, other studies reported immediately infective metacercariae isolated from jellyfish. In this case, jellyfish could be considered as true intermediate hosts. Stunkard [46] described *Mnemiopsis leidyi* as true host for *Neopechona pyriforme* (Linton, 1900) unencysted metacercariae. Ctenophore *Pleurobrachia pileus* has been defined as true hosts also for for *Opechona bacillaris* (Cobbold, 1858) [57].

Most of the studies focused on the detection and identification of trematodes, without investigating the number of parasites and potential relations of intensity with body size or environmental parameters.

In recent years, the metacercariae of *Opechona bacillaris* (Molin, 1859) were recorded in *Pleurobrachia pileus* from Galway Bay, western Ireland [91]. Here, data about prevalence (P) were

assessed during three years, ranging to over 40% during summer. Other lepocreadiids, *Opechona* sp, were recorded in *Mnemiopsis mccradyi* Mayer (30% prevalence, 2–20 intensity) in the Argentine Sea [58]. Up to the present day, most of the studies addressing ctenophores-parasites relationships has been spatially limited to south America and Northern Europe [60,91]. No data from the Mediterranean Sea is available.

This study, for the first time, aims to fill this gap about the occurrence of digenean parasites in *Mnemiopsis leidyi,* the most abundant ctenophore in the Mediterranean Sea.

Mnemiopsis leidyi is a native species from North and South America [38]. After its introduction in the Sea of Azov in 1988, *Mnemiopsis leidyi* spread over the eastern Mediterranean Sea. In the last decade, it settled in the Northern Adriatic Sea and France [34], Israel [119], and Spain [120].

The Gulf of Trieste (north Adriatic Sea) is a semi-enclosed basin characterized by an average depth of 20 m over a surface area of 500 km^2 [121]. The water column is widely influenced by seasonality; however, its oceanographic conditions and the abundance of preys may have favored the establishment of *Mnemiopsis leidyi* in the area. Unlike the black Sea, where this species bloomed exponentially, the presence of predators, *Beroe ovata sensu mayer*, *Beroe Cucumis* and *Beroe forskalii*, may had maintained *Mnemiopsis leidyi* populations under control [34].

The knowledge of Ctenophora – parasite dynamics is fundamental to shed light on the potential role of this organisms as carriers of parasites and their trophic interactions with the fish compartment [60]. Particularly, the objectives of this research were to 1) determine infection parameters, prevalence (P) and intensity (I), of metacercariae in *Mnemiopsis leidyi* collected year-round from 2018 to 2021 in three different sites of the North Adriatic Sea: Trieste and Grado Lagoon (Italy) and Piran (Slovenia); 2) identify the parasite species through morphological and molecular analysis; 3) test if infection parameters change in the different areas and different time of the year.

To the authors knowledge, this work is the first attempt to study these parasites dynamics in Mediterranean ctenophores.

2. Materials & Methods

Mnemiopsis leidyi individuals were collected in three sites of the north Adriatic Sea: Grado Lagoon (Italy), Grignano/Trieste (Italy) and Piran (Slovenia) between 2018 and 2020 (Fig. 1).
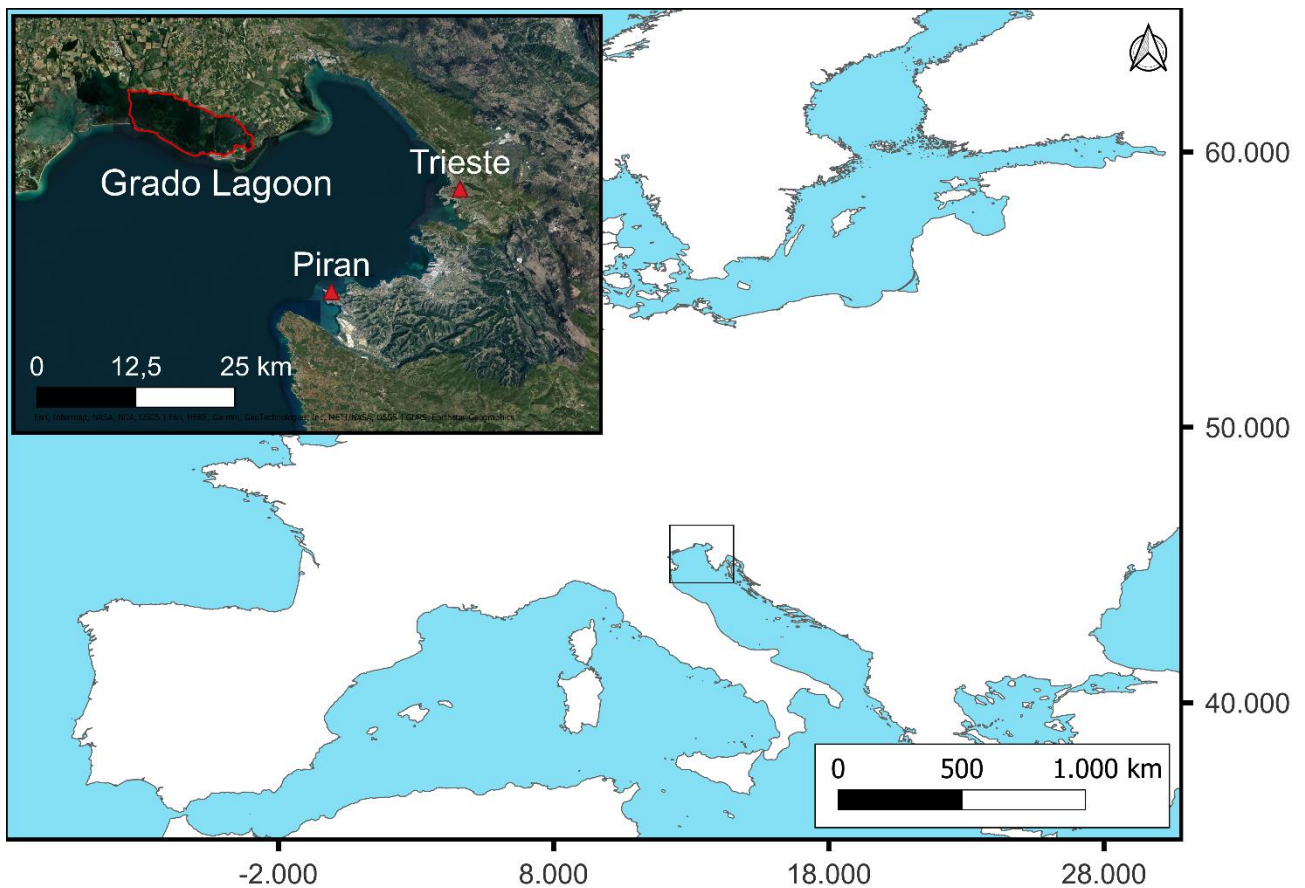

Figure 1. Sampling area of *Mnemiopsis leidyi*.

Ctenophores were collected through diving sessions using containers of adequate size to avoid damages. Samples were brought to the lab and body length was measured with a precision caliper. A total of 324 individuals were collected (Table 1 shows locations, month of sampling and mean body length ± dev std).

Table 1. Year, month of sampling, location and mean body length ± dev std of *Mnemiopsis leidyi*

Year - Month - Site	N° samples	Mean (TBL)	sd(TBL)	Min	Max
2017 – Oct - Piran	13	6.4	1.4	4.2	8.6
2017 – Nov - Piran	10	7.4	1.0	5.9	9.6
2017 – Dec -Piran	7	9.3	1.2	6.9	10.5
2018 – Jul - Piran	5	6.4	1.8	3.8	8.2
2018 – Aug - Piran	24	7.0	1.8	2.5	10.1
2018 – Sep - Piran	11	8.1	1.0	5.8	9.1
2018 – Nov - Piran	54	6.4	2.2	0.4	10.5
2018 – Dec - Piran	18	7.6	1.1	5.4	9.5
2019 – Jan - Piran	13	7.7	1.4	3.9	9.0
2019 – Feb - Piran	15	8.6	1.0	6.9	10.2
2019 – Mar - Piran	10	8.2	1.4	6.5	10.5
2019 – Jul - Piran	9	6.9	2.1	3.4	9.3
2019 – Sep - Grignano	17	5.2	1.4	3.0	8.0
2019 – Oct - Grignano	18	4.8	1.6	0.3	7.0
2019 – Nov - Grignano	12	6.6	1.4	3.9	8.0
2019 – Oct - Lagoon	69	3.5	2.1	0.3	9.0
2021 – Sep - Lagoon	7	5.2	1.2	4.0	7.3
2021 – Nov - Grignano	12	6.8	1.3	5.0	8.6

2.1 Parasite Count

Ctenophores were dissected and the presence of parasites was evaluated under a stereomicroscope (Leica Mz-6). Prevalence (P) and intensity (I) values were defined following Bush et al. [1]. All individuals have not been fixed, since common fixative do not properly work on Ctenophora [122,123].

2.2 Parasite identification

For identification, parasites were extracted from fresh tissues and preserved in 70% or 96% ethanol for molecular analysis and 10% hot formalin for morphological analysis following Cribb & Bray [104]. For morphological analysis, metacercariae were subjected to microscopical observation after clarification in Amman's lactophenol. All measurements were taken with the imaging software Fiji ImageJ [124] and expressed in micrometers, as ranges with mean values in parentheses.

For molecular analysis, genomic DNA was extracted from five metacercariae by PureLink® Genomic DNA Kit (Life Technologies, Carlsbad, CA, USA), following the manufacturer's instructions.

The amplification of the D1-D3 region of 28S rDNA was performed with primers U178_f (5′-GCACCCGCTGAAYTTAAG-3′) and L1642_r (5′-CCAGCGCCATCCATTTTCA-3′) [105], following Gustinelli et al. [106]. The PCR products were electrophoresed on 1% agarose gel stained with SYBR® Safe DNA Gel Stain (Thermo Fisher Scientific, Carlsbad, CA, USA) in 0.5X TBE. All amplicons were purified by NucleoSpin Gel and PCR Cleanup (Mackerey-Nagel, Düren, Germany, CA, USA) and sequenced with an ABI 3730 DNA analyzer (StarSEQ, Mainz, Germany). 28S rDNA amplicons were sequenced with the internal primers 900F (5′-CCGTCTTGAAACACGGACCAAG-3′) and EDC2 (5′-CCTTGGTCCGTGTTTCAAGACGGG-3′) of Lockyer et al. [105].

The DNA trace files were assembled with ContigExpress (VectorNTI Advance 11 software, Invitrogen, Carlsbad, California) and the consensus sequences were compared with previously published data by BLAST tools (https://blast.ncbi.nlm.nih.gov/Blast.cgi). Multiple sequence alignments of the newly generated sequences together with the all the sequences reported by Curran et al. [90], were built by BioEdit 7.2.5 [107]. Pairwise distance, using a Kimura 2-parameter model and maximum likelihood (ML) tree (BIC = GTR + G, bootstrap of 1000 replicates) were obtained by MEGA version X [108].

2.3 Statistical analysis

A generalized linear model (GLM) was applied to assess the potential relationship between Intensity/Length (I/L) ratio (used to normalize infection data, since organisms of similar size were not available for some sampling events), location, and month of sampling. The statistical models were developed under the R statistical environment v.3.6.2 [109], package "stats" [109]. Its specifications were as follows: the I/L ratio has been selected as the response variable, location and month of sampling have been defined as fixed effect. Plots were performed using 'GGplot2' package [110].

A posteriori pair-wise comparisons were performed among locations and months of sampling via package "multcomp" [125] (Table S1)..

3. Results

3.1 Parasite Count

Length, prevalence, and intensity recorded in the three sites in the different months are reported in table 2. Considering all the samples, 2342 parasites have been counted, 1417 in Piran, 560 in Grado Lagoon and 365 in Grignano.

Table 2. Year, month of sampling, location, prevalence and mean intensity ± dev std.

Year - Month - Site	N° samples	P	mean(INT)	sd(INT)	Min	Max
2017 – Oct - Piran	13	100	6.5	3.6	1.0	13.0
2017 – Nov - Piran	10	90	5.9	5.0	0.0	18.0
2017 – Dec -Piran	7	71	6.6	5.5	0.0	13.0
2018 – Jul - Piran	5	100	14.0	10.9	3.0	27.0
2018 – Aug - Piran	24	83	7.3	7.5	0.0	26.0
2018 – Sep - Piran	11	90	6.5	6.9	0.0	20.0
2018 – Nov - Piran	54	77	4.1	5.7	0.0	26.0
2018 – Dec - Piran	18	91	10.4	14.5	0.0	51.0
2019 – Jan - Piran	13	92	4.4	2.9	0.0	10.0
2019 – Feb - Piran	15	100	16.8	14.8	2.0	52.0
2019 – Mar - Piran	10	80	3.3	3.3	0.0	11.0
2019 – Jul - Piran	9	77	17.8	17.7	0.0	47.0
2019 – Sep - Grignano	17	88	3.3	2.6	0.0	9.0
2019 – Oct - Grignano	18	88	5.6	5.0	0.0	20.0
2019 – Nov - Grignano	12	100	9.0	4.6	3.0	19.0
2019 – Oct - Lagoon	69	97	7.1	6.0	0.0	26.0
2021 – Sep - Lagoon	7	100	10.3	8.6	4.0	29.0
2021 – Nov - Grignano	12	100	8.3	5.0	2.0	20.0

Prevalence was considerably high in all areas and month of sampling, 291 ctenophores out of 324 were infected by digeneans. At a first look, without considering seasonality of sampling, intensity showed a positive correlation with body size and no statistical differences have been found in mean intensity in the three areas (Fig. 2-3).
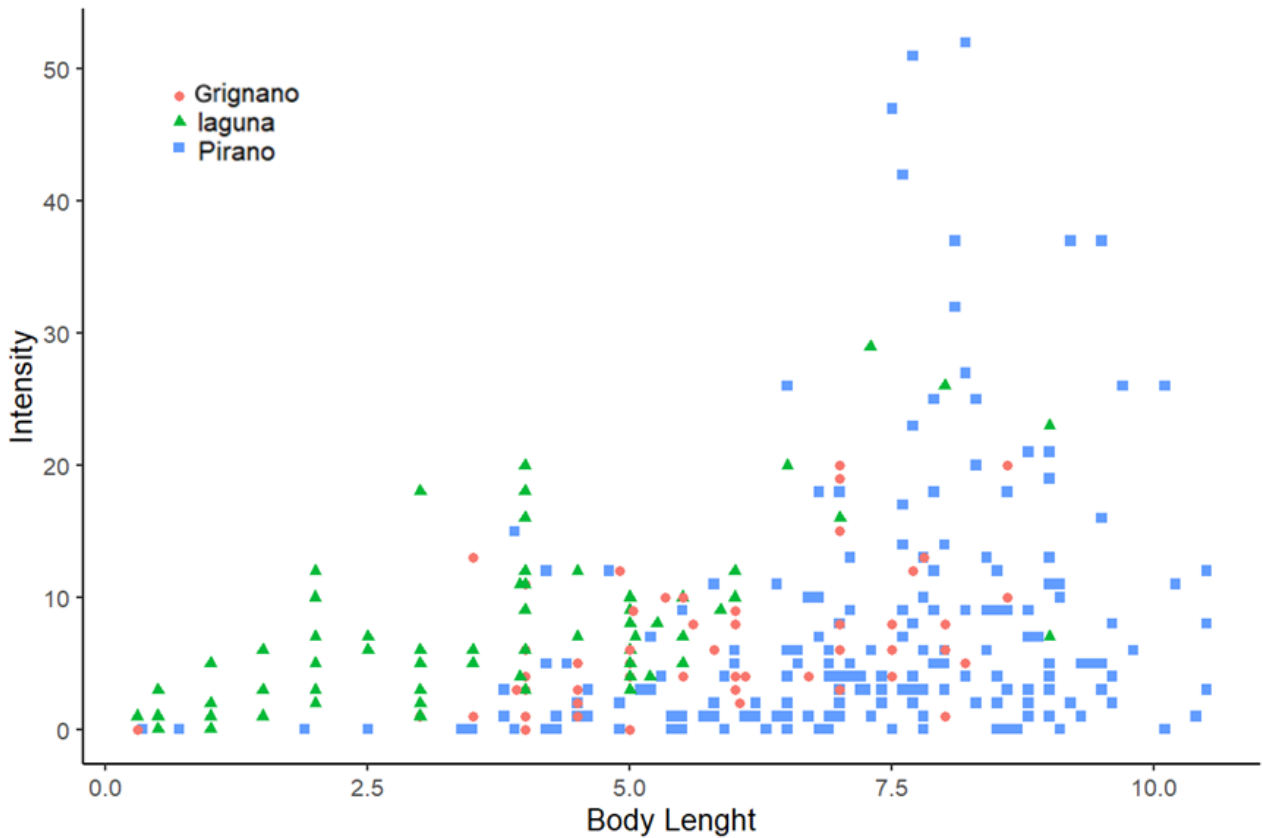
Figure 2. Scatterplot for body length vs intensity in the three areas: red circles, Grignano; green triangles, Grado lagoon; blue squares, Piran.

However, Piran is the site that records the highest values in the months of December 2018 (51) and February 2019 (52), followed by Grado Lagoon and Grignano. On the other hand, based on the Intensity/body length (I/L) ratio (Fig. 3), the highest values are observed in Grado Lagoon, with similar values between Piran and Grignano.
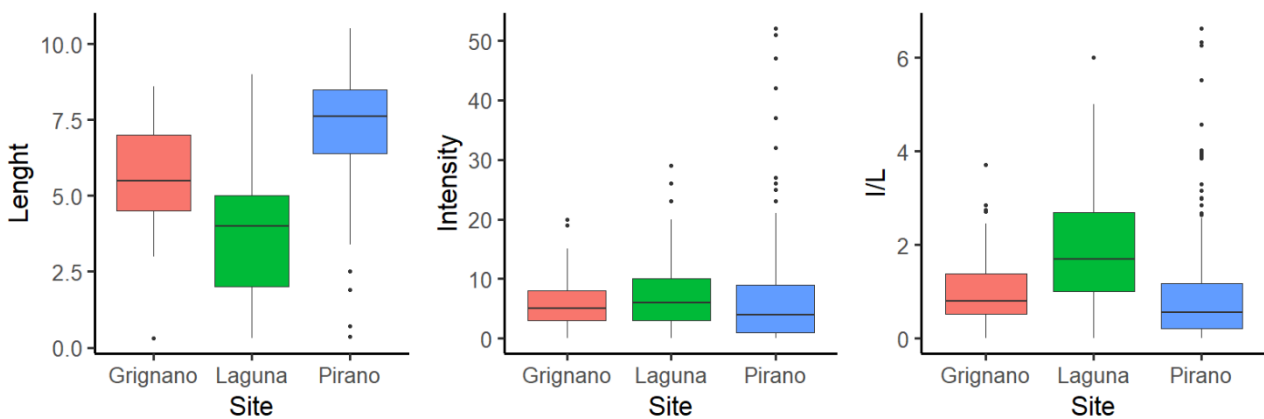

Figure 3. Boxplot of length, intensity and I/L ratio in the three areas.

Along the year (Fig. 4), different trends are observed in the three locations. In Piran, the mean intensity remains almost constant, with the exception of the three peaks recorded in February 2018 and both July 2017 and 2018. In Grignano and Grado Lagoon intensity grows overtime from September to November. This trend is even more highlighted by the I/L ratio, confirming higher parasite density in lagoon individuals.
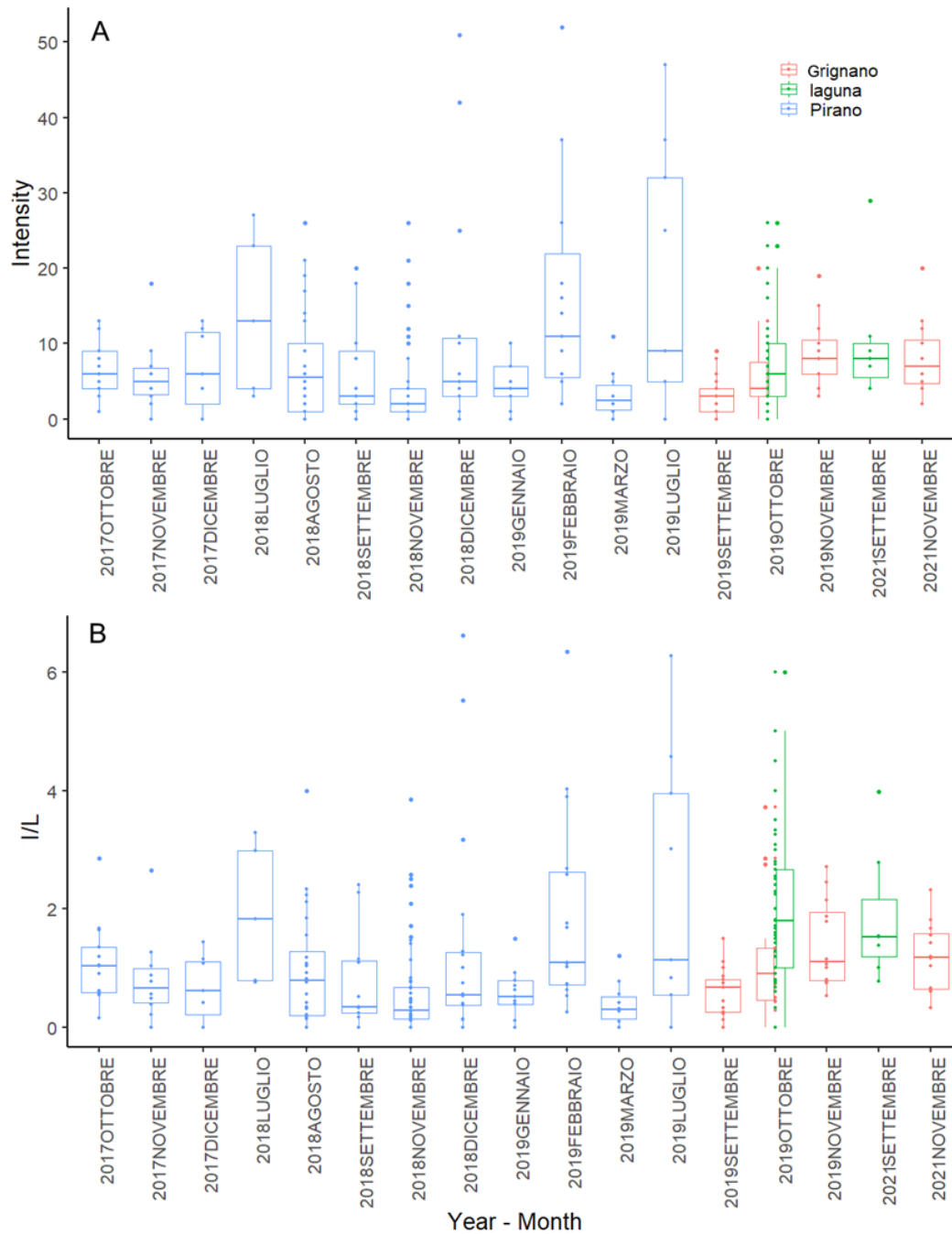

Figure 4. Boxplot of Intensity **(a)** and I/L ratio **(b)** in the three areas (see legend) for each sampling month and year. For each plot, the thick horizontal line represents the median of the distribution, the

box includes 50% of the data, and the whiskers reach the highest and lowest value within 75% of the distribution. Open circles represent single values outside 75% of the distribution.

3.2 Statistical analysis

Model outputs showed that the number of parasites is influenced by both ctenophore length, location and month of sampling. Formulas, coefficients, goodness of fit R2 and P values are reported in Table 3.

Table 3. Generalized linear model (GLM) coefficients (intercept and treatment), p value and variance explained (R2) for log(intensity) (response variable) vs Location and month of sampling (fixed effect) and Anova table.

Predictors	Estimates	CI	p	df
(Intercept)	0.47	-0.03 – 0.98	0.067	312.00
TBL	0.25	0.20 – 0.30	**<0.001**	312.00
luogo [laguna]	0.44	0.12 – 0.75	**0.008**	312.00
luogo [Pirano]	-0.57	-0.84 – -0.30	**<0.001**	312.00
Mese [DICEMBRE]	-0.14	-0.58 – 0.29	0.520	312.00
Mese [FEBBRAIO]	0.54	0.03 – 1.04	**0.038**	312.00
Mese [GENNAIO]	-0.31	-0.84 – 0.21	0.242	312.00
Mese [LUGLIO]	0.73	0.22 – 1.25	**0.005**	312.00
Mese [MARZO]	-0.76	-1.33 – -0.18	**0.010**	312.00
Mese [NOVEMBRE]	-0.19	-0.55 – 0.17	0.301	312.00
Mese [OTTOBRE]	0.07	-0.37 – 0.50	0.765	312.00
Mese [SETTEMBRE]	-0.33	-0.76 – 0.11	0.145	312.00
Observations	324			
R^2	0.320			
Anova Table				

Column1	Df	Deviance	Resid. Df	Resid. Dev	Pr(>Chi)
NULL			323	278.30	
TBL	1	29.029	322	250.27	8.047e-12 ***
luogo	2	38.72	320	211.54	9.404e-15 ***
Mese	8	24.50	312	187.04	2.206e-06 ***

A posteriori pair wise test showed differences in INT and I/L in the different areas and in the different times of the year (table S1-3).

3.3 Parasite identification

The morphological analyses allowed to assign all the unencysted metacercariae analyzed to the family Lepocreadiidae. Their morphology (Fig. 5) was consistent with the description of metacercariae of the genus *Clavogalea* Bray (1985) as described by Bray and Gibson [83] and fitted with the measures provided by Motta et al. (present study) in *Rhizostoma pulmo* (Table 4).
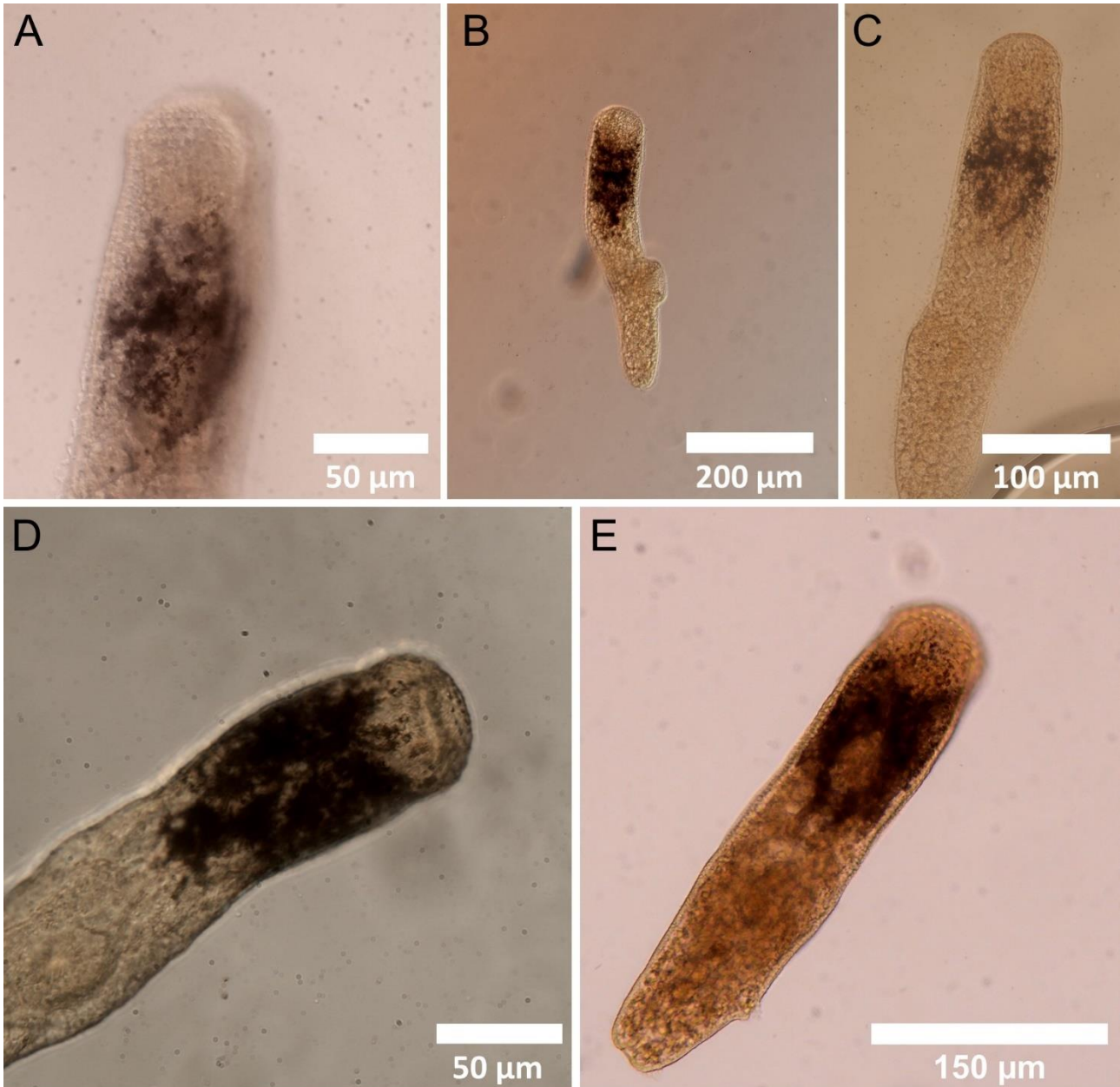
Figure 5. Lepocreadiid metacercariae from *Mnemiopsis leidyi* (**a-d**), *Rhizostoma pulmo* **(e)** (from Motta et al.), light microscopy. (**a-c-d**) anterior region showing double rows of oral spines characteristic of the genus *Clavogalea.*

Table 4. Measurements (µm) and ratios of Digenea specimens from *Rhizostoma pulmo* and *Mnemiopsis leidyi*.

Anatomical measures	Species	
	Clavogalea sp.	Metacercariae
Mean(min-max) µm	*Rhizostoma pulmo*	*Mnemiopsis leidyi*
Body Length	215.4 - 461.6 (336.5)	254.1-448.2 (364.6)
Body Width	54.8 - 107.6 (81.6)	53.0-90.5 (76.8)
Oral sucker Length	45.6 - 71.5 (60)	41.0-71.0 (58.8)
Oral sucker Width	44.7 - 80.4 (55.9)	28.7-68.1 (51.6)
Ventral sucker Length	40.9 - 63.0 (51.5)	30.5-66.4 (51.1)
Ventral sucker Width	42.1 - 69.8 (54.0)	33.4-60.5 (49.0)
Pharynx Length	36.5 - 40.5 (39.0)	28.4-46.6 (35.7)

4. Discussion

Ctenophora parasites, and especially Digenea metacercariae, have not been properly addressed by the scientific community and data on their occurrence are scarce [70,91]. This study, for the first time, tried to fill the gap about Digenea dynamics in Mediterranean ctenophores. Together with Motta et al. (2022, in press), who observed Digenea metacercariae in *Rhizostoma pulmo* (scyphomedusae), this is the first record of Ctenophora as second intermediate hosts for trematodes in the Adriatic Sea.

All areas showed high prevalence of parasites in every month of sampling (87.5 Piran, 94 Grignano, 98.5 Grado Lagoon), therefore this species show a noticeable tolerance for environmental conditions (water temperature range between about 9.2°C during winter and about 25°C during summer [126]). At the same time, prevalence suggests that *Mnemiopsis leidyi* is an important host for *Clavogalea* sp. all year round.

Clavogalea sp. has been recorded once in gelatinous zooplankton in the Adriatic Sea, infecting *Rhizostoma pulmo* (Motta, 2022). This genus, erected by Bray [88], is characterized by enlarged oral spines while its other features are very similar to *Opechona* sp. [89]. In the fish host, no observations are available for *Clavogalea* genus in the Mediterranean Sea, adult stages have been described only in *Trachinotus botla* from south Africa and *Clavogalea trachinoti* (synonymized with *Stephanostomum trachinoti* Fischthal & Thomas, 1968, and *Opechona pseudobacillaris* Fischthal & Thomas, 1970 [89] from Australia).

Comparing the different places and time of sampling, the highest densities (I/L) have been recorded in Grado Lagoon, while the highest intensities have been measured in February and July in Piran. In the three areas, *Clavogalea* sp. intensity increase also in relation with *Mnemiopsis leidyi* body length. This has already been reported in other studies on north Adriatic jellyfish (Motta et al., 2022) and it is in line with Yip [91], who theorized that bigger and older individuals are characterized by wider body surfaces and longer times of exposure for intercept and being parasitized by swimming cercariae.

Infection in the second intermediate host for digeneans is also related to cercaria release from the first hosts (commonly benthic gastropods) and to the characteristics of the areas, which may favor or penalize parasite transmission to the second intermediate hosts.

Piran and Grignano share similar environments in the Gulf of Trieste, this may support the similar numbers observed in the same months of sampling, with the exception of November-Piran 2021, which is slightly higher compared to November 2017/18 in Piran. Differently, in the same period, Grado Lagoon record the highest values of parasite density (I/L). While Grignano and Pirano bays are open basins, Grado Lagoon is a semi-closed area where parasite can scarcely scatter. This factor, along with lagoon shallow waters may provide a more prone environment for parasite-jellyfish encounter. Several anthropic activities taking place in Grado (commercial suction dredge fishing, shellfish production, touristic maritime traffic) are responsible to a significant increase in water turbulence, another factor that may favor the dispersion of cercariae in the water column.

No records of lepocreadiid first hosts and sporocysts or cercariae in benthic gastropods are available from the three areas. According to literature, the family Nassaridae could host digeneans

leporeadidids, *Opechona* sp. cercariae have been observed in *Nassarius pygmaeus* from Scandinavia [57], *Stephanostomum*-like cercariae from Australian Nassaridae [97], and Lepocreadiids, probably *Opechona* sp., were identified in *Buccinanops cochlidium* from Argentina [96]. In the north Adriatic, this family is present with two species, *Tritia mutabilis* and *Tritia varicosa* [98,99], typically found in fine sands and fine muddy sands between 2 and 15 m depth [100].

Seasonal fluctuations may be linked to the release of free swimming cercariae from the benthic gastropod, theorized to happen during the host spawning peak in cold months and in the months with highest temperature [96,127]. The intensity peaks observed during February and July in Piran may be related to a recent spawning event of these species. Cocci et al. [128] defines February as the start of *Tritia mutabilis* spawning period in the north Adriatic. Similarly, Polidori et al. [99] state that spawning occurs in late winter, early spring, thus matching the peak observed in February. The presence of parasites during the other months may be related to the increase of water temperature, peaking its maximum in July in the north Adriatic (Ispra, 2021). However, gastropods spawning does not happen once, Mallet et al. [129] found immature females with ongoing oogenesis between October and November, suggesting the occurrence of another reproductive period in late autumn. This could support the increase in intensity observed in Grignano and Grado Lagoon between September and November.

Comparing our results with the only two studies which addressed ctenophores lepocreadiids, a noticeable difference in both intensity and prevalence stands out. Morandini et al. [70] recorded 12.5% P and 1-6 intensity range in 48 *Mnemiopsis mccrady* and 80% prevalence and 1-13 intensity range in 5 *Beroe* sp. from southeastern Brazil. No information of ctenophore length is given. Yip [91] recorded about 10% prevalence and 1-5 intensity range in *Pleurobrachia pileus* from Western Ireland. The north Adriatic Sea is a semi-enclosed basin, and the Gulf of Trieste is located at its deeper site, thus it can act as a better sink site for free swimming cercariae compared to the Irish and Brazilian coasts, exposed to the open ocean. Another important factor is the abundance of the first hosts but, even if Nassaridae are generally present in shallow waters in tropical and temperate latitudes [130], data of presence and abundance of digeneans in Brazilian and Irish gastropods are scarce [96]. Similarly, no

records of lepocreadiids in gastropods are available from the north Adriatic Sea but, there, *Tritia* gastropods are an important commercial species, and their presence is monitored. In the north Adriatic, even if recently declining due to overfishing, *Tritia* mollusks are abundant [98] and they may be a potential source for cercariae infesting ctenophores in the area.

As for the first hosts, no final hosts of *Clavogalea* sp. have been found in the north Adriatic. Similarly, no records of fish eating ctenophores are available for the area. In literature, *Mnemiopsis leidyi* principal predators are other Ctenophora of *Beroe* genus [131], present in north Adriatic as *Beroe ovata sensu mayer*, *Beroe forskalii* and *Beroe cucumis* [34]. The fish-Ctenophora predation dynamics are still uncertain, even if gelatinous zooplankton was erroneously considered as a scarce energy source for the fish compartment, studies confirmed that it can be significant part of fish diet when other sources are lacking [76,132,133].

Surprisingly, ctenophores have been demonstrated to be also potential preys for herbivores [134]. The rabbithfish *Siganus rivulatus* (Siganidae) and surgeonfish *Zebrasoma desjardinii* (Acanthuridae) actively selected and fed until disintegration on local ctenophores [134]. However, to date, predatory interactions between fish and ctenophores, and the role of Ctenophora as parasite transmitters, are scarcely known and they have to be properly clarified [75]. The high values of prevalence registered in this study in all the three areas suggest that Ctenophora are true and not accidental intermediate host of lepocreadiid digeneans, fundamental for their life cycle in the north Adriatic Sea. As already reported by Motta (2022) for *Rhizostoma pulmo*, also *Mnemiopsis leidyi* could be common part of the diet of fish, since trophic interactions are needed for *Clavogalea* sp. individuals to close their cycles. Furthermore, it would be interesting to investigate the role of beroids. As mentioned, *Beroe* species diet exclusively rely on other ctenophores, in particular lobata such as *Mnemiopsis leidyi* [131,135,136]. The three species of the north Adriatic, *Beroe ovata sensu mayer*, *Beroe forskalii* and *Beroe cucumis* [34], could act as a "second" second intermediate host or, being one trophic level above, as a concentrator of parasites (in a similar mechanism of pollutants biomagnification). It could also be that digeneans are not adapted to beroids and do not colonize their bodies after *Mnemiopsis leidyi* host tissues digestion. In this case, Beroida could be a dead-end of digeneans life cycles. Similarly,

to date, no data about Beroida predators are available, only one study found Beroida-like tissues in cod stomachs, together with other preys. Even in this case, with no known predators, Beroida could be a dead-end again.

As a conclusion, addressing predation over gelatinous plankton with traditional methods is challenging due to the scarce durability of their tissues in fish stomachs [39,137]. The presence of parasites can be another way to assess these dynamics, integrating traditional trophic ecology protocols. However, the picture about gelatinous plankton parasites is still incomplete and several topics have to be addressed such as their complete life cycle (host species and potential effects on them) and the differences in infection patterns between other gelatinous zooplankton species in the north Adriatic Sea.

Supplementary materials

Table S1. Pairwise comparison among locations for intensity as dependent variable (upper table) and

I/L as dependent variable (lower table)

```
          Simultaneous Tests for General Linear Hypotheses

Multiple Comparisons of Means: Tukey Contrasts


Fit: glm(formula = log(INT) ~ TBL + luogo + Mese, family = gaussian(link = identity),
    data = TM2)

Linear Hypotheses:
                      Estimate Std. Error z value Pr(>|z|)
laguna - grignano == 0    0.4351     0.1632   2.666   0.0205 *
Pirano - grignano == 0   -0.5715     0.1393  -4.102   <0.001 ***
Pirano - laguna == 0     -1.0066     0.1786  -5.636   <0.001 ***
---
Signif. codes:  0 '***' 0.001 '**' 0.01 '*' 0.05 '.' 0.1 ' ' 1
(Adjusted p values reported -- single-step method)

> summary(glht(fit3, mcp(luogo="Tukey")))

          Simultaneous Tests for General Linear Hypotheses

Multiple Comparisons of Means: Tukey Contrasts


Fit: glm(formula = log(TL) ~ luogo + Mese, family = gaussian(link = identity),
    data = TM2)

Linear Hypotheses:
                      Estimate Std. Error z value Pr(>|z|)
laguna - grignano == 0   0.31227    0.08759   3.565  0.00101 **
Pirano - grignano == 0  -0.19577    0.07552  -2.592  0.02550 *
Pirano - laguna == 0    -0.50804    0.09303  -5.461  < 0.001 ***
---
Signif. codes:  0 '***' 0.001 '**' 0.01 '*' 0.05 '.' 0.1 ' ' 1
(Adjusted p values reported -- single-step method)
```

Table S2. Pairwise comparison among months of sampling for intensity as dependent variable

```
Multiple Comparisons of Means: Tukey Contrasts


Fit: glm(formula = log(INT) ~ TBL + luogo + Mese, family = gaussian(link = identity),
    data = TM2)

Linear Hypotheses:
                          Estimate Std. Error z value Pr(>|z|)
DICEMBRE - AGOSTO == 0    -0.14355    0.22280  -0.644   0.9992
FEBBRAIO - AGOSTO == 0     0.53800    0.25764   2.088   0.4603
GENNAIO - AGOSTO == 0     -0.31295    0.26718  -1.171   0.9582
LUGLIO - AGOSTO == 0       0.73492    0.26049   2.821   0.1011
MARZO - AGOSTO == 0       -0.75575    0.29289  -2.580   0.1816
NOVEMBRE - AGOSTO == 0    -0.18895    0.18229  -1.037   0.9801
OTTOBRE - AGOSTO == 0      0.06616    0.22104   0.299   1.0000
SETTEMBRE - AGOSTO == 0   -0.32634    0.22333  -1.461   0.8619
FEBBRAIO - DICEMBRE == 0   0.68155    0.25315   2.692   0.1395
GENNAIO - DICEMBRE == 0   -0.16940    0.26491  -0.639   0.9993
LUGLIO - DICEMBRE == 0     0.87847    0.26064   3.370   0.0198 *
MARZO - DICEMBRE == 0     -0.61219    0.28972  -2.113   0.4435
NOVEMBRE - DICEMBRE == 0  -0.04540    0.18219  -0.249   1.0000
OTTOBRE - DICEMBRE == 0    0.20971    0.22373   0.937   0.9896
SETTEMBRE - DICEMBRE == 0 -0.18279    0.22274  -0.821   0.9958
GENNAIO - FEBBRAIO == 0   -0.85095    0.29413  -2.893   0.0836 .
LUGLIO - FEBBRAIO == 0     0.19692    0.29129   0.676   0.9989
MARZO - FEBBRAIO == 0     -1.29375    0.31621  -4.091   <0.01 **
NOVEMBRE - FEBBRAIO == 0  -0.72695    0.22375  -3.249   0.0293 *
OTTOBRE - FEBBRAIO == 0   -0.47184    0.25976  -1.816   0.6516
SETTEMBRE - FEBBRAIO == 0 -0.86434    0.25764  -3.355   0.0212 *
LUGLIO - GENNAIO == 0      1.04787    0.29923   3.502   0.0125 *
MARZO - GENNAIO == 0      -0.44279    0.32591  -1.359   0.9044
NOVEMBRE - GENNAIO == 0    0.12400    0.23418   0.529   0.9998
OTTOBRE - GENNAIO == 0     0.37911    0.26697   1.420   0.8802
SETTEMBRE - GENNAIO == 0  -0.01339    0.26709  -0.050   1.0000
MARZO - LUGLIO == 0       -1.49067    0.32269  -4.620   <0.01 ***
NOVEMBRE - LUGLIO == 0    -0.92388    0.22593  -4.089   <0.01 **
OTTOBRE - LUGLIO == 0     -0.66876    0.25752  -2.597   0.1752
SETTEMBRE - LUGLIO == 0   -1.06126    0.26030  -4.077   <0.01 **
NOVEMBRE - MARZO == 0      0.56679    0.26339   2.152   0.4167
OTTOBRE - MARZO == 0       0.82190    0.29391   2.796   0.1077
SETTEMBRE - MARZO == 0     0.42940    0.29286   1.466   0.8600
OTTOBRE - NOVEMBRE == 0    0.25511    0.16056   1.589   0.7962
SETTEMBRE - NOVEMBRE == 0 -0.13739    0.16405  -0.837   0.9951
SETTEMBRE - OTTOBRE == 0  -0.39250    0.17102  -2.295   0.3262
---
Signif. codes:  0 '***' 0.001 '**' 0.01 '*' 0.05 '.' 0.1 ' ' 1
(Adjusted p values reported -- single-step method)
```

Table S3. Pairwise comparison among months of sampling for I/L as dependent variable

```
            Simultaneous Tests for General Linear Hypotheses

Multiple Comparisons of Means: Tukey Contrasts


Fit: glm(formula = log(TL) ~ luogo + Mese, family = gaussian(link = identity),
    data = TM2)

Linear Hypotheses:
                            Estimate Std. Error z value Pr(>|z|)
DICEMBRE - AGOSTO == 0       0.02980    0.12148   0.245  1.00000
FEBBRAIO - AGOSTO == 0       0.37447    0.13991   2.677  0.14527
GENNAIO - AGOSTO == 0       -0.15328    0.14638  -1.047  0.97885
LUGLIO - AGOSTO == 0         0.39457    0.14295   2.760  0.11802
MARZO - AGOSTO == 0         -0.27011    0.15999  -1.688  0.73672
NOVEMBRE - AGOSTO == 0      -0.11018    0.10003  -1.101  0.97109
OTTOBRE - AGOSTO == 0       -0.03445    0.12029  -0.286  1.00000
SETTEMBRE - AGOSTO == 0     -0.19695    0.12261  -1.606  0.78657
FEBBRAIO - DICEMBRE == 0     0.34467    0.13883   2.483  0.22555
GENNAIO - DICEMBRE == 0     -0.18308    0.14535  -1.260  0.93660
LUGLIO - DICEMBRE == 0       0.36477    0.14189   2.571  0.18573
MARZO - DICEMBRE == 0       -0.29991    0.15905  -1.886  0.60346
NOVEMBRE - DICEMBRE == 0    -0.13998    0.09851  -1.421  0.88001
OTTOBRE - DICEMBRE == 0     -0.06425    0.11904  -0.540  0.99980
SETTEMBRE - DICEMBRE == 0   -0.22675    0.12137  -1.868  0.61532
GENNAIO - FEBBRAIO == 0     -0.52775    0.16107  -3.276  0.02696 *
LUGLIO - FEBBRAIO == 0       0.02011    0.15796   0.127  1.00000
MARZO - FEBBRAIO == 0       -0.64457    0.17354  -3.714  0.00589 **
NOVEMBRE - FEBBRAIO == 0    -0.48464    0.12051  -4.022  0.00166 **
OTTOBRE - FEBBRAIO == 0     -0.40892    0.13780  -2.968  0.06807 .
SETTEMBRE - FEBBRAIO == 0   -0.57142    0.13982  -4.087  0.00126 **
LUGLIO - GENNAIO == 0        0.54785    0.16372   3.346  0.02111 *
MARZO - GENNAIO == 0        -0.11683    0.17880  -0.653  0.99916
NOVEMBRE - GENNAIO == 0      0.04310    0.12797   0.337  0.99999
OTTOBRE - GENNAIO == 0       0.11883    0.14436   0.823  0.99568
SETTEMBRE - GENNAIO == 0    -0.04367    0.14630  -0.298  1.00000
MARZO - LUGLIO == 0         -0.66468    0.17600  -3.777  0.00470 **
NOVEMBRE - LUGLIO == 0      -0.50475    0.12403  -4.070  0.00155 **
OTTOBRE - LUGLIO == 0       -0.42903    0.14088  -3.045  0.05442 .
SETTEMBRE - LUGLIO == 0     -0.59152    0.14286  -4.140  0.00109 **
NOVEMBRE - MARZO == 0        0.15993    0.14334   1.116  0.96872
OTTOBRE - MARZO == 0         0.23565    0.15815   1.490  0.84838
SETTEMBRE - MARZO == 0       0.07316    0.15991   0.457  0.99994
OTTOBRE - NOVEMBRE == 0      0.07572    0.08719   0.869  0.99376
SETTEMBRE - NOVEMBRE == 0   -0.08677    0.09003  -0.964  0.98755
SETTEMBRE - OTTOBRE == 0    -0.16250    0.09262  -1.754  0.69369
---
Signif. codes:  0 '***' 0.001 '**' 0.01 '*' 0.05 '.' 0.1 ' ' 1
(Adjusted p values reported -- single-step method)
```

Chapter 3

Digeneans of infrequent gelatinous zooplankters (Scyphozoa – Hydrozoa – Cubozoa) from the Gulf of Trieste

Gregorio Motta [1,2*], Monica Caffara [3], Maria Letizia Fioravanti [3], Massimo Avian [1], Antonio Terlizzi [1,2], Perla Tedesco [3]

[1]Department of Life Science, University of Trieste, 34127 Trieste, Italy.

[2]Department of Integrative Marine Ecology (EMI), Stazione Zoologica Anton Dohrn – Italian National Institute for Marine Biology, Ecology and Biotechnology, 80121 Napoli, Italy.

[3]Department of Veterinary Medical Sciences, Alma Mater Studiorum University of Bologna, Ozzano dell'Emilia, 40064 Bologna, Italy.

1. Introduction

Aurelia aurita, *Aequorea forskalea*, *Cothyloriza tubercolata, Chrysaora hysoscella* and *Carybdea marsupialis* are common species of the Gulf of Trieste but their presence is stochastic and hugely influenced by seasonality [138]. *Aequorea forskalea* (Hydrozoa) and *Aurelia aurita* (Scyphozoa) usually spawn in the same period, between February and June [138]. *Aequorea forskalea* usually disappear at the beginning of summer, while *Aurelia aurita* is still present during the season. On the other hand, *Carybdea marsupialis* is mainly present during summer and the majority of individuals are observed in Grado lagoon, suggesting the preference of this species for warmer waters [132,139]. *Chrysaora hysoscella* is rare in the north Adriatic Sea nowadays, even if coastal blooms during spring (1989) of this species were observed in the Gulf of Trieste [140]. Last, *Cothyloriza tubercolata* is the rarest species of ones above, spawning during spring/summer [138]. As in the two previous chapters, parasites of these species have been studied in a few works, from South America [60,70,141] and Japan [63]; no data about Mediterranean jellyfish is available.

Their random presence in the Gulf of Trieste made the sampling of a consistent number of specimens really hard. One of the major issues in gelatinous zooplankton research (exacerbated with rare and random spawning species) is being in the right place at the right moment. Without the possibility of being at Sea every day (that is the case of this PhD), the likelihood of encounter with these species was limited. That is why these species have been omitted, for the moment, in submitted papers, waiting to have a more robust dataset. However, these data are all first records of digeneans in these species in the Mediterranean Sea, and they can give useful hints to understand these parasites dynamics in gelatinous zooplankton in the north Adriatic Sea.

2. Materials and methods.

Aurelia aurita, *Aequorea forskalea*, *Cothyloriza tubercolata* and *Carybdea marsupialis* (Fig. 1) individuals were collected in two sites of the north Adriatic Sea: Grado Lagoon (Italy) and Grignano/Trieste (Italy). A total of 113 individuals were collected (Table 1 shows locations and month of sampling for each species).
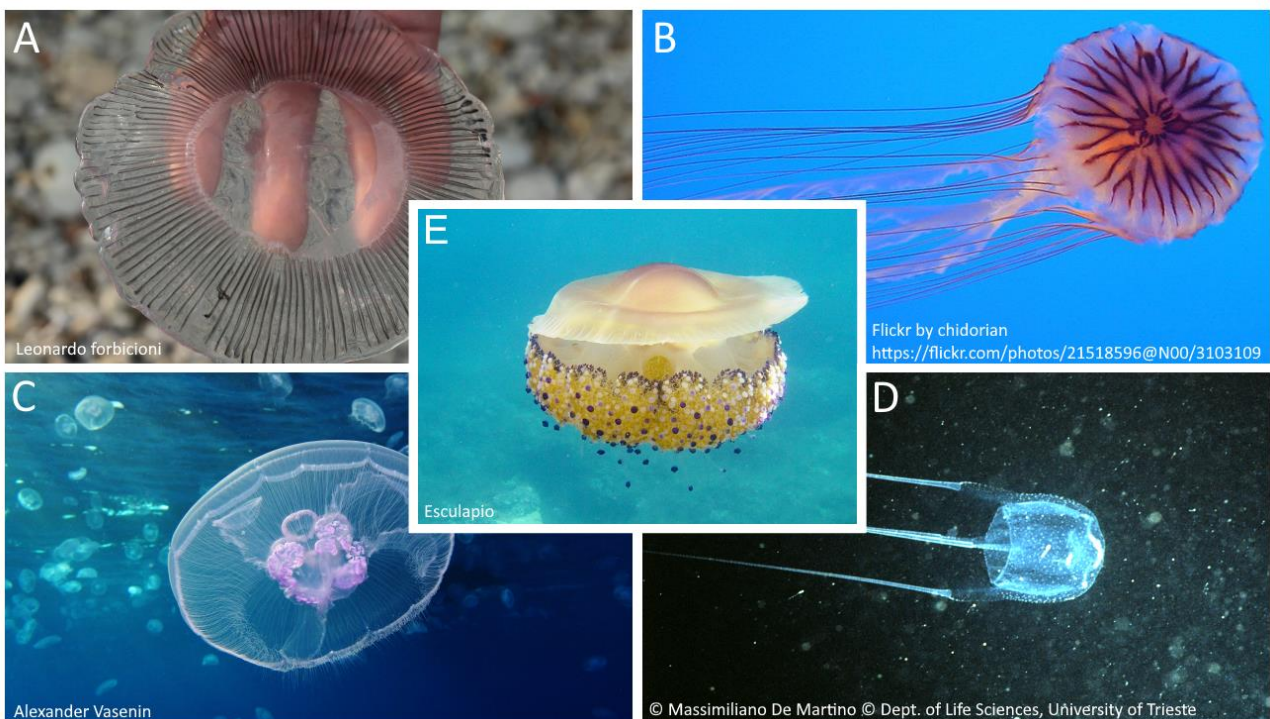
Figure 1. Species collected in the Gulf of Trieste. **(a)** *Aequorea forskalea*; **(b)** *Chrysaora hysoscella*; **(c)** *Aurelia aurita*; **(d)** *Carybdea marsupialis*; **(e)** *Cothyloriza tubercolata*.

Table 1. Locations, month of sampling and number of organisms collected for each species

Species	Location	Date of sampling	N° samples
Aurelia aurita	Grignano	12/02/2020	69
		28/04/2020	
		01/06/2020	
		09/07/2020	
		21/07/2020	
		27/07/2020	
		02/07/2021	
Aequorea forskalea	Grignano	2017	35
		12/02/2020	
		27/07/2020	
		25/03/2021	
		26/03/2021	
Cothyloriza tubercolata	Trieste	07/09/2020	3
Carybdea marsupialis	Grado Lagoon	28/07/2021	5
Chrysaora hysoscella	Trieste	2019	1

2.1 Parasite count and identification

Methods of sampling, sample processing, dissection and identification are the same of the ones reported in the two papers above for *Rhizostoma pulmo* and *Mnemiopsis leidyi*, therefore they will not be reported again to avoid redundancy for the reader.

2.2 Statistical analysis

A generalized linear model (GLM) was applied to assess the potential relationship between intensity, jellyfish diameter and month of sampling for *Aurelia aurita*; and a linear model (LM) was applied to assess the potential relationship between intensity, jellyfish diameter and month of sampling (taking in consideration we have only two sampling events) for *Aequorea forskalea*. The statistical models

were developed under the R statistical environment v.3.6.2 [109], package "stats" (version 3.6.2) [109].

Their specifications were as follows: intensity has been selected as the response variable, diameter and month of sampling have been defined as fixed effects. When significant, a posteriori pair-wise comparisons were performed among months of sampling via package "multcomp" [125] (Table S1). Plots were performed using 'GGplot2' package [110]. Tables were made with sjPlot (version 2.8.10) [142].

3. Results

3.1 Parasite count

All jellyfish species presented parasites (Table 2). Except for *Aurelia aurita* (0.65 prevalence), the other jellyfish samples were all parasitized by digeneans. The highest intensities have been observed in *Aurelia aurita* (256) and *Aequorea forskalea* (412) (Table 2, Fig. 2). *Carybdea marsupialis* and *Chrysaora hysoscella* showed the lowest mean intensities (1.3 and 10, respectively), *Cothyloriza tuberculata* recorded 48 mean intensity, but its size was 4-5 times bigger compared to the other species (Fig. 2).
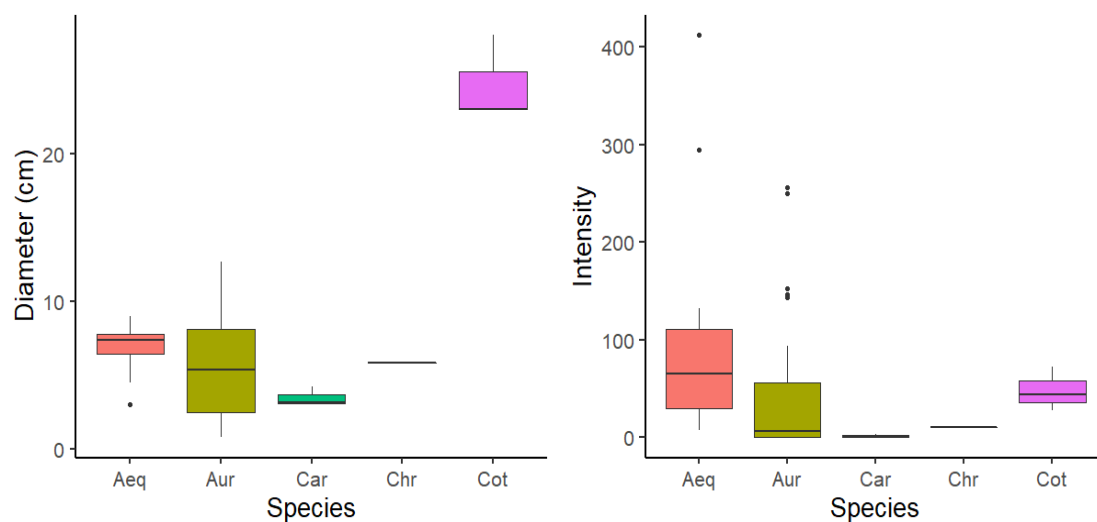
Figure 2. Boxplot of Diameter **(a)** and intensity **(b)** for all the species sampled: *Aequorea forskalea* (red); *Aurelia aurita* (light green); *Carybdea marsupialis* (dark green); *Chrysaora hysoscella* (black); *Cothyloriza tubercolata* (purple).

Table 2. Number of samples, size, prevalence and mean, min and max intensity ± dev std for each species collected.

Species	N° samples	Mean diameter (cm)	Prevalence	Mean Intensity	Sd Intensity	Min Intensity	Max Intensity
Aurelia aurita	69	5.8	0.65	36.66	55.38	0	256
Aequorea forskalea	35	6.84	1	82.4	79.47	7	412
Cothyloriza tubercolata	3	24.66	1	48	22.27	28	72
Carybdea marsupialis	5	3.44		1.2	1.3	0	3
Chrysaora hysoscella	1	5.87	1	10	0	10	10

As mentioned, the dataset for these species is not robust since their presence is stochastic in the Gulf of Trieste.

Only *Aurelia aurita* and *Aequorea forskalea* results will be reported, being the only species with a sufficient number of observations.

At a first sight, showed a positive relation with body size in both *Aurelia aurita* and *Aequorea forskalea* (Fig. 3).
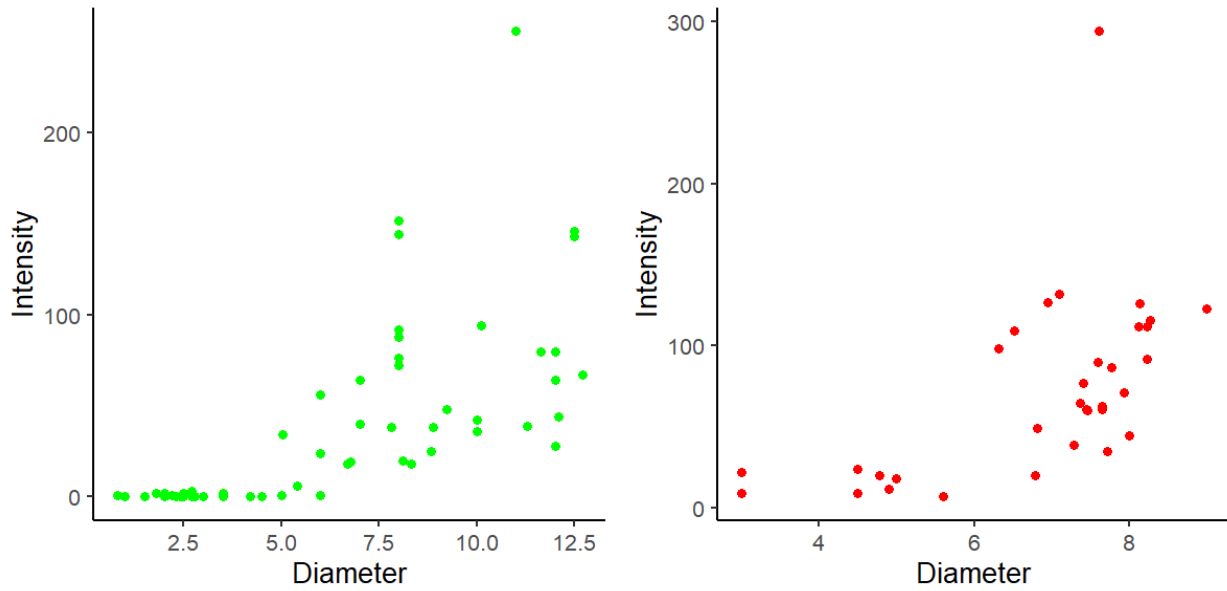
Figure 3. Scatterplot for intensity vs diameter for *Aurelia aurita* (green) and *Aequorea forskalea* (red).

If we take in consideration the variations due to seasonality, it was not possible to measure statistically significant effects for *Aequorea forskalea*, whose intensity seems to be mainly driven by the dimension of the jellyfish (Table 3). The conditional is due to the lack of similar size *Aequorea forskalea* in the two sampling events, making it impossible to assess the real effect of size and seasonality in parasite intensity (Fig. 4).

Table 3. GLM summary for *Aequorea forskalea.*

Predictors	Estimates	CI	p	df
(Intercept)	-65.41	-111.62 – -19.21	**0.007**	26.00
Diam ombr	21.71	11.82 – 31.60	**<0.001**	26.00
mese [MAR]	-20.15	-66.33 – 26.02	0.378	26.00
mese []	-44.20	-99.16 – 10.75	0.110	26.00
Observations	30			
R^2 / R^2 adjusted	0.600 / 0.554			

Anova Table					
Column1	Df	Sum sq	Means q	F value	Pr(>F)
Diameter	1	26016	26015.8	36.14	2.388e-06 ***
Mese	2	2034	1017	1.41	0.26
Residuals	26	18715	719.8		

Differently, it is more evident the effect of seasonality on parasite intensity in *Aurelia aurita* (Fig. 4, Table 4-S1). Jellyfish sampled in May are way bigger compared to July samples, but their intensity is lower. Similarly, samples from February and April, the colder months, record the lowest intensities.
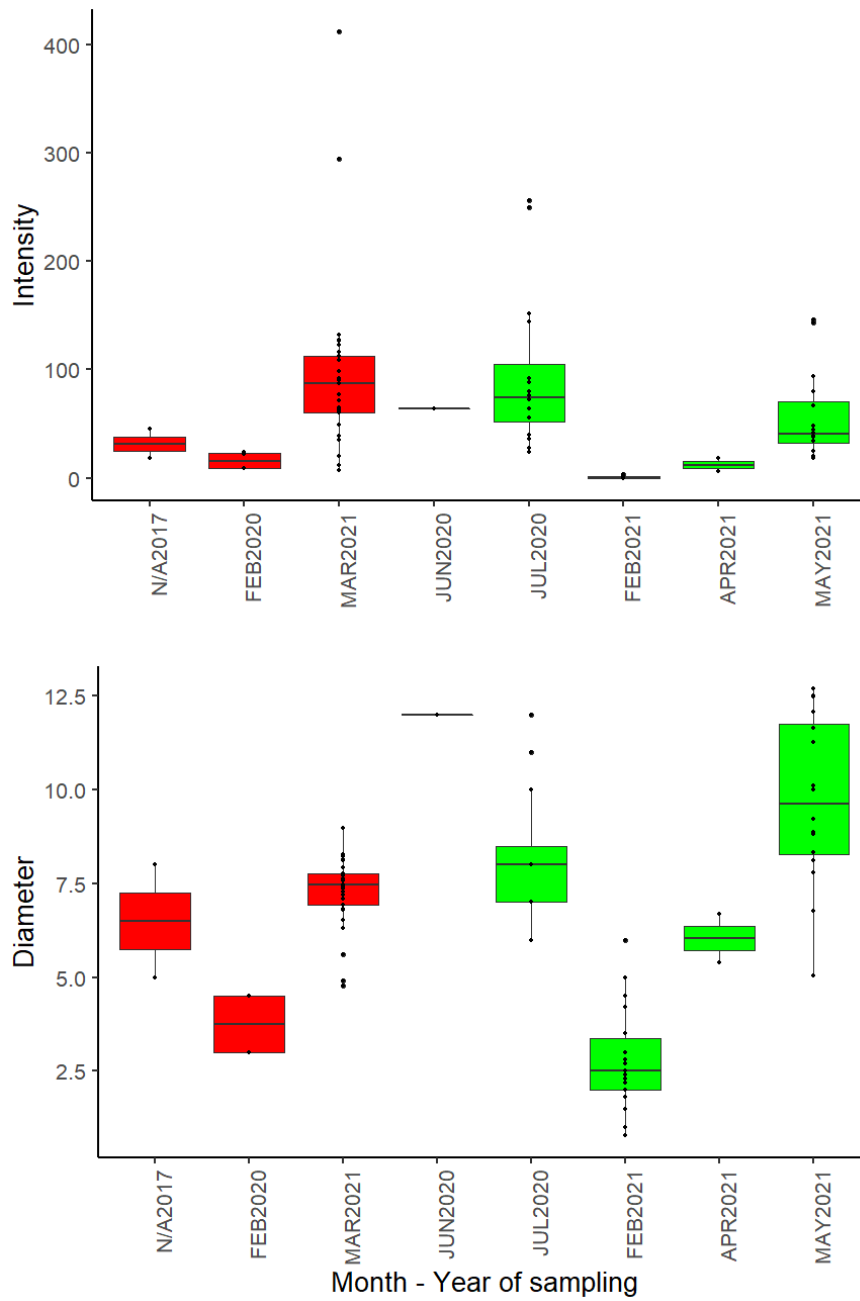
Figure 4. Boxplot of intensity **(a)** and diameter **(b)** in each sampling month for *Aequorea forskalea* (red) and *Aurelia aurita* (green). The thick horizontal line represents the median of the distribution, the box includes 50% of the data, and the whiskers reach the highest and lowest value within 75% of the distribution. Open circles represent single values outside 75% of the distribution.

Table 4. GLM summary for *Aurelia aurita.*

Species	glm(log(INT) ~ diameter + mese, family= gaussian(link =			
Aurelia aurita	identity)			

Predictors	Estimates	CI	p	df
(Intercept)	1.86	0.99 – 2.73	**<0.001**	62.00
diameter	0.03	0.01 – 0.06	**0.018**	62.00
mese [FEB]	-1.83	-2.63 – -1.04	**<0.001**	62.00
mese [JUL]	1.62	0.82 – 2.42	**<0.001**	62.00
mese [JUN]	1.21	-0.13 – 2.55	0.082	62.00
mese [MAY]	1.05	0.23 – 1.88	**0.015**	62.00
Observations	68			
Pseudo.R.squared	McFadden	0.645278		
	Cox and Snell (ML)	0.931451		
	Nagelkerke (Cragg and Uhler)	0.946316		

3.2 Parasite identification

The majority of digeneans were assigned to *Clavogalea* genus, as the morphological analysis totally matched the measures taken in both *Rhizostoma pulmo* and *Mnemiopsis leidyi* (Fig. 5, table S2).
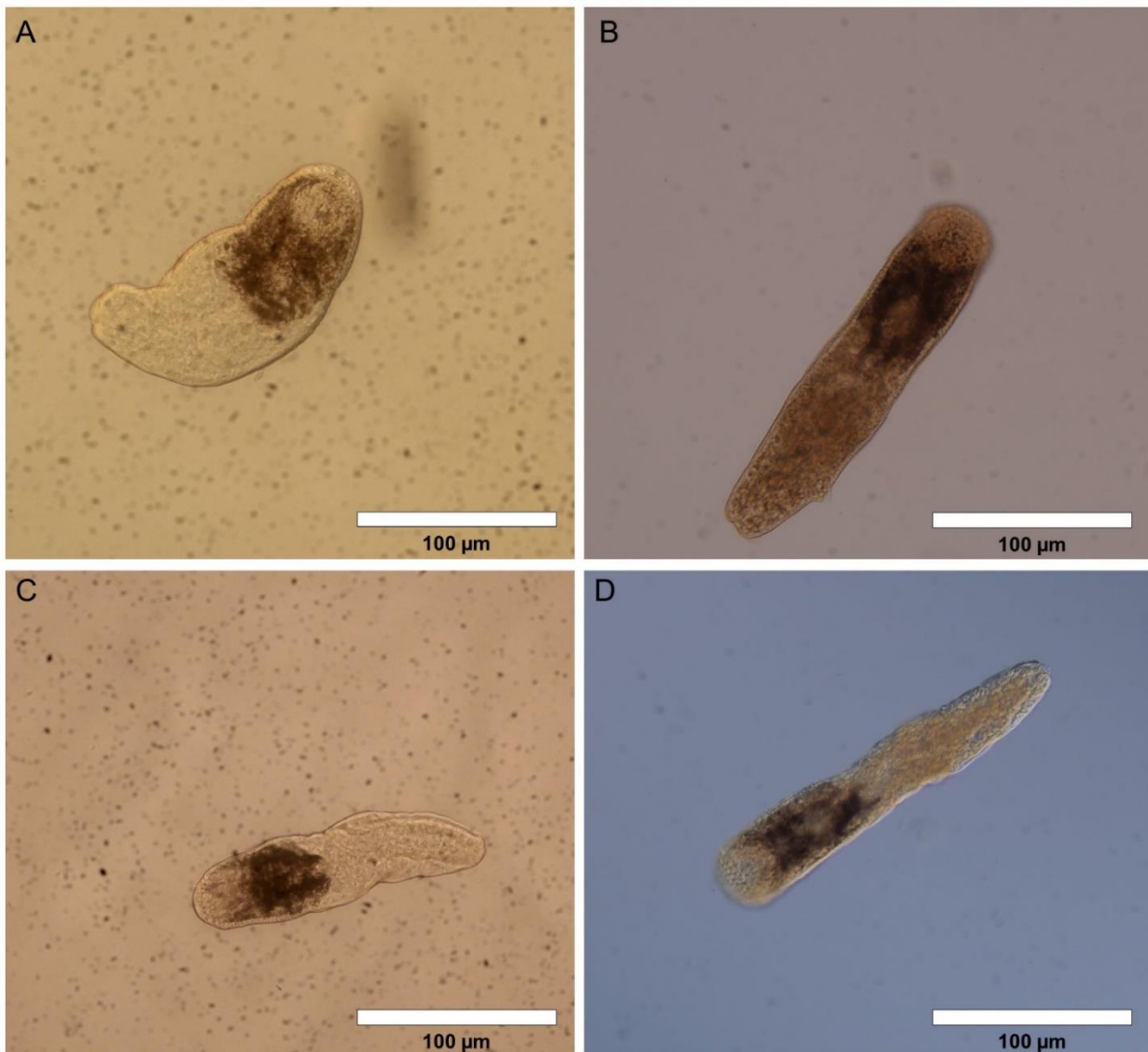
Figure 5. Lepocreadiid metacercariae from **(a-c)** *Aurelia aurita,* **(b)** *Rhizostoma pulmo,* **(d)** *Aequorea forskalea,* light microscopy: anterior region showing double rows of oral spines characteristic of the genus *Clavogalea.*

Surprisingly, in *Aequorea forskalea*, a second parasite (Figure S1 shows the overall abundance of *Clavogalea* sp. and *Opechona* sp. in *Aequorea forskalea*) has been found. It was extracted from already formalin fixed specimens, so only morphological analyses were feasible (Fig. 6).
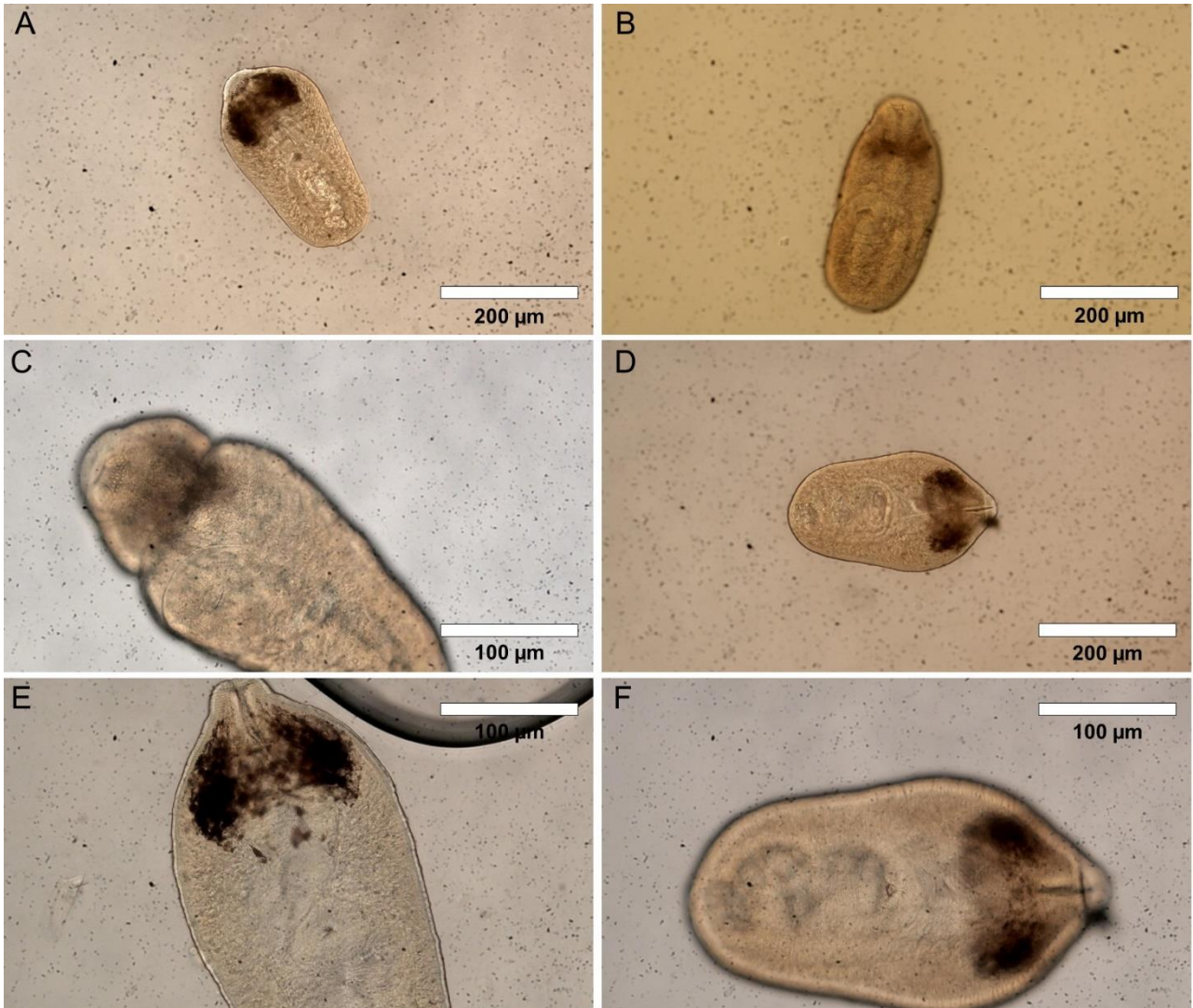
Figure 6. Metacercariae from *Aequorea forskalea*, light microscopy.

In literature, similar metacercarie, species *Opechona bacillaris*, extracted from *Pleurobrachia pileus*, were described by Køie [57], while Martorelli [116] provided the description of *Opechona* sp. from Argentinian jellyfish . Morphologically, these metacercariae are very similar, as pictures confirm (Fig. 7). The oral sucker could be found invaginated (Fig. 7 A-C) or everted [57] (Fig. 7 B-D), covered with spines that extend all over the anterior end of the body [57] (Fig. 7 D). In Table 6 a comparison of our data with measurements made by Køie [57], and Martorelli [116], is provided.
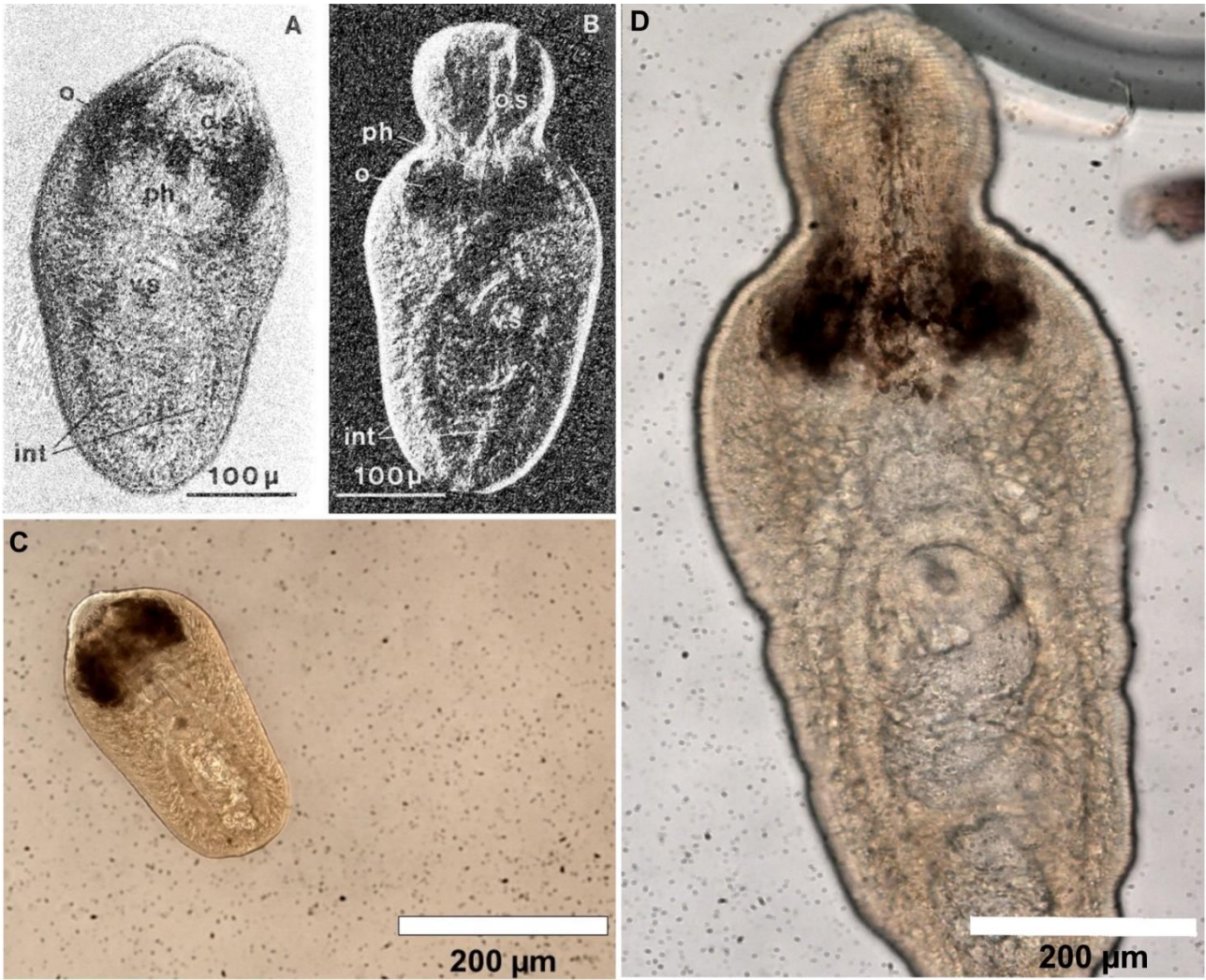
Figure 7. *Opechona bacillaris* metacercariae. **(a)**, **(b)**, extracted from *Pleurobrachia pileus*. modified after Køie [57]. **(c)**, **(d)**, extracted from *Aequorea forskalea*. Abbreviations: o, ocellus; o.s., oral sucker; ph, pharynx; v.s., ventral sucker; int, intestinal caecum.

Table 6. Measurements (µm) and ratios of Digenea specimens from *Pleurobrachia pileus, Olindias sambaquiensis* and *Mnemiopsis leidyi*.

Anatomical measures	Species		
Mean(min-max) µm	*Opechona bacillaris* (Køie) [57]	*Opechona* sp. (Martorelli) [116]	Metacercariae (PhD work)
Body Length	366-460(404)	282-440(345)	297-510(352.8)
Body Width	189-241(217)	130-210(167)	112-185(149.9)
Oral sucker Length	102-142(120)	62-80(67)	45-83(65.4)
Oral sucker Width	108-120(113)	55-75(63)	45 -78(63.6)
Ventral sucker Length	53-66(60)	40-43(41)	48-83(59.7)
Ventral sucker Width	57-74(67)	40-43(41)	47-66(56.8)
Pharynx Length	30-47(36)	35-40(39)	28-46(39.2)
Pharynx Width	26-34(29)	37-50(39)	27-42(37.4)

After this first sight, no *Aequorea forskalea* or *Aurelia aurita* was found during sampling days in the Gulf during autumn/winter 2021 and spring 2022. In a recent sampling (May 2022) parasites from fresh sampled *Aequorea forskalea* have been dissected and fixed in ethanol and sent for molecular analysis, results will be available soon. At the moment, the molecular analyses are still in progress.

4. Discussion

Prevalence and intensity indicate that all jellyfish in the area are potential true hosts for digeneans parasites. At the same time, considering all the gelatinous zooplankton species investigated in this area (including *Rhizostoma pulmo* and *Mnemiopsis leidyi*), it evident that *Clavogalea* sp. is a generalist species, adapted to infect "gelatinous bodies", since it has been found in different organisms of different phyla and classes, from Ctenophora to Cnidaria (inside this phylum it has been

found in both Scyphozoa, Hydrozoa and Cubozoa). Its presence is elevated during all the year, even if it was impossible to monitor its temporal variations in a single species due to seasonality of jellyfish in the area. However, high intensities (much higher compared to other studies) have been recorded all year long, with important peaks during the warmer months both in *Aurelia aurita*, *Rhizostoma pulmo* and *Mnemiopsis leidyi*. This, once again, support the thesis that intensity peaks may be related to release events of the first hosts, positively correlated with water temperature [95,127,128,143].

As for *Rhizostoma pulmo* and *Mnemiopsis leidyi*, even in these rarer species the intensities recorded in the Gulf of Trieste are much higher compared to the available literature. Kondo et al. [63], observed the intensity of *Lepotrema clavatum* in *Aurelia aurita* ranging from 1 to 247.0 individuals, peaking during summer. The max intensity recorded in Adriatic *Aurelia aurita* is 256, similar to Kondo, but the size of jellyfish analyzed has to be taken in consideration, since our specimen were half the size of the Japanese study. *Aurelia aurita* ranged from 5.8 to 29.0 cm (13.3 ± 3.8 cm) in Kondo vs 1 to 12.5 cm (5.8 ± 3.8 cm) in this study. *Aequorea forskalea* digeneans have been studied by Nogueira Júnior et al. [141] in Brazil. There, 20 specimens of *Aequorea forskalea* (size range 14–32 mm), hosted 1 parasite for a 10% prevalence. Regarding *Cothyloriza tuberculata*, this is a first record for this species.

These results support the theory that the Gulf of Trieste provide a potential favorable environment for Digenea life cycles, at least for the first host-jellyfish transfer. Further studies on the abundance and the infection parameters of the first hosts, together with fish parasite investigation, are needed to complete the whole picture.

Regarding the second species found in *Aequorea forskalea*, morphological analyses point towards *Opechona* genus. This identification is supported by several characteristics typical of this genus, such as spinous integument denser anteriorly, black anterior eyespot pigment encircling the pharynx, oral sucker subterminal and larger than ventral sucker, caecal bifurcation (anterior to acetabulum) with two long lateral intestinal caeca, reaching posterior end [58,70,83,116]. However, we could not define the species because there are no available descriptions about the metacercaria juvenile stages (except for *Opechona bacillaris* [57]. It is evident that our specimen, despite being very similar in terms of body

shape, it is smaller compared to *Opechona bacillaris* described in the Baltic Sea, even if some features (ventral sucker and pharynx) are quite similar. The most similar metacercaria is *Opechona* sp. described by Martorelli [116], extracted from *Olindias sambaquiensis* (Table 6). A few other studies provided a description of *Opechona* metacercariae. Morandini [70] described individuals of *Opechona* sp., but their dimension are half the size of Adriatic metacercariae (164-202 μm length, 80-128 μm width). It is hard to compare these stages with the adult descriptions, since digeneans metacercariae body change during maturation to the adult stage found (and morphologically described) in the definitive hosts-fish. It is evident that molecular analysis will be fundamental to tighten the circle about its phylogeny.

At the same time, we could not infer if this species is present only during the colder months, where blooms of *Aequorea forskalea* are predominant and no "size-processable" *Rhizostoma pulmo* is present or if this species is peculiar of this hydrozoan and it is not hosted by other gelatinous species. It will be fundamental the investigation of the potential first host species, in order to discover if its presence in jellyfish is related to a strictly seasonal release by the first host or if it is related to the parasite biology. However, all these observations of *Clavogalea* sp. and *Opechona* sp. (waiting for the identification of the second species) in North Adriatic jellyfish are first-time records [60]. *Opechona* genus, as mentioned above, has been observed in several gelatinous zooplankton species, from Ctenophora [57,58,70] to scyphomedusae [63,70] and hydromedusae [58,67,116,141] in both south Atlantic and Pacific Ocean.

Conversely, *Clavogalea* genus was never found in gelatinous zooplankton (considering all the available worldwide literature) and, at the same time, these are the first digenean species ever described in Adriatic gelatinous zooplankton, no other data are currently available.

As a conclusion, the presence of digeneans in all the gelatinous species in the gulf of Trieste suggest, as already mentioned, that these organisms are preys for fish in the area, since predation is needed to close the life cycle of parasites [58]. It would be odd if jellyfish are parasite dead-ends after being so much infested. The only different situation is the one of *Carybdea marsupialis*. Despite being sampled during summer in Grado Lagoon, the most favorable season and place for digeneans

transmission, as shown with other species, this cubozoan shows really low intensity. Different hypothesis could be made for this. First, *Carybdea marsupialis* is the most venomous jellyfish in the Mediterranean Sea, together with *Pelagia noctiluca*, much more toxic if compared to all the other species in this study [144,145]. This may interfere with parasite colonization, even if no data about the effect of jellyfish poisons on Trematoda is available. Plus, Cubozoa are known to be fast swimmers, over 1 m/s [28] in the wild current-assisted (in laboratory the highest speed ever recorded is 115 mm · s-1 [29]). Since infestation needs physical contact, *Carybdea marsupialis* velocity may be a disadvantageous factor, compared to all other species that are more "stationary".

Supplementary material

Table S1. GLM *Aurelia aurita.* Pair wise comparison of intensity between months of sampling.

Contrast	estimate	SE	Df	t. ratio	p-value
APR - FEB	1.835	0.407	62	4.509	0.0003
APR - JUL	-1.619	0.407	62	-3.975	0.0017
APR - JUN	-1.208	0.683	62	-1.769	0.4007
APR - MAY	-1.051	0.421	62	-2.497	0.1046
FEB - JUL	-3.453	0.271	62	-12.757	<.0001
FEB - JUN	-3.043	0.639	62	-4.763	0.0001
FEB - MAY	-2.886	0.315	62	-9.148	<.0001
JUL - JUN	0.411	0.562	62	0.731	0.9486
JUL - MAY	0.567	0.198	62	2.859	0.0441
JUN - MAY	0.157	0.551	62	0.285	0.9985

Table S2. Measurements (µm) and ratios of digenean metacercariae.

Anatomical measures Mean(min-max) µm	Species		
	Clavogalea sp. *Rhizostoma pulmo*	Metacercariae *Mnemiopsis leidyi*	Metacercariae Pool from Aur-Aeq-Cot-Car
Body Length	215.4 - 461.6 (336.5)	254.1-448.2 (364.6)	305.4-391.8 (355.8)
Body Width	54.8 - 107.6 (81.6)	53.0-90.5 (76.8)	77.3-117.9 (93.9)
Oral sucker Length	45.6 - 71.5 (60)	41.0-71.0 (58.8)	58.3-76.1 (65.4)
Oral sucker Width	44.7 - 80.4 (55.9)	28.7-68.1 (51.6)	43.7-71.6 (55.1)
Ventral sucker Length	40.9 - 63.0 (51.5)	30.5-66.4 (51.1)	38.3-61.7 (50.9)
Ventral sucker Width	42.1 - 69.8 (54.0)	33.4-60.5 (49.0)	28.1-59.7 (49.5)
Pharynx Length	36.5 - 40.5 (39.0)	28.4-46.6 (35.7)	27.2-37.7 (31.3)
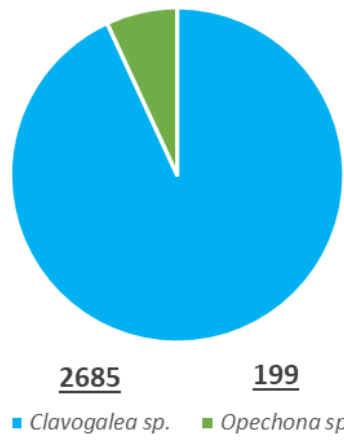
Figure S1. Total intensity of *Clavogalea* sp. and *Opechona* sp. in *Aequorea forskalea.*

Chapter 4.

Digenean parasites in North Adriatic fish

Gregorio Motta [1,2*], Monica Caffara [3], Maria Letizia Fioravanti [3], Massimo Avian [1], Antonio Terlizzi [1,2], Perla Tedesco [3]

[1]Department of Life Science, University of Trieste, 34127 Trieste, Italy.

[2]Department of Integrative Marine Ecology (EMI), Stazione Zoologica Anton Dohrn – Italian National Institute for Marine Biology, Ecology and Biotechnology, 80121 Napoli, Italy.

[3]Department of Veterinary Medical Sciences, Alma Mater Studiorum University of Bologna, Ozzano dell'Emilia, 40064 Bologna, Italy.

*These authors contributed equally to this work.

1. Introduction

Fish have been shown to be definitive hosts a huge number of different parasites, including digeneans (Phylum: Platyhelminthes, Class: Trematoda) [146]. The number of new digenean parasites described is steadily increasing, now including about 18000 species in about 2500 genera [147,148]. As an example, Cribb [149] estimated that the Australian fish species (about 3000) could host up to 5500 species of digeneans. Manter [150] stated that digeneans are mainly host specific, since most of their records came from single host species or from related genera. The adult stage of these parasites is commonly found in the digestive tract of fish, but they are able to infect other tissues like gills or brain [146].

Intestinal digeneans have been demonstrated to cause scarce harm to the fish, even if present in high numbers. Differently, extraintestinal parasites, infecting the gills, liver, brain, testis, etc. are potentially pathogenic [151]. The presence of blood flukes (sanguinicolids) could cause considerable damage to the gills and impair respiration [147,151]. These worms can physically obstruct the passage of blood, cause thrombosis and tissue necrosis [146,152,153]. Even worse, the emersion of miracidia, with gill tissue rupture, could led to death of infected fish [146,152].

In parallel with fish health, digeneans could interfere with human economic activities, in particular aquaculture [151,154,155]. The high density of individuals in the cages directly favor the exchange of parasites between farmed fish [151]. Problems related with digeneans infections may include mortality of farmed fish, growth delay and sometimes loss of market value [146]. The presence of digeneans may lead to the impossibility of selling the fish and a reject by consumers, decreasing the overall values of the products [156–159].

From a global perspective, considering the rapid expansion and intensification of mariculture taking place in the last decades [160], the economic issues related to Digenea infections may increase exponentially.

This work, even if still under construction (some datasets, in particular about digeneans identification, are incomplete), is the first attempt to check for the presence of jellyfish parasites in north Adriatic fish, in order to obtain fundamental information about their life cycle and definitive fish hosts in the Gulf of Trieste. To date, few studies focused on digeneans in the area and they only aimed at assessing presence and anatomically describing adults digeneans in north Adriatic fish [161–163]. Thus, this work would be an important step forward both for jellyfish, digeneans and fish ecology for the area.

2. Materials and methods

81 individuals of common fish species were collected by fishermen in the Gulf of Trieste in summer 2022 (Fig. 1).

Figure 1. Species collected (not complete) from the Gulf of Trieste. **(a)** *Trachurus trachurus*; **(b)** *Mullus barbatus*; **(c)** *Scomber scombrus*; **(d)** *Zosterisessor ophiocephalus*; **(e)** *Pagellus erythrinus*; **(f)** *Engraulis encrasicolus*; **(g)** *Merlangius merlangus*.

Samples were brought to the lab and their body length was measured. Then, the digestive apparatus (Stomach, intestine, villi) was removed (Fig. 2) and dissected in order to check the presence of digenean parasites. Two protocols were followed: intestines of species characterized by a huge

number of pyloric caeca (>30) were macerated with a blender in a vertebrate saline solution following Cribb and Bray [104].
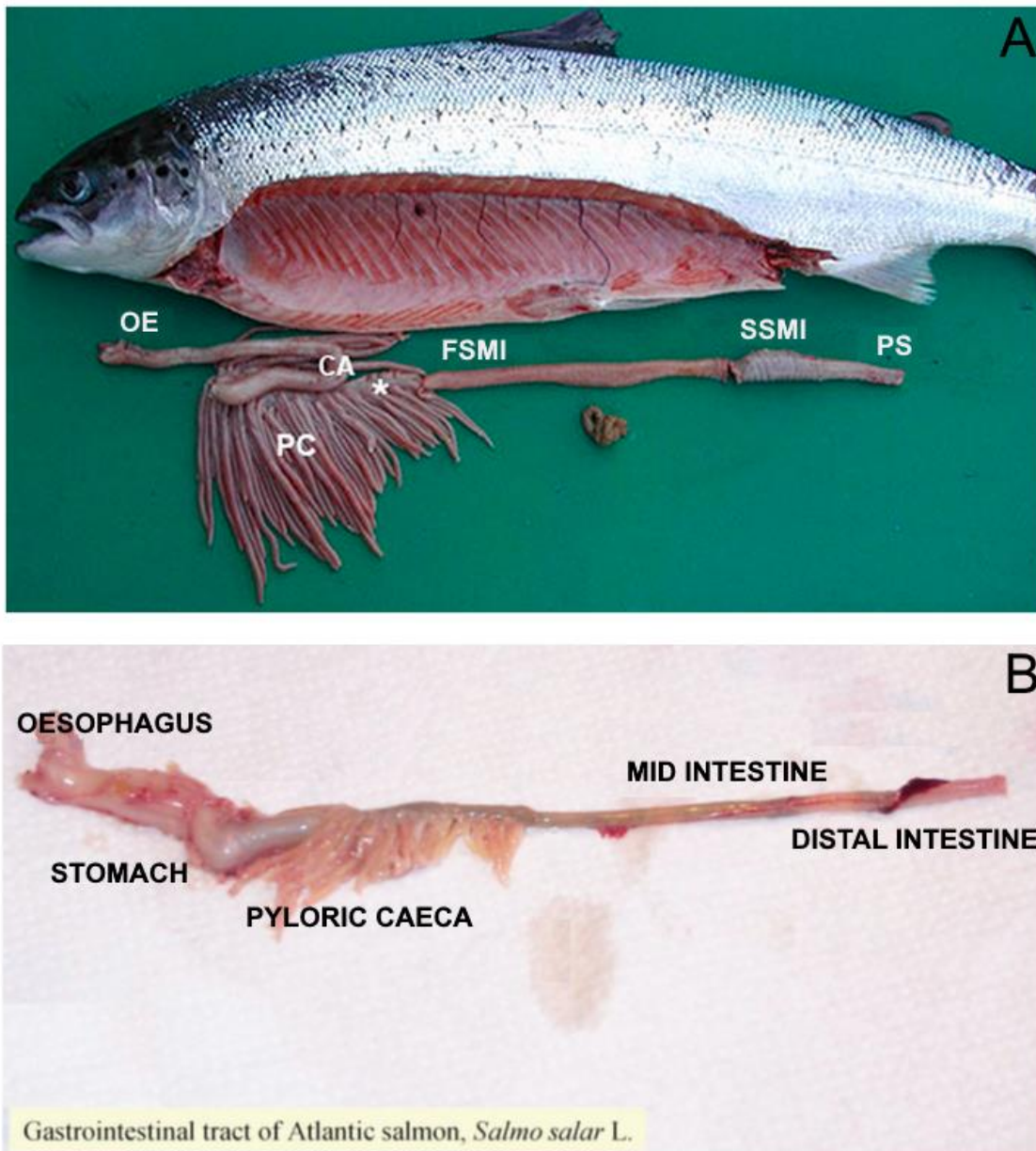
Figure 2. (a) Macroscopic image of the gastrointestinal tract of the Atlantic salmon. OE - oesophagus, CA - cardia, PC - pyloric caeca, FSMI - first segment of the mid-intestine, SSMI - second segment of the mid-intestine, PS - posterior segment. Taken from [164], modified after [165] **(b)** Gastrointestinal tract of Atlantic salmon showing oesophagus, stomach, pyloric caeca, mid intestine and distal intestine. Modified after [166]

The resulting mixture was left "resting" for 5 minutes to let the parasites sink. Parasites were then collected and counted in petri dishes under a stereomicroscope (Leica Mz-6) and pictures were taken

at light microscopy. The supernatant was removed after checking for floating parasites. In species characterized by a limited number of caeca, each caecum was cut with a chirurgical blade and gently pressure was applied to it to let the contents spill over. For both kind of digestive systems, stomachs were cut and washed with vertebrate saline to collect their contents. Prevalence (P) and intensity (I) values were defined following Bush et al. [1].

2.1 Parasite count and identification.

For identification, parasites extracted from fresh tissues were preserved in 70% ethanol for molecular analysis and 10% hot formalin for morphological analysis following Cribb & Bray [104].

For morphological analysis, metacercariae were subjected to microscopical observation after clarification in Amman's lactophenol. All measurements were taken with the imaging software NIS-Elements expressed as ranges with mean values in parentheses.

For molecular analysis, genomic DNA was extracted from five metacercariae by PureLink® Genomic DNA Kit (Life Technologies, Carlsbad, CA, USA), following the manufacturer's instructions.

The amplification of the D1-D3 region of 28S rDNA was performed with primers U178_f (5′-GCACCCGCTGAAYTTAAG-3′) and L1642_r (5′-CCAGCGCCATCCATTTTCA-3′) [105], following Gustinelli et al. [106]. The PCR products were electrophoresed on 1% agarose gel stained with SYBR® Safe DNA Gel Stain (Thermo Fisher Scientific, Carlsbad, CA, USA) in 0.5X TBE. All amplicons were purified by NucleoSpin Gel and PCR Cleanup (Mackerey-Nagel, Düren, Germany, CA, USA) and sequenced with an ABI 3730 DNA analyzer (StarSEQ, Mainz, Germany). 28S rDNA amplicons were sequenced with the internal primers 900F (5′-CCGTCTTGAAACACGGACCAAG-3′) and EDC2 (5′-CCTTGGTCCGTGTTTCAAGACGGG-3′) of Lockyer et al. [105].

The DNA trace files were assembled with ContigExpress (VectorNTI Advance 11 software, Invitrogen, Carlsbad, California) and the consensus sequences were compared with previously published data by BLAST tools (https://blast.ncbi.nlm.nih.gov/Blast.cgi). Multiple sequence alignments of the newly generated sequences together with the all the sequences reported by Curran et al. [90], were built by BioEdit 7.2.5 [107]. Pairwise distance, using a Kimura 2-parameter model and

maximum likelihood (ML) tree (BIC = GTR + G, bootstrap of 1000 replicates) were obtained by MEGA version X [108].

3. Results

3.1 Parasite Count.

33 of 81 specimens analyzed were parasitized by trematode metacercariae. Intensity values ranged between 0 up to over 200 (recorded in *Merlangius merlangus*). Mean, min and max intensity for species are reported in Table 1.

Table 1. Comparison of mean, standard deviation, min and max intensity for each fish species sampled from the Gulf of Trieste.

Species	N° samples	Mean lenght (cm)	Prevalence	Mean Intensity	Sd Intensity	Min Intensity	Max Intensity
Scomber scombrus	16	20.47	0.31	0.375	55.38	0	11
Merlangius merlangus	27	22.38	0.91	68.36	79.47	0	>200
Engraulis encrasicolus	10	11.27	0	0	0	0	0
Trachurus trachurus	13	14.91	0.15	1	1.3	0	13
Mullus barbatus	3	12.48	0	0	0	0	0
Boops boops	4	19.81	0	0	0	0	0
Oblada melanura	3	17.75	0	0	0	0	0
Pagellus erythrinus	4	14.51	0	0	0	0	0

Prevalence was considerably high in *Merlangius merlangus*. On the other hand, several species did not seem to be parasitized by digenean metacercariae.

3.2 Parasite identification

Metacercariae from *Merlangius merlangus* were morphologically analyzed and amplified. Two similar morphotypes were found. The preliminary molecular analysis gave the highest similarity 98.7% with *Stephanostomum pristis*, *Stephanostomum gaidropsari* matched for 95.7%. for one morphotype (from this point called M1), while the other (M2) gave bad sequences, thus only morphological analysis are available. Molecular analysis of metacercariae from S*comber scombrus* are in progress, only morphological analysis was performed. The measures taken for *Stephanostomum*-like metacercariae were compared with literature and the most similar descriptions (M1) were the ones provided by Bartoli and Bray [167] for *Stephanostomum gaidropsari* (Fig.3, Table 2), while M2 (thinner, smaller OS diameter and oral spines compared to M1) did not match any available description in terms of both body measurement, while a similarity in shape with *Stephanostomum pristis* was noticed (Fig. 4, Table 2).
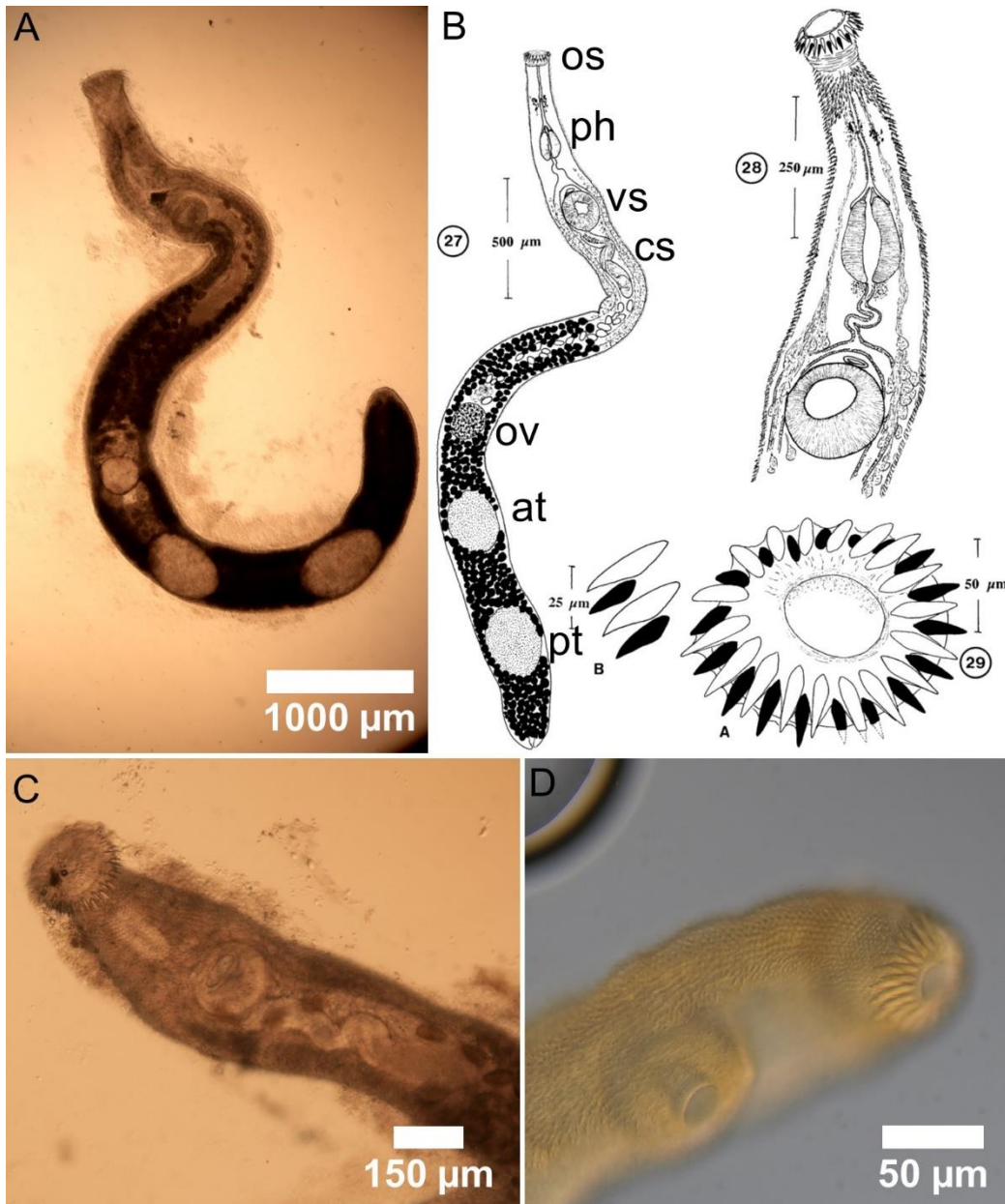
Figure 3. *Stephanostomum* metacercariae, M1, from *Merlangius merlangus*, light microscopy: **(a)** whole body, ventral view, **(b)** *Stephanostomum gaidropsari* from [167]: ventral view. 28. Paratype: ventral view of the forebody. 29. Paratype: oral sucker. A. Apical view. Modified after [167], **(c)** magnified view of the hindbody, with focus on oral spines, **(d)** detail of anterior region of immature specimen. Abbreviations: anterior sucker (as), pharynx (ph), ventral sucker (vs), cirrus (cs), ovary (ov), anterior and posterior testes (at-pt).
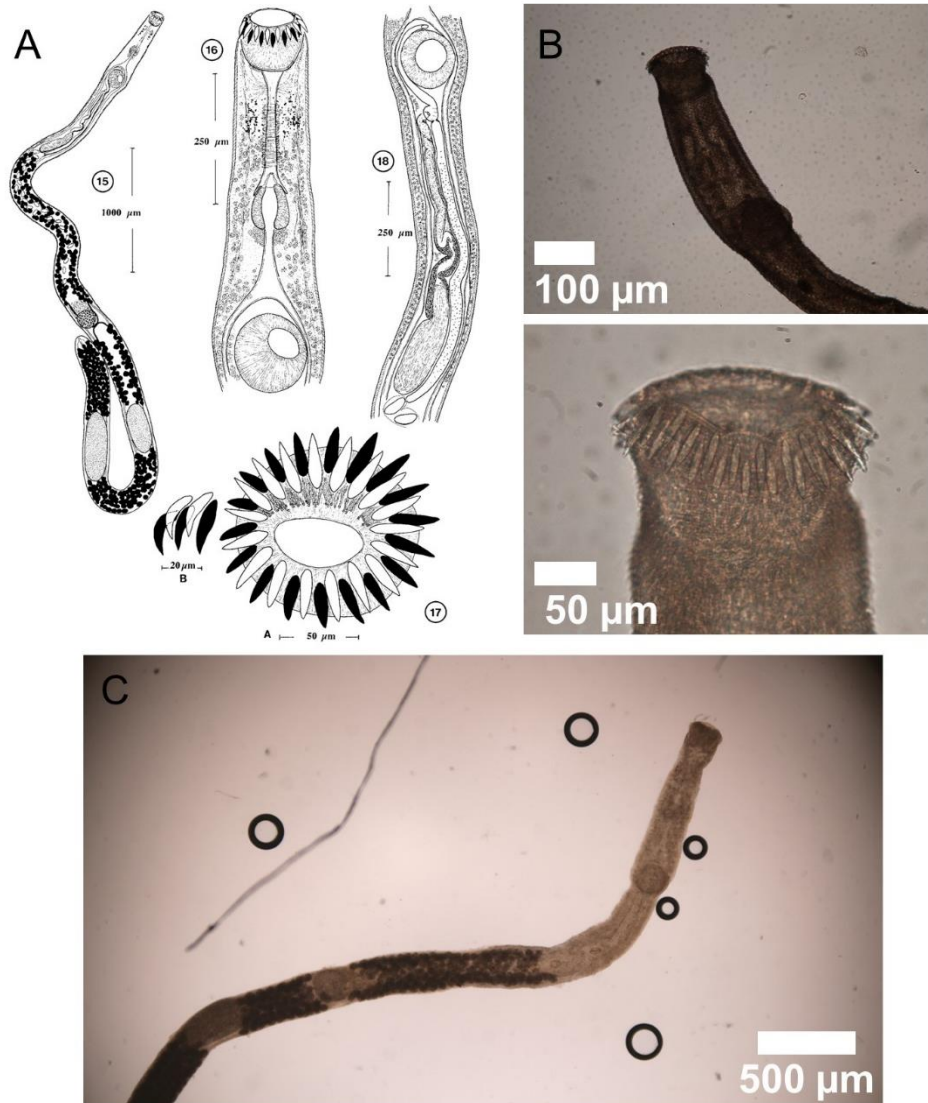
Figure 4. *Stephanostomum* metacercariae, M2, from *Merlangius merlangus*, light microscopy: **(a)** *Stephanostomum pristis* from [167]: ventral view. 28. Paratype: ventral view of the forebody. **(b)** forebody (upper); detail of oral sucker spines (lower). **(c)** whole body, ventral view.

Table 2. Measurements (µm) and ratios of Stephanostomum-like specimens from *Merlangius merlangus.*

Anatomical measures Mean(min-max) µm	Species			
	Stephanostomum gaidropsari [167]	*Stephanostomum M1* (PhD work)	*Stephanostomum M2* (PhD work)	*Stephanostomum pristis* [167]
Body Length	3400-5376 (4237)	2513.70-6070.40 (4151.41)	3151.35-6304.58 (4523.57)	6310-10550 (8104)
Body Width	224-373 (302)	239.32-422.71 (313.62)	162.75-320.20 (224.89)	208-415 (271)
Oral sucker Length	69-100 (85)	126.66-270.66 (209.65)	109.54-198.22 (156.04)	104-130 (112)
Oral sucker Width	100-130 (110)	129.44-203.03 (159.66)	87.35-168.52 (130.59)	104-130 (122)
Ventral sucker Length	171-234 (199)	140.11-252.79 (183.55)	128.03-196.16 (160.95)	148-202 (175)
Ventral sucker Width	152-221 (190)	149.40-278.22 (183.55)	111.75-184.34 (155.79)	141-204 (167)
Pharynx Length	122-176 (154)	88.87-183.64 (127.62)	101.79-144.88 (116.42)	82-130 $\times$ (110)
Pharynx Width	87-145 (109)	49.70-92.68 (67.81)	71.57-80.72 (74.82)	72-111 (89)
Forebody	468-829 (649)	419.54-930.99 (600.56)	174.95-1155.9 (769.15)	490-773 (627)

Hindbody	2614-4314 (3383)	2087.60-5521.21 (3468.13)	2558.47-5261.58 (3746.41)	5586-9594 (7302)
Ovary length	133-203 (171)	78.69-237.31 (165.88)	116.68-393.62 (185.03)	139-250 (205)
Ovary to testis	133-346 (226)	55.64-384.42 (233.92)	218.0-426.77 (323.15)	720-1,173 (892)
Anterior testis	282-506 (383)	257.45-666.25 (355.14)	214.95-495.46 (338.56)	410-752 (540)
Posterior testis	325-506 (416)	198.58-863.18 (448.40)	207.58-616.30 (392.82)	506-650 (607)
Intertesticular space	133-586 (309)	135.80-736.62 (372.58)	122.49-660.12 (376.16)	640-1,519 (1,014)
Post-testicular space	373-682 (478)	340.90-846.65 (573.19)	283.14-880.12 (606.17)	645-1,652 (1,164)
Oral sucker/pharynx ratio	1: 1.52-2.55 (1.82)	1.360-2.08 (1.55)		
Ventral sucker/pharynx ratio	1: 0.66-0.89 (0.77)	1.21-1.67 (1.43)		
Forebody/hindbody ratio	1: 4.24-6.90 (5.25)	3.83-10.05 (5.91)		

Metacercariae from *Scomber scombrus* included three different organisms, the most abundant was assigned to the genus *Lecithocladium*, its measure almost fitted the description of *Lecithocladium* made by Keser et al. [87] in *Scomber scombrus* from Turkey (Fig. 5, Table S2). The other two species fit with the description of *Helicometra fasciata* (Fig. 6, Table S1) by Paradižnik and Radujković [162]

in north Adriatic *Scomber scombrus* specimens, and *Opechona* sp. by Akmirza [168] in the Aegean Sea (Fig. 7, Table S2).
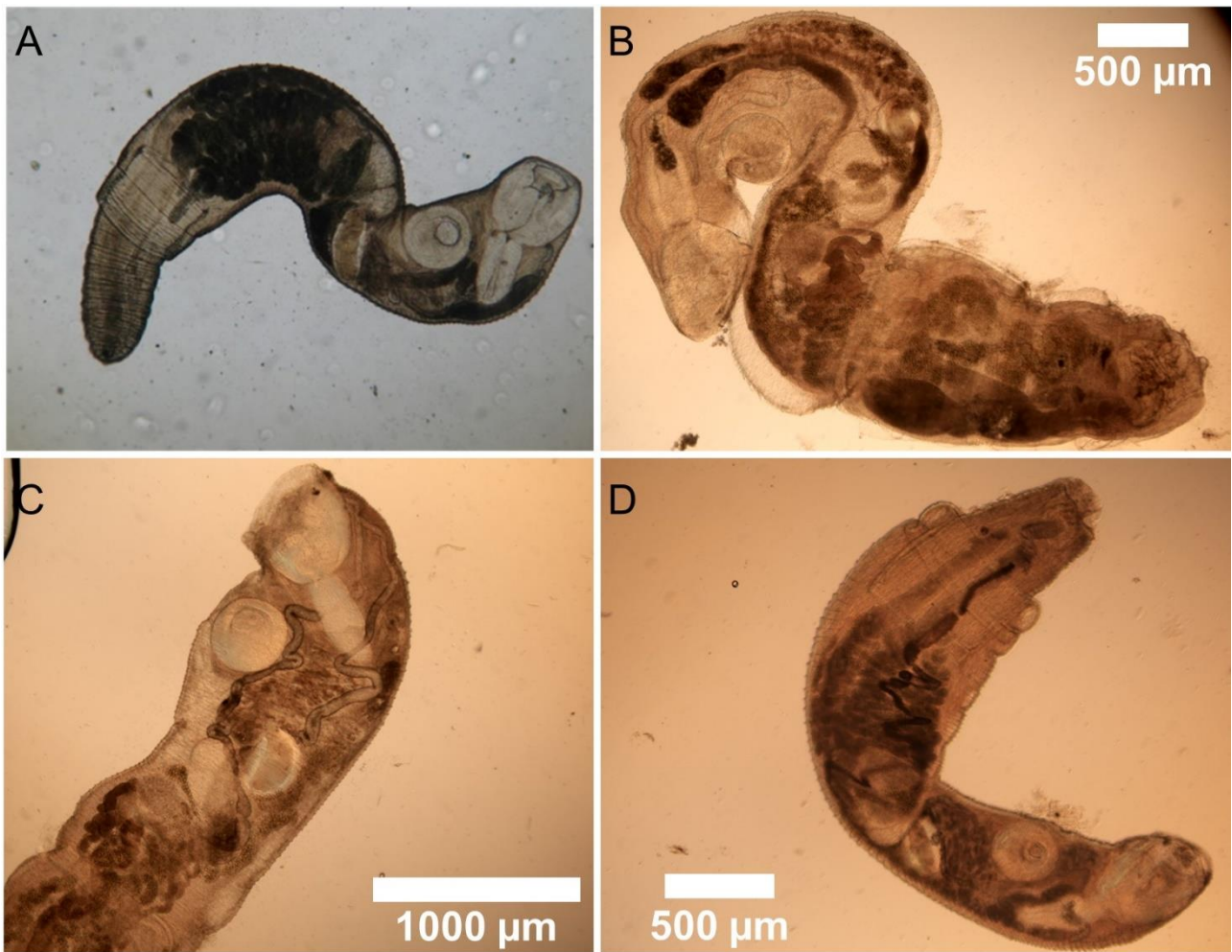
Figure 5. *Lecithocladium* metacercariae from *Scomber scombrus*. (**a**) *Lecithocladium excisum* taken from [168]; (**b-d**) metacercariae from the present study.

Figure 6. *Opechona* metacercariae from *Scomber scombrus*. **(a)** *Opechona olssoni* taken from [168]. **(b-d)** metacercariae from the present study.
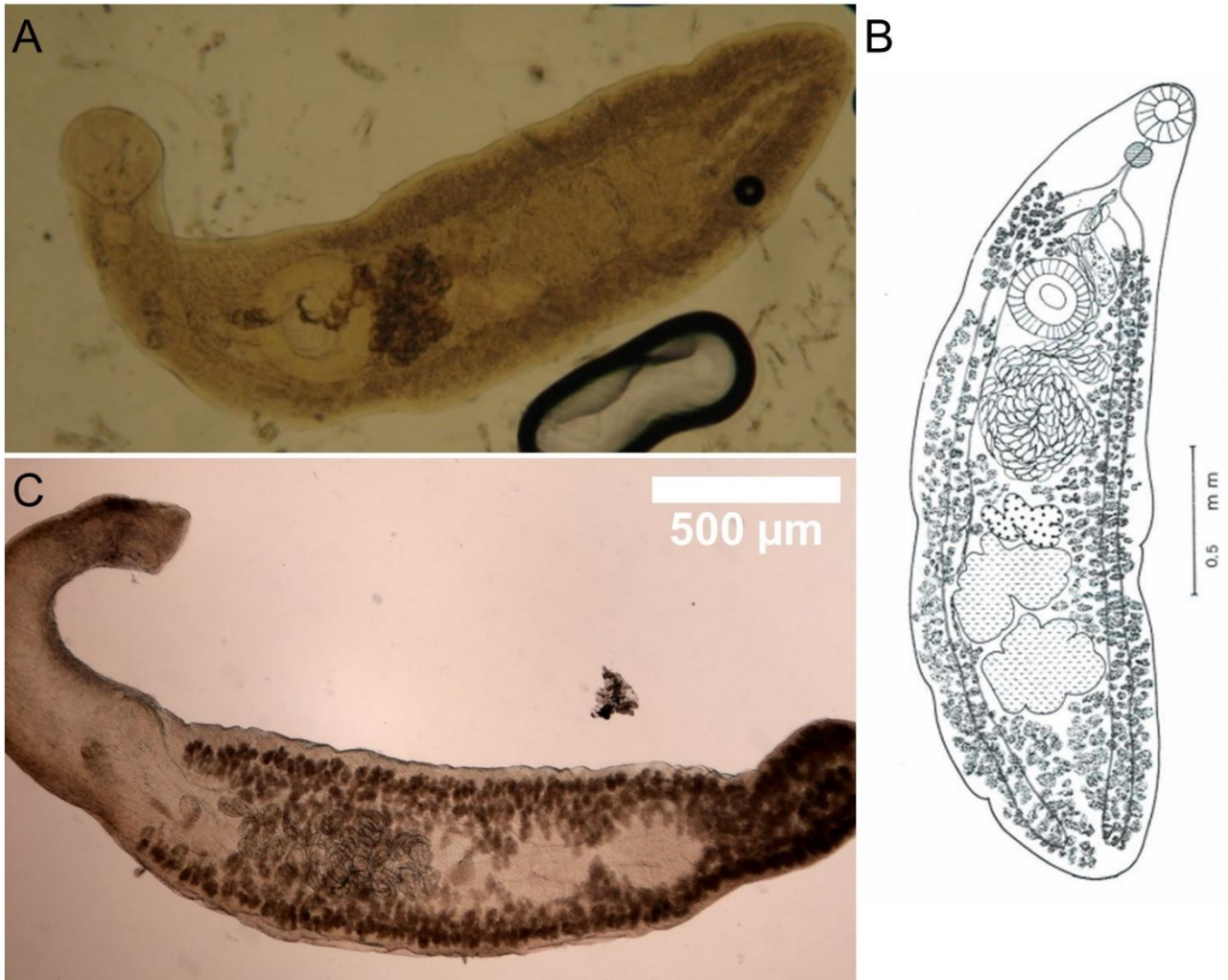
Figure 7. *Helicometra* metacercariae from *Scomber scombrus.* **(a)** *Helicometra fasciata* taken from

[168], **(b)** *Helicometra fasciata* taken from [162] **(c)** damaged metacercaria from the present study.

4. Discussions

As mentioned above, few studies focused on digeneans life cycle in the area and they aimed at anatomically describing adults digeneans in north Adriatic fish [161–163].

Unfortunately, the most abundant parasite in jellyfish, *Clavogalea* sp., was not found. Considering the high mean prevalence and intensity of *Clavogalea* sp. in all the gelatinous plankton species in the Gulf of Trieste, we can assume that none of these fish species include jellyfish in their diet. However, we have to consider that fish have all been sampled over the minimum landing size, so we have to narrow our theory. Adult fish may not eat jellyfish, but we do not have enough data about their juvenile stages. These stages could be key moments for parasite transfer for some fish species. For example, juveniles of species like *Merlangius merlangus* [169] have been demonstrated to live in a commensalism relationship with *Rhizostoma octopus* while juveniles of *Trachurus mediterraneus* have observed in association with *Rhizostoma pulmo* and *Cotylorhiza tuberculata* [103]. It is still unclear if this relationship is just for shelter or if these species actually feed on jellyfish tissues. Parasitology may help investigating these relationships since it is complex to address them with other methods. Moreover, for this first study, we mostly focused on invertebrate predators. Surprisingly, recent research demonstrated that ctenophores may be prey for herbivores [134]. The rabbitfish *Siganus rivulatus* (Siganidae) and surgeonfish *Zebrasoma desjardinii* (Acanthuridae) actively selected and fed until disintegration on local ctenophores [134].

Opechona genus adults have been found in *Scomber scombrus* in a recent sampling (June 2022). Currently, samples of this genus have been sent for molecular analysis to be compared with the metacercariae found in *Aequorea forskalea*. However, intensity in the jellyfish was so low that it would be hard to theorize a trophic relation between *Scomber scombrus* and the hydromedusa. At the same time, the absence of *Clavogalea* sp. adults (despite their abundance in *Aequorea forskalea*) would suggest that fish got the parasites from another intermediate host.

From a broader perspective, even if we could not complete the picture on jellyfish digeneans, this study gave new information about fish parasites in the Gulf of Trieste.

Stephanostomum is a common genus of digeneans in fish. Cribb et al. [170] stated that *Stephanostomum* Looss, 1899 is the second Digenea genus according to the number of described species, 107, parasitizing fishes.

To date, only Jardas, I. & Hristovski [161], Paradižnik, V. & Radujković [162] and Radujkovic, B. & Sundic [163] investigated fish digeneans from Croatia and Montenegro listing over 160 species. In the north Adriatic *Stephanostomum* genus has been only observed in *Lophius piscatorius* [171], *Umbrina cirrosa* and *Trisopterus minutus* [162]. In the whole Mediterranean Sea, Bartoli and Bray [167,172] found several individuals of *Stephanostomum* in different fish from the Natural Reserve of Scandola (Corsica), and the Gulf of Marseilles. Of the two *Stephanostomum*-like morphotypes, our identification came closest with *Stephanostomum gaidropsari*, with the only noticeable differences in oral sucker dimensions, for M1 while M2 did not match any available description, despite a similar shape with *Stephanostomum pristis*. The molecular analysis for M1 fitted best with *Stephanostomum pristis*, but the identity % is not high enough to confirm the species.

Taking in consideration that these are preliminary results (other morphological and molecular analysis are needed to have robust information), data could be interpreted in several ways. We could be observing new species never described before (and that is not an uncommon event within this poorly described organisms), we could be observing different maturation stages of different species (explaining the variability of the measures) or, maybe, the lack of sequences for *Stephanostomum gaidropsari* (only 1 available) is not enough to consider this match sufficiently accurate and reliable. In fact, it has to be considered that most of the digeneans studies relied on old records based on morphological descriptions and handmade anatomical tables, no microscopy images or molecular data are available for most of digenean species. This could lead to misidentifications where the two different, but morphologically similar, species could be mistaken each other or as a single species (with potentially mistaken related sequences attribution, if no other sequence is available for that species), or individuals of the same species, at different stages of maturity, different body sizes, or fixed in convoluted postures, could be described as different species. These issues could be intensified by the fact that no study focused on following and describing all the stages of growth and maturation

of digeneans, we have descriptions only for the "presumed" fully-grown adult stages. This could be the case for M2, since its shape recalls *Stephanostomum pristis,* but the size is much smaller, it could be an immature stage of this species. A second run of molecular analysis are needed to shed light on these species.

Comparing our preliminary results with the available literature, *Merlangius merlangus* has been demonstrated as an host for several *Stephanostomum* species, *pristis* included, as described by Deslongchamps [173], Shotter [174] and Bartoli and Bray [167,172]. *Stephanostomum gaidropsari* was only observed in *Gaidropsarus mediterraneus* [167], so, if M1 will be confirmed as *Stephanostomum gaidropsari* or as a new species, this could be a first record for this species in *Merlangius* in the north Adriatic Sea. In the study by Bartoli and bray, *Stephanostomum pristis* parasites were also hosted by *Engraulis encrasicolus*. In our study, no digenean parasite was observed in this species. The absence of any *Stephanostomum* in *Engraulis encrasicolus* (despite the high prevalence and intensity recorded in *Merlangius merlangus*, confirming the presence of the parasite in the area) could support the idea that we are observing a different parasite species with different hosts, or this species could behave differently in the Adriatic Sea.

Lecithocladium, *Opechona*, and *Helicometra*, on the other hand, are common parasites genera of *Scomber scombrus* [83,87,90,168]. *Lecithocladium* has been described from the Aegean Sea and the coasts of turkey, and our specimen match its description. *Opechona* and *Helicometra* have been described both in the Turkish Sea and the north Adriatic [162,168], so we confirm this species as host for this genera also in the Gulf of Trieste.

Concluding, even if we did not succeed in finding the definitive fish hosts of digenean species present in jellyfish, this work updated the current state of the art and knowledge about digenean parasites in the fish compartment, including a potential first record of *Stephanostomum gaidropsari* (or a new species?) in Adriatic *Merlangius merlangus*, another description of *Stephanostomum pristis,* and three records of *Helicometra fasciata, Lecithocladium* and *Opechona* sp. in *Scomber scombrus* from the north Adriatic Sea.

The continuation of this study will focus on both new fish species and, most important, the already analyzed species but at smaller size, in order to include the juvenile stages. Finding the key definitive host for jellyfish digeneans is necessary to obtain fundamental information (the number of definitive hosts, their abundance in the north Adriatic, assessing the number of parasites hosted by these species) about parasite life cycles and to better understand the role of jellyfish in the ecosystem's food webs. Once completed, this work would be an important step forward both for jellyfish, digeneans and fish ecology.

Supplementary material

Table S1. Measurements (mm) of Digenea specimens from *Scomber scombrus.*

Anatomical measures min-max mm (mean)	Species	
	Helicometra fasciata [168]	(PhD work)
Body Length	2.6 – 4.0	3.45
Body Width	0.6 – 0.7	0.59
Oral sucker	0.20	0.19
Ventral sucker	0.16	0.16
Ovary	0.14 - 0.26	0.19
testis	0.30 – 0.40	0.30

Table S2. Measurements (µm) of Digenea specimens from *Scomber scombrus.*

Anatomical measures Min-max (mean) µm	Species			
	Opechona bacillaris [83]	*Opechona* sp. (PhD work)	*Lecithocladium excisum* [87]	*Lecithocladium* sp. (PhD work)
Body Length	2160-4550	3128.6-3212.1 (3170.3)	7671	3892.6-6871.3 (5065.9)
Body Width	366-492	518.2-616.4 (567.3)	903	631.6-973.2 (852.5)
Oral sucker Length	328-379	290.5-368.7 (329.6)	459	482.1-591.7 (519.5)
Oral sucker Width	220-284	189.3-358.8 (274.0)	421	314.3-502.7 (417.4)

Ventral sucker Length	170-221	166.9-178.0 (172.4)	407	321.8-387.9 (355.1)
Ventral sucker Width	164-216	155.7-188.9 (172.3)	362	287.2-385.6 (348.20)
Pharynx Length	120-152	145.8-216.1 (181.0)	413	377.7-489.6 (441.7)
Pharynx Width	96-130	123.5-176.0 (149.8)	206	174.3-366.4 (248.2)
Ovary lenght	131-202	214.7-335.9 (275.3)		
Anterior testis	240-348	304.9-385.6 (345.2)		
Posterior testis	279-350	381.8-381.8 (381.8)		

General conclusions and future studies

This PhD work is the first attempt to investigate jellyfish digeneans in the Mediterranean Sea with a modern approach made by a combination of traditional morphological analysis, molecular analysis (fundamental to overcome the issues related with the "age" and holes of bibliography about these organisms), and statistical analysis (to better describe prevalence and intensity dynamics).

First of all, every gelatinous zooplankton species in the Gulf of Trieste resulted to be host to digenean parasites in every sampling location and month. In fact, *Clavogalea* sp. is present all year long in every site, even if ecologically different from each other, such as Grado Lagoon and the bays of Trieste and Piran. This indicates a noticeable tolerance of this species to seasonal variations, considering that (water temperature range between about 9.2°C during winter and about 25°C during summer). *Opechona* sp., on the other hand, is present only in *Aequorea forskalea* (blooming winter - spring), so we could not state if the presence of this parasite is limited by the presence of the intermediate host or limited by environmental conditions.

In parallel, the high prevalence recorded in every gelatinous species (>80%) suggests that the gelatinous zooplankton in the Gulf of Trieste is an important intermediate host of lepocreadiid digeneans and therefore plays a key role in their life cycle. Similarly, the yearlong presence of the parasite indicates a constant cercaria release from the first hosts, fundamental aspect that needs to be addressed in the near future. From a broader perspective, high prevalence and intensity supports the hypothesis that the gelatinous zooplankton is a component of fish diet in the gulf of Trieste, since trophic interactions are necessary for these parasites to complete their cycles.

Addressing predation over gelatinous plankton with traditional methods is challenging due to the scarce durability of their tissues in fish stomachs. The presence of parasites can be another way to assess these dynamics, parasitological data may be a useful tool to evaluate trophic interactions between fish and gelatinous organisms, an important but still under investigated aspect that needs to be fully clarified in jellyfish ecology.

The high infection values observed in our study also hint that the characteristics of the gulf of Trieste could provide a favorable spot for digeneans proliferation and transmission. Its warmer and shallow waters (mean depth 20 m), compared to the studies made in the south Atlantic Ocean or Japan Sea, may favor both cercaria release (positively correlated with water temperature) and the encounter between swimming cercariae and the second intermediate hosts. Plus, the anthropic activities in the Gulf, and in particular in Grado Lagoon, involved in the increase of resuspension (suction dredge fishing, dredging, turbulence caused by maritime traffic in shallow waters) may impair the "natural" dynamics of the water column, thus making parasites even more available with unpredictable effects on the ecosystems. For example, digenean belonging to *Opechona* sp. were found in gonads and digestive gland of *Buccinanops cochlidium* (Nassaridae) from San Jose´ Gulf, Argentina [95]. Here, the presence of the parasite interfered with the host metabolism causing a reduction of the penis dimension and a so called "parasitic castration" (the parasites occupied the gonads leaving no room for gametes). It is evident that the presence of these parasites could affect traditional biomarkers analysis for ecotoxicological studies, potentially increasing or altering their results. Digenea (at least in gastropods), could act as a supplementary "pollutant" that has to be taken in consideration in this kind of studies, making the understanding of the whole picture of environmental status even more complex, especially in areas like the Gulf of Trieste where their abundance is remarkable.

In conclusion, although it was not possible to identify the parasite at species level, due to the scarcity of literature information (at both morphological and molecular level) available for these organisms particularly in the considered area, our work provides important information on the role of gelatinous zooplankton as intermediate host for lepocreadiids, and useful data as basis for future studies aimed to shed light on the life cycle of these parasites in the Mediterranean Sea.

This work could be considered a sort of first step, a "cornerstone" about jellyfish parasites and jellyfish ecology in the north Adriatic since it started investigating this huge hole of knowledge about this topic, provided important data (first record of *Clavogalea* and *Opechona* genus in jellyfish and in the area, highest values of digeneans ever recorded in jellyfish if compared to studies made in other areas of the world) and opened up numerous questions that still need to be addressed. Similarly, the

related work on fish parasite aimed to find the definitive host of this species did not record any *Clavogalea*, leaving the life cycle of this organisms still unclear but, we described a potential first record of *Stephanostomum gaidropsari* (or a new *Stephanostomum* species, still under investigation) in *Merlangius merlangus* from the north Adriatic. Potential juvenile stages of *Stephanostomum pristis* were also observed in this fish, as already reported in several studies from the Mediterranean Sea. Similarly, records of *Helicometra fasciata, Lecithocladium* sp. and *Opechona* sp. were made in *Scomber scombrus*, confirming this fish as a common host for these parasites.

Concluding, future studies on different topics are needed to complete the picture about jellyfish, their parasites and their position in the ecosystem of the Gulf of Trieste. Studies will need to address local gastropods in order to find the potential first host and the potential relationships between the parasites, their host and its physiology, and external factors like seasonality. A similar approach needs to be taken to shed light on the definitive fish host, in order to "close" the life cycle. For all the hosts, it would be interesting to investigate the potential impact or effect due to the presence of parasites. To date, digeneans have been declared to not harm the jellyfish (no study focused on "true" biomarkers analysis), but, as mentioned above, some species can cause severe castration to the gastropod first host or interfere with fish metabolism and potentially cause mortality, with severe repercussions on economic activities if these hosts would be commercial species. Last, since no historical data regarding digeneans in gelatinous zooplankton in the area is available, jellyfish still need to be monitored to check if the parasitological values and the species involved recorded during these 3 years will change or if they will remain constant overtime.

Chapter 5

A novel endocast technique providing a 3D quantitative analysis of the gastrovascular system in *Rhizostoma pulmo*: an unexpected through-gut in cnidaria

Massimo Avian[1*¶], Lucia Mancini[2,#a], Marco Voltolini[2,#b], Delphine Bonnet[3], Diego Dreossi[2], Vanessa Macaluso[1], Nicole Pillepich[1], Laura Prieto[4], Andreja Ramšak[5], Antonio Terlizzi[1,6], Gregorio Motta[1,6¶]

[1] Department of Life Science, University of Trieste, Trieste, Italy.

[2] Elettra-Sincrotrone Trieste S.C.p.A., S.S. 14 Area Science Park, Basovizza, Trieste Italy.

[3] MARBEC, Université de Montpellier, CNRS, Ifremer, IRD, Montpellier, France.

[4] Group Ecosystem Oceanography, Department of Ecology and Coastal Management, Instituto de Ciencias Marinas de Andalucia (CSIC), Cádiz, Spain.

[5] National Institute of Biology, Marine Biology Station, Piran, Slovenia.

[6] Department of Integrative Marine Ecology (EMI), Stazione Zoologica Anton Dohrn, Napoli, Italy.

[#a] Current Address: Slovenian National Building and Civil Engineering Institute, Ljubljana, Slovenia.

[#b] Current Address: Department of Earth Science Ardito Desio, University of Milano, Milano, Italy.

* Corresponding author

E-mail: avian@units.it (MA)

[¶]These authors contributed equally to this work (MA and GM)

Abstract

The investigation of jellyfish gastrovascular systems mainly focused on stain injections and dissections, negatively affected by thickness and opacity of the mesoglea. Therefore, descriptions are incomplete and data about tridimensional structures are scarce. In this work, morphological and functional anatomy of the gastrovascular system of *Rhizostoma pulmo* (Macri 1778) was investigated in detail with innovative techniques: resin endocasts and 3D X-ray computed microtomography. The gastrovascular system consists of a series of branching canals ending with numerous openings within the frilled margins of the oral arms. Canals presented a peculiar double hemi-canal structure with a medial adhesion area which separates centrifugal and centripetal flows. The inward flow involves only the "mouth" openings on the internal wing of the oral arm and relative hemi-canals, while the outward flow involves only the two outermost wings' hemi-canals and relative "anal" openings on the external oral arm. The openings differentiation recalls the functional characteristics of a through-gut apparatus. We cannot define the gastrovascular system in *Rhizostoma pulmo* as a traditional through-gut, rather an example of adaptive convergence, that partially invalidates the paradigm of a single oral opening with both the uptake and excrete function.

1. Introduction

Cnidaria is a Precambrian phylum comprising about 10.000 living known species, and nearly 4,055 of these are Medusozoa [12]. Nowadays, jellyfish have become increasingly important for the scientific community as jellyfish blooms have been observed to increase all over the world [72,175,176]. Jellyfish can play a dominant role in structuring planktonic communities, and they may directly and indirectly interact and interfere with human economic and recreational activities, ecosystem services, public health and local wildlife [177]. Thus, a deep knowledge about their biology, physiology, anatomy, and ecology is required to understand the dynamics of blooms and to predict their occurrence and impacts, also in relation to climate change.

Within Cnidaria, the gastrovascular apparatus is based mainly of a central cavity, the stomach, connected with the outside through a single opening, the "mouth", and from which a series of extensions, pouches or canals, branch out, reaching the periphery of the organism. The internal fluid circulation is ensured by the ciliary motion of the gastrodermic layer that delimits the "gastrovascular" system. To provide a constant exchange of internal fluids, a double circulation (in and out) has therefore developed, both in the anatomical polyp body plan (with the formation of one or two ciliated furrows, the siphonoglyphs, in several anthozoans), and in the medusa one [16,92,178].

The Medusozoa are a monophyletic group with a wide range of gut anatomies and digestive mechanisms [19]. This Subphylum is characterized by a sac-like gut with a single opening that acts both as mouth and anus [16,178]. Ciliary currents carry food to the gut through the mouth as well as perform food egestion from the same oral opening [178]. This general idea is supported by anatomical and physiological studies [179–181]. Within the clade Acraspeda, staurozoans maintain a roughly polyp-like circulation pattern even in the benthic medusa stage, whilst in the Rhopaliophora (Cubozoa and Scyphozoa) clade jellyfish exhibit a series of pouches (Cubozoa; Coronatae, Pelagiidae, Cyaneidae, Drymonematidae and Phacellophoridae within Semaeostomeae scyphozoans) or canals (Ulmaridae within Semaeostomeae, and Rhizostomeae) reaching the umbrella margins. However, most of the jellyfish maintain a single central opening, the cruciform mouth. In gastrovascular systems thus structured, the inward and outward circulation begins to be spatially separated with the appearance

of the umbellar canals in the Ulmaridae, characterized by centrifugal flows in the adradial canals, and centripetal flows in the perradial canals. In the stomach, the outward perradial currents flow outside the umbrellar gastrovascular system from the peripheral base of the gastro-oral groove (= the edges of the cruciform manubrium canal) while the inward currents flow in the proximal part of the groove (= the medial portion of the cruciform manubrium canal [16,118,182]. A further increase in complexity, with the regression of the central mouth replaced by a network of oral arm canals (initially four, originating by the cruciform grooves of the original mouth, with a complicated course due to the hypertrophic development of the four genital sinuses) is present in the Rhizostomeae only. Some benthic Cambrian medusozoan fossils, very well preserved, probably cubozoans, are devoid of radial canals [183,184], so the potential evolutionary steps could have been the extension of broad gastric pouches up to the umbrella margins (in swimming medusae), the reduction of broad gastric pouches by fusion between exumbrellar and subumbrellar gastroderm [183], their ramification, especially in the inter- and adradial areas (involved to centrifugal fluxes), and the reduction of the single central mouth with the origin of a network of oral arms canals, which led to the appearance of numerous mouths, a specialization for a planktophagous diet, in rhizostomean medusae. Within these adaptations, the network of oral arms canals and related "mouths" must therefore make up for both incoming and outgoing flows, and, to date, the most widespread idea (in the absence of experimental evidence) hypothesized that the direction of the ciliary currents within the oral arm canals may be reversible. According to this theory, the internal circulation rely on the same single opening (or many) for both ingestion and egestion of food. However, Arai and Chan [185] demonstrated that the hydromedusan *Aequorea victoria* possess other openings in addition to the central mouth. *Aequorea victoria* was shown to egest material from both its gastrovascular cavity through its mouth, but also through radial subumbrellar papillae and pores [185]. Despite this is not being a proper trough-gut, it was the first observation that collides with the single oral opening paradigm of Cnidarian anatomy. Similarly, in Ctenophora, Presnell [186] proved that *Mnemiopsis leidyi* possess a proper unidirectional tripartite through-gut. This evidence deeply collides with the common theories of the evolution of the metazoan through-gut, although its origin is currently a matter of debate [187]. Furthermore, other recent studies

are now discussing the hypothesis that Ctenophora may be the first branching extant metazoan phylum [188–191].

The common statements on the metazoan evolution take it for granted that the first through-gut appeared within Bilateria [192,193]. Except for Porifera and Placozoa, the other non-Bilateria phylum such as Cnidaria and Ctenophora are thought to possess simple digestive systems for the extracellular breakdown of ingested food [194]. A hypothesis concerning the through-gut origin speculates that it may have appeared in the elder metazoans, and it may have been lost in successive phyla until Bilateria or ctenophores converged to an analogue organ close to the bilaterian through-gut [186]. However, at least in the cnidarians, and especially in the jellyfish body plan, it seems that the gastrovascular system has undergone various adaptations, some of which seem an adaptive convergence with the bilaterian through-gut, like the *Aequorea* group, and other taxa, which developed an innovative complex network of anastomosed canals both in the umbrella (similar to a capillary network) and the oral arms, with relative increase of the openings ("mouths") with the outside.

Rhizostoma pulmo (S1 Fig) is one of the first jellyfish species formally described in history [80], however, up to now, a complete description of its gastrovascular system is still missing, despite being a rather common jellyfish along the coasts of the Mediterranean Sea [81,195]. As part of a research on defining the phylogenetic pattern of the *Rhizostoma* genus, the morphology and functional anatomy of the species *Rhizostoma pulmo* were analyzed in detail.

In this work, we investigated the morphology of the gastrovascular system of jellyfish by using a novel approach combining resin endocasts and laboratory-based X-ray computed microtomography (µCT). The µCT data acquisition of the cast replicating the gastrovascular system of the medusa opened, for the first time, the opportunity to describe its manubrium system topology in a fully

quantitative fashion. The comprehension of the gastrovascular system and its circulation pattern are very important to understand jellyfish feeding physiology and their role in the trophic webs.

Our main objectives were:

1) to create a new protocol for the investigation of the morphology of gastrovascular systems in jellyfish by using epoxy resins in order to create solid three-dimensional (3D) casts of the vascular systems.

2) to describe and measure the morphology of the umbrellar and manubrium gastrovascular system from X-ray μCT.

3) to investigate the circulation pattern among the complex canal system of *Rhizostoma pulmo*.

2. Results

2.1 Morphological analyses

As a result of contrast injections (see S3 Fig), cast experiments (Fig 1a) and X-ray µCT (Fig 1b), it has been possible to analyze the gastrovascular structure of *Rhizostoma pulmo*. The present study allowed us to provide new and original morphological-anatomical details both at umbrellar and manubrium level. All diameter values in this work refer to the jellyfish apparent diameter, not the real diameter (see Methods, S1a Fig).
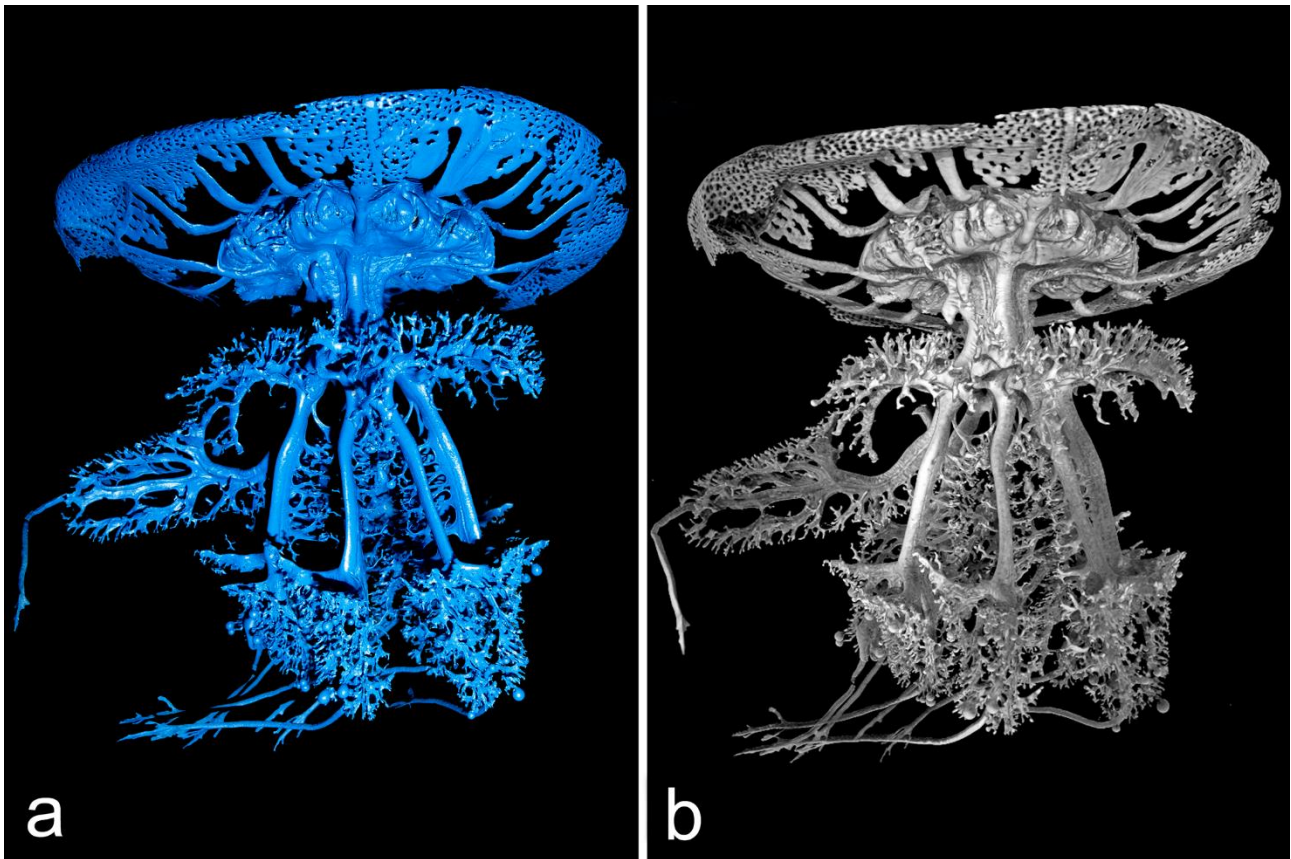
Fig 1. *Rhizostoma pulmo* gastrovascular system of the manubrium. **(a)** Resin endocast of the whole gastrovascular system of a specimen of 14.6 cm in diameter. **(b)** 3D rendering obtained by X-ray microtomographic data of the resin endocast showed in (a). Tomographic reconstruction performed with an isotropic voxel size of 62.0 µm.

Umbrella

At umbrellar level, the stomach is four sided, from which sixteen radial canals originate. Four cross shaped straight perradial canals originating from the peripheral ring canal are literally immersed in the subumbrellar mesoglea layer (Fig. 2).
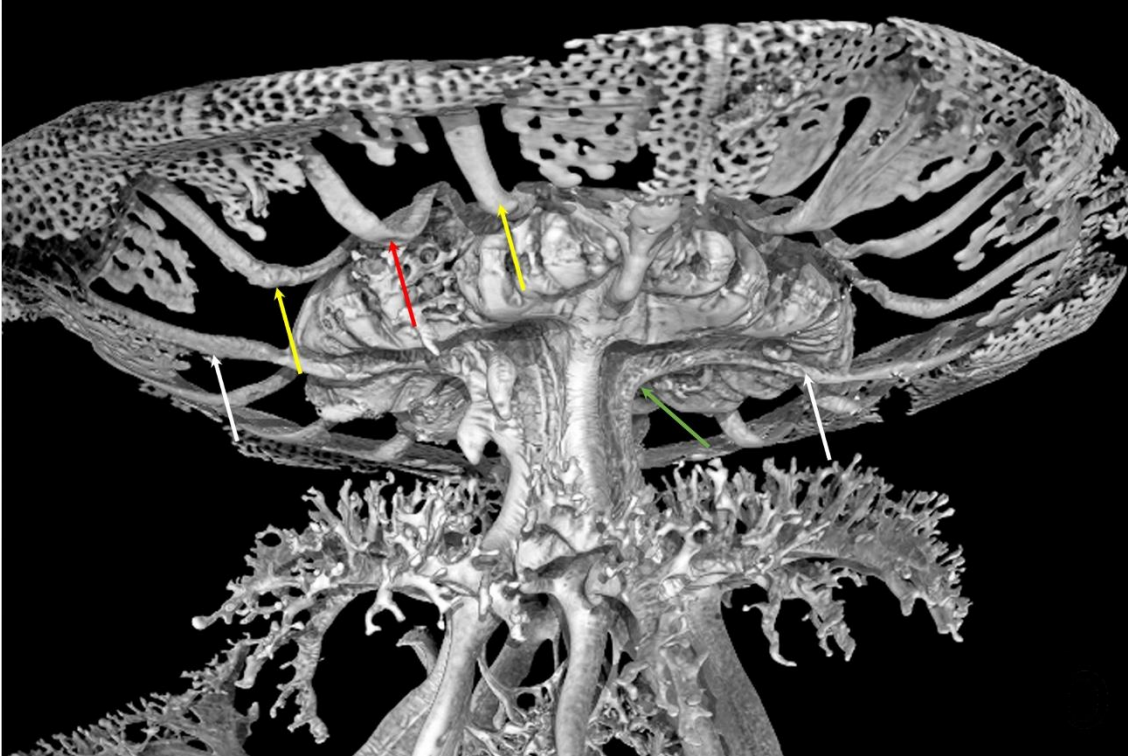
Fig 2. Volume rendering of the resin endocast obtained via X-ray µCT, showing an enlarged view of Fig 1b: detail of the stomach, subumbrellar view. The radial canals per quadrant, emerging from the stomach are visible. Arrows indicate: two perradial canals (white), one interradial canal (red), two adradial canals (yellow) and the perradial canal passage into the manubrium (green). CT reconstruction performed with an isotropic voxel size of 62.0 µm.

In specimens of about 5-10 cm in diameter, the two subumbrellar edges that delimit these canals from the stomach are in slight contact, starting to virtually isolate them (Fig 3a, b). In larger medusae these edges adhere more widely, making the perradial canals practically independent from the overlying stomach (Fig 3c, d). They are alternated with the four interradial canals as well the eight adradial canals. All inter- adradial canals origin from the upper part of the stomach, then they bend downwards before getting straight in the distal umbrellar portion, just over the coronal muscle (Fig 2, Fig 3c, Fig 4b).

The endocasts also showed that the stomach roof is not concave, but convex (Fig 4a-d).

This central upper convexity can be better seen in younger specimens, less than 15 cm in diameter. Later on, this convexity develops a central, protruding, flattened four-sided pyramid that continues distally with four small ridges exactly corresponding to the perradia (Fig 4c, d).

The stomach floor is cruciform, composed by four interradial triangular areas, alternated with four perradial depressions which correspond to the perradial canals (Fig 3a, b, S2c, d Fig).
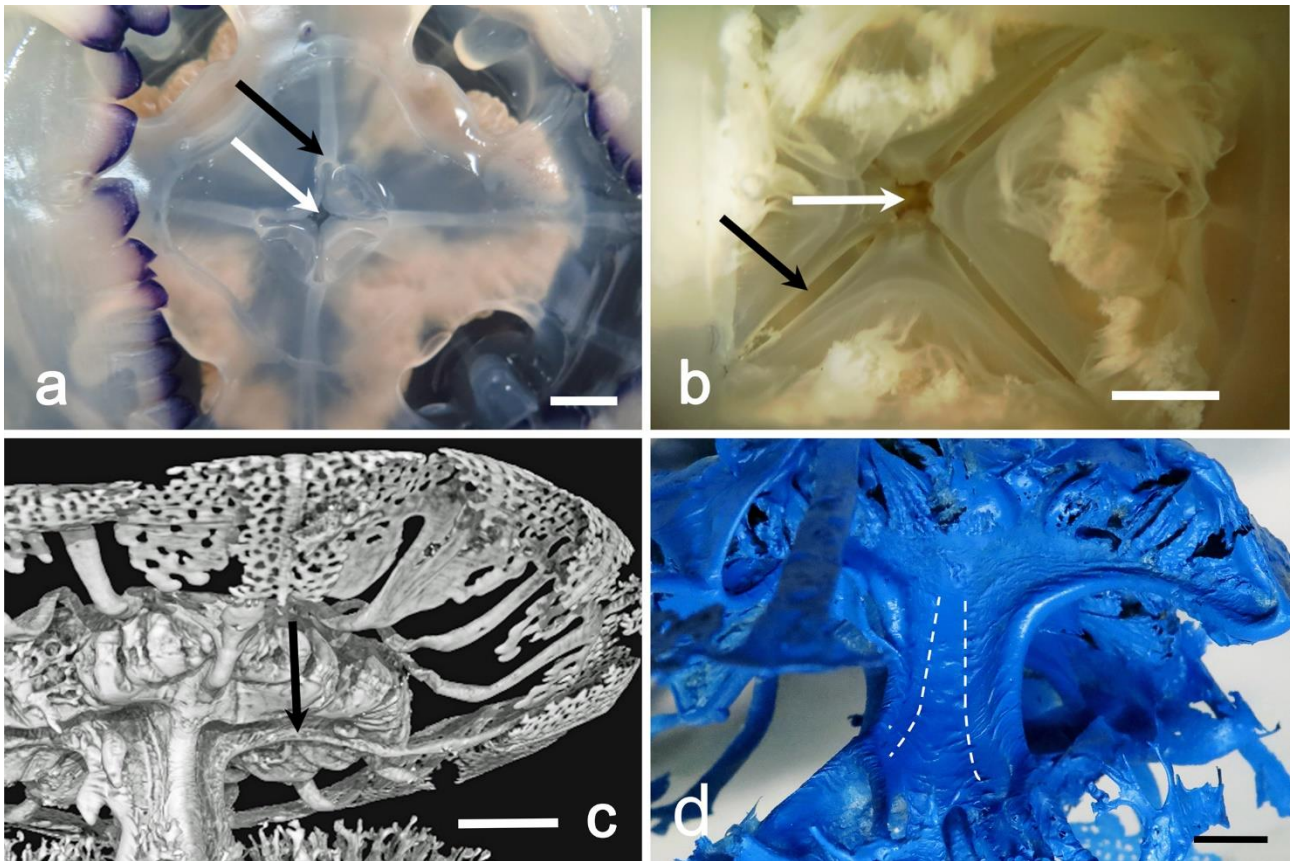
Fig 3. Relationship of the perradial canals and the juvenile mouth opening. **(a)** Subumbrellar view of a young medusa, manubrium excised. White arrow indicates the remnant of the original mouth. Black arrow indicates the section of one perradial canal. The edges that delimit the canals are still partially adjacent (scale bar = 1 cm). **(b)** Exumbrellar view of the stomach floor of another young specimen. White arrow indicates the quadrangular central remnant of the mouth. Black arrow indicates the still partially opened edges of a perradial canal (scale bar = 0.5 cm). **(c)** Volume rendering of the subumbrellar region of the resin endocast, obtained by X-ray μCT. Black arrow indicates a protruding perradial canal from the stomach floor. CT reconstruction performed with an isotropic voxel size of 62.0 μm. **(d)** Endocast of a larger specimen (35 cm diam.). The area of adherence of the perradial

123

canal edges is noticeably increased. Dashed lines indicate the end of the adhering stripes in the proximal portion of the manubrium (scale bar = 1 cm).
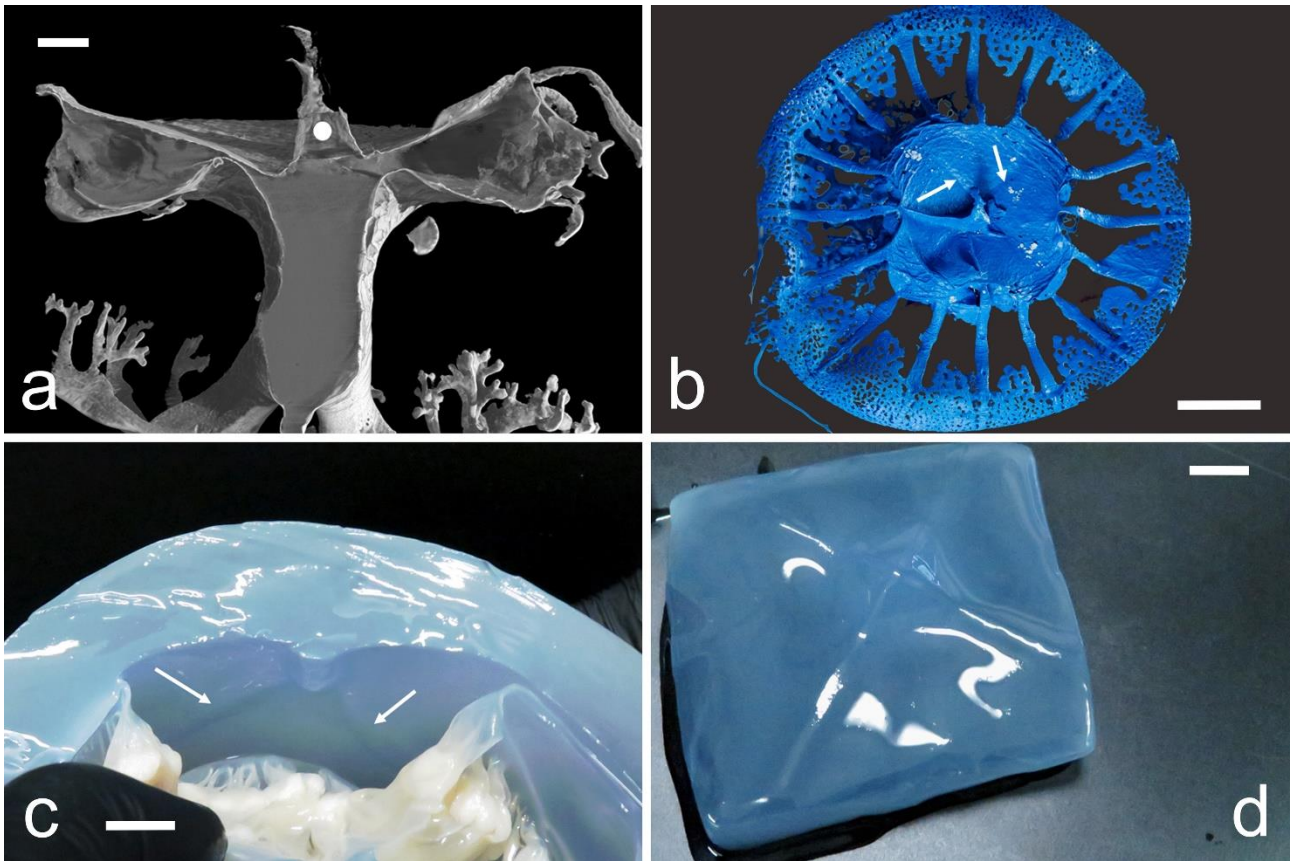
Fig 4. Morphology of the exumbrellar limit of the stomach. **(a)** Median sagittal section of the endocast showed in Fig. 1b, evidencing the convexity of the stomach roof. White spot indicates the artefact due to the resin injection. CT reconstruction performed with an isotropic voxel size of 62.0 µm. **(b)** Endocast exumbrellar view. White arrows indicate two of the four perradial outlined ridges (scale bar = 1 cm). **(c)** Interradial section of a 29 cm adult evidencing the upper central protruding pyramid. Arrows indicate two of the perradial ridges (scale bar = 1.5 cm). **(d)** Subumbrellar view of the stomach roof of a specimen of 33 cm diam. showing the central protruding square pyramid and the four perradial ridges (scale bar = 1 cm).

Manubrium

The gastrovascular system of the manubrium starts with a deep cruciform opening, the edges of which correspond to the perradial canals. This cruciform opening is the residual of the central mouth of the ephyra - post-ephyra stages (Fig 3a, b, Fig. 5a, b, Fig. 6a-d, S2c, d Fig). In adults, the mouth opening,

still open in the post-ephyra phase (up to a diam. of about 3 cm, S2a, b Fig), is almost sealed (S3a Fig).

From the edges of this cruciform opening originate four apparently flattened canals. The canals section is not simply flattened, rather recall an eight shape, compressed in the median portion. This portion is not fused (as the stains injections in fixed samples seemed to evidence, S3b Fig), but the gastrodermic layer of both sides is in contact through a specular crenulation (Fig 5c, d). This structure simulates a double canal system. In living specimens, these adhesions limit the communication between the two hemi-canals. Comparing the same canal's cross-sections of a specimen with a diameter of 18 cm with an adult specimen of 26.1 cm, and calculating an "adherence ratio" (adhering stripe width/canal total width) (Fig 5c, d) it was possible to observe that the ratio remains rather constant, with a value of 0.35 for the young specimen, and of 0.36 for the adult one, even if the adhering stripe width increases from 2.88 mm to 3.53 mm in the adult.

In the proximal portion of the manubrium, between the genital sinuses and the scapulae (= scapulets, epaulettes), the outer hemi-canal bifurcates into two, while the inner hemi-canal bifurcates just below (two overlapped "Y"-shape branches, Fig 5a, b), forming a total of eight hemi-canals, one for each oral arm. At scapulae level (each oral arm has two scapulae), two hemi-canals (the distal and the proximal) bifurcates into two lateral hemi-canals which continue into the scapulae (Fig 5e-g). The endocast also highlighted the pattern of the scapular canal emergence from the oral arm canals. The disposition of the upper secondary ramified scapular canalicula seems mostly related with the upper hemi-canal. The most distal, always dichotomously branched, is connected with the lower hemi-canal. This canalicular pattern undergoes further complications in larger specimens, where some lateral canaliculi also connect with the lower hemi-canal (Fig 5f, g).

Within each scapula the canals branch into many tiny canals reaching the upper frilled margins, ending in multiple openings (Fig. 5g).
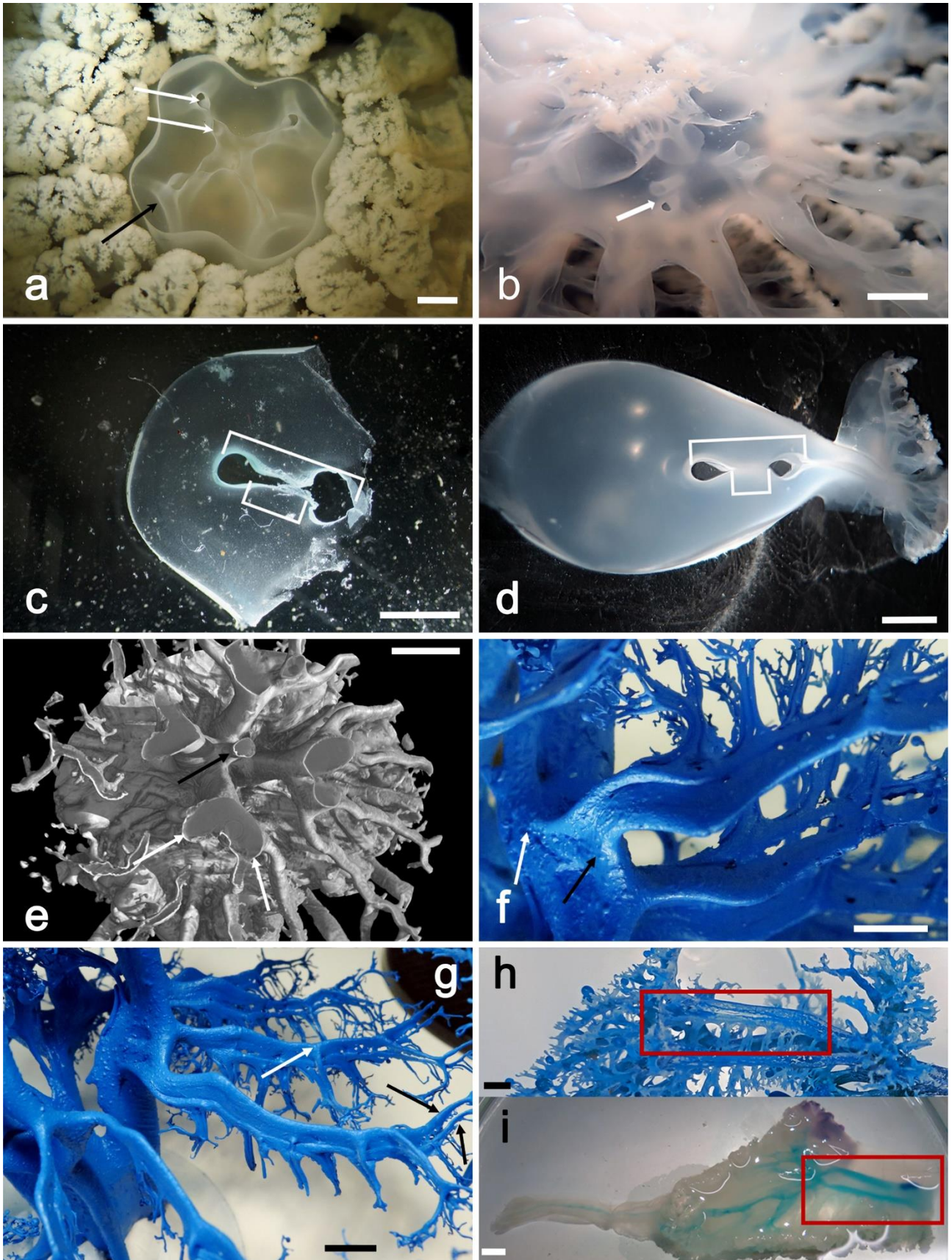
Fig. 5 Morphology of the manubrium gastrovascular system. **(a)** Manubrium section over the emergence of the scapulae, exumbrellar view. Visible the hemi-canals pattern (white arrows) branching from the central cavity, the internal one partially emerging. Black arrow indicates one of

the further dichotomic branches of the oral arms duplication (scale bar = 0.5 cm). **(b)** Section at subscapular level, subumbrellar view (scale bar = 1 cm). Arrow indicates one of the hemi-canal structures. **(c)** Transverse section of an oral arm at sub scapular level. Larger square bracket indicates the total canal length, smaller one the medial adhering area (scale bar =0.5 cm). **(d)** Same as in (c) (scale bar = 0.5 cm). **(e)** Subumbrellar 3D rendering of a specimen sub-volume obtained by X-ray µCT; white arrows indicate the dichotomization of two oral arms main canals, black arrow indicates the remnant of the juvenile central mouth opening. CT reconstruction performed with an isotropic voxel size of 62.0 µm. **(f)** Endocast of a specimen of 32 cm diam. showing the emergence of the scapular hemi-canal. Arrows indicate the upper (white) and lower (black) hemi-canal (scale bar = 1 cm). **(g)** Scapular canal system, upside down view. White arrow indicates one branching connected to the lower canal, black arrows indicate the terminal dichotomic branching maintaining the two hemi-canals pattern (scale bar = 1 cm). **(h)** Endocast of one oral arm, showing the two hemi-canals pattern (scale bar = 1 cm). **(i)** Stain injected in the oral arm evidences the hemi-canal pattern. Red squares indicate the correspondent trait as in (h). The juvenile anastomoses on the left will disappear in more developed medusae (scale bar = 1 cm).

However, it was noticed that, especially in the smaller ones, like that of 14.6 cm in diameter measured by X-ray µCT measurements (Fig 1, Fig 3c, Fig 4a, Fig 5e), the resin injected into the gastrovascular system tends to slightly dilate the shape of the canals, reducing or masking the medial narrowing present in most of the canal system. In larger specimens (diam. ≥20 cm) this effect is strongly reduced, and, in some cases, it has been observed that the resin forms a very thin layer in the median area of adherence, thus making the two distal portions of the canals appearing clearly thicker (Fig. 3d, Fig. 5f-h). In larger medusae the origin of the lower scapular hemi-canal starts from the outer, distal oral arm hemi-canal, while the upper one starts from the internal, proximal hemi-canal of the oral arm. The adhering, medial portion of the scapular canal, begins from the corresponding adhering area of the oral arm canal, slightly sloped (Fig. 5f). This canal pattern is symmetrical, since each oral arm gives rise to two scapulae, one on each side (Fig 5g).

The other two hemi-canals continue under the scapulae (Fig. 5b, Fig. 5h) to the three-winged portion of the oral arm (S1b Fig). Here, in the initial part, in specimens with a diameter smaller than 15-20 cm, the two hemi-canals anastomose and subsequently fuse in the central part (Fig. 5i, S3b Fig) sending many lateral branches to the marginal opening of each wing. The fused canal continues into the terminal club, where it branches again at its ending (Fig. 5i). In larger medusae (diam. > 20 cm), however, the anastomosed tract regresses, and the two hemi-canals remain separated until the beginning of the terminal club canal, which is the only segment that remains undivided.

2.2 Image processing and analysis of the X-ray µCT data

The most complete endocast from a specimen of 14.6 cm in diameter was firstly visualized by means of virtual sectioning and using 3D rendering procedures (Fig 1b).

In addition to the computed morphometric analysis of the tomographic data (discussed in the next paragraph), the X-ray µCT data also allowed the investigation of the less accessible areas of the gastrovascular system, impossible to be properly examined by visual observations. The endocasts analyses already evidenced that the remnant of the juvenile central mouth opening (the central canal) continues with a small canal that apically branches into a series of small distal canals and relative openings right in the center of the oral arms (Fig 5e, Fig 6a-d, S1-4 Videos). However, its position and the complexity of the surrounding canals pattern masked this area, thus making it impossible to have a clear picture of this structure, and to describe it in detail.
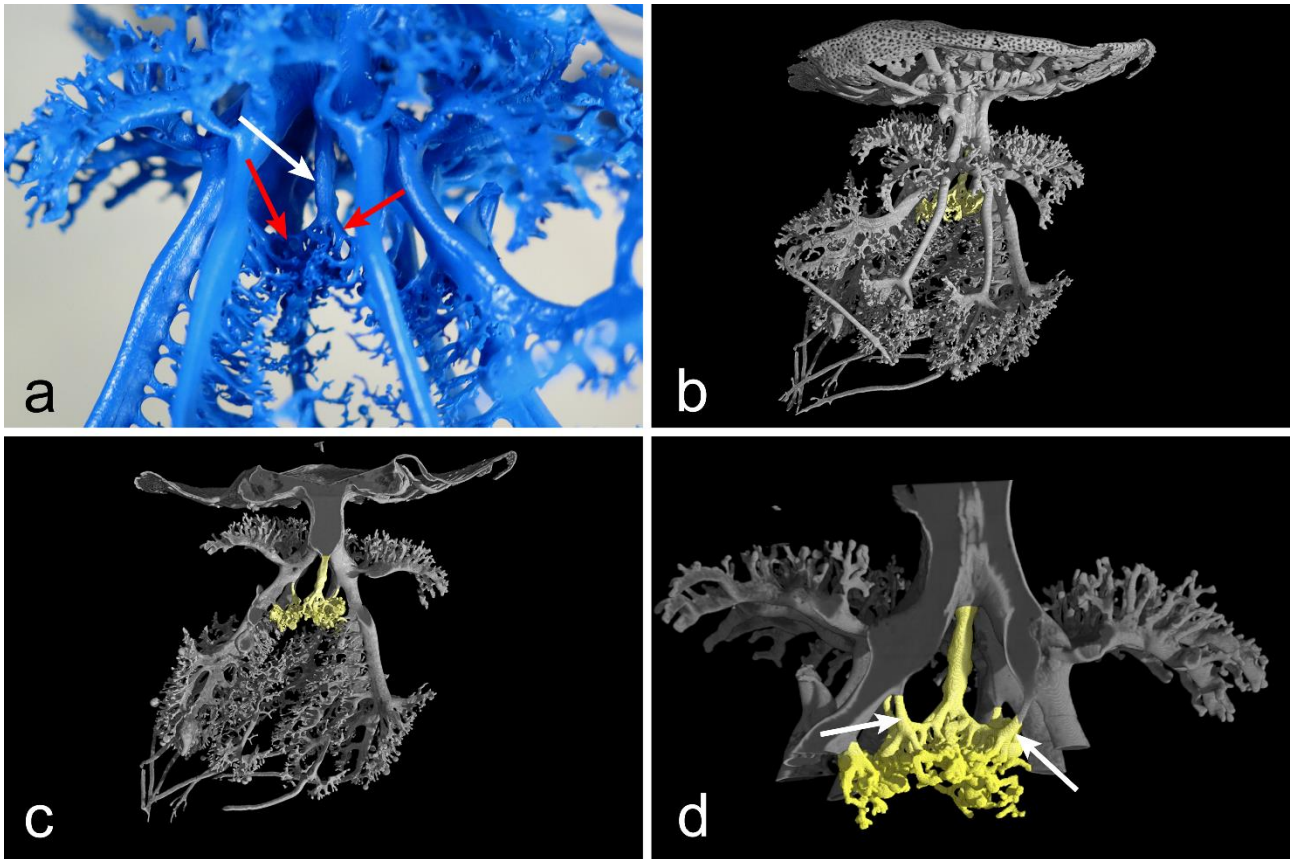
Fig 6. Morphology of the manubrium gastrovascular system. **(a)** Proximal internal region of the manubrium, showing the projection of the juvenile central mouth (white arrow), distally branching into a series of small canals with terminal openings (red arrows). **(b)** Volume rendering obtained by X-ray µCT showing the hidden central canal and its branches (yellow). **(c)** Longitudinal section of the volume shown in (b), highlighting two lateral canals connected with two oral arms. **(d)** Magnification of the region showed in (c), featuring all the four transverse connections with the proximal bifurcations of the emerging eight oral arms (arrows indicate two of them). CT reconstruction performed with an isotropic voxel size of 62.0 µm.

The 3D rendering and the consequent longitudinal sections highlighted that, in correspondence of the dichotomy of the oral arms (from the four proximal to eight distal) there are four transverse canals connecting the central canal with the point of emergence of the eight oral arms canals (Fig 6b-d; S1-4 Videos), slightly asymmetrically shifted to the left one. This connections pattern was observed in other endocasts of larger specimens, but it was slightly different, both in number (maybe two or three)

and symmetry (some connections seem to finish exactly in the middle of the dichotomic oral arm canals).

2.3 Morphometric analysis of the tomographic data

A graphical summary of the morphometric analysis of the tomographic data is shown in Fig 7.
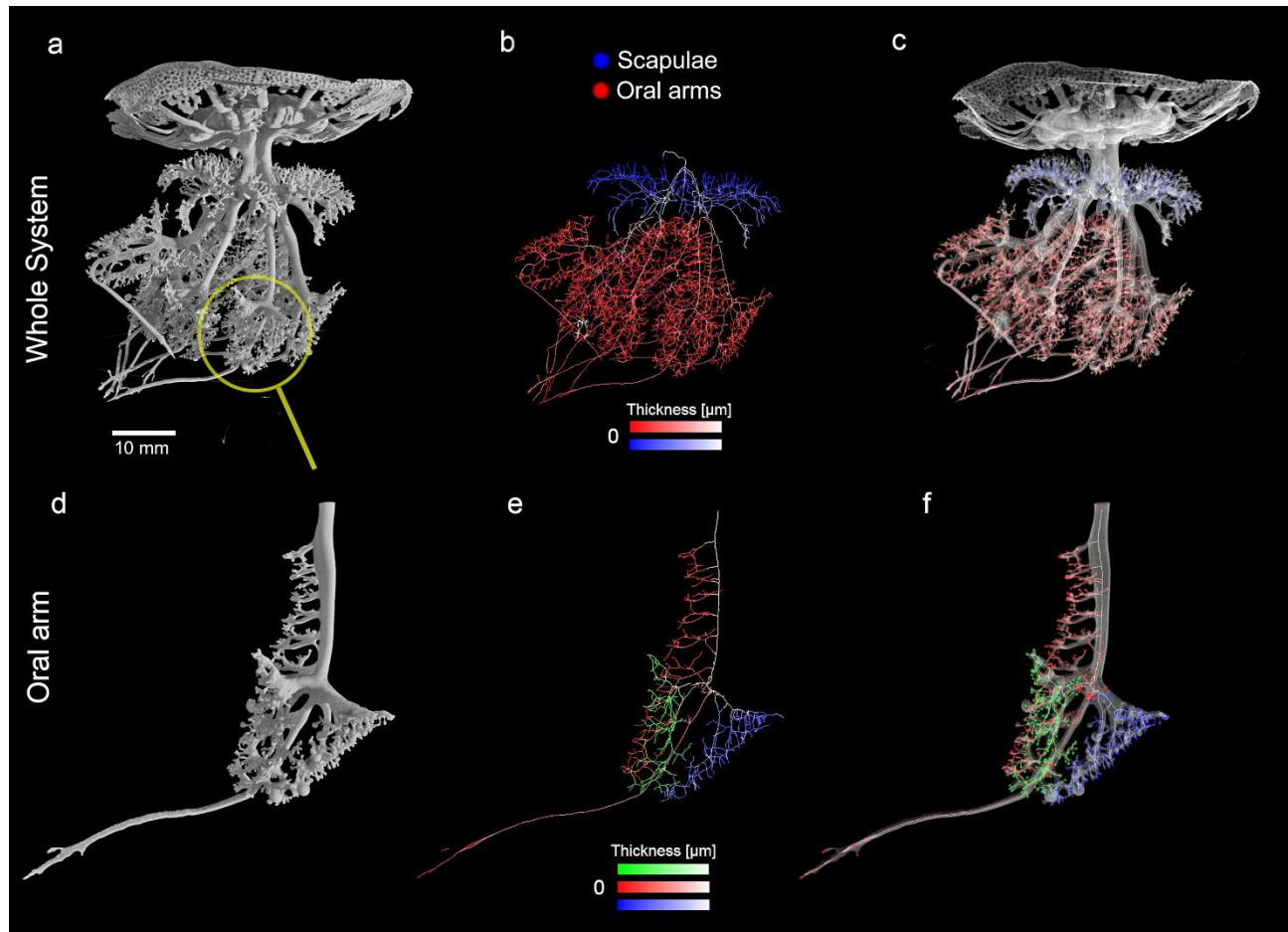
Fig. 7. Graphical summary of the results of the quantitative analysis on the gastrovascular system. **(a)** 3D rendering of the whole cast of the gastrovascular system measured via X-ray µCT. **(b)** Isosurface rendering showing the segmented gastrovascular system of the whole manubrium; false colors refer to the two different structures analyzed (blue = scapulae, red = oral arms). Color intensity is proportional to the local thickness values in the medial axis at that specific voxel. **(c)** Volume rendering of the cast; medial axes analysis, high intensity colors indicate the smaller canals. **(d)** Volume rendering of a single oral arm. **(e)** Thickness-labeled skeleton of the three-winged portions, each characterized by a specific hue (red, green, and blue). **(f)** Openings of the three different wings

labeled with the three different colors as in (e). CT reconstruction performed with an isotropic voxel size of 62.0 µm.

The total volume of the gastrovascular system and the single volumes of umbrella, scapulae, central canal and oral arms of the 3D digitalized endocast (specimen of 14.6 cm in diameter), are of 26.050 cm³, 11.591 cm³, 5.955 cm³, 0.193 cm³ and 8.312 cm³, respectively.

The volume rendering of the whole cast measured via X-ray µCT shown in (a), the yellow circle highlights the arm used for the more specific analysis of the single oral arm reported in (d). In (b), the hue refers to the two different structures analyzed (blue = scapulae, red = oral arms), the intensity being proportional to the local thickness values in the medial axis at that specific voxel (e.g., in the oral arms light pink indicates a wide canal, while the strong red shows the thinner canals). In (c), a highly transparent volume rendering of the cast and the canals pattern has been superimposed to better highlight the context of the medial axes analysis, with the high intensity colors being more distributed close to the distal openings, while the low intensity colors being localized in the large canals of the system, as expected. In the panels (d-f), the analysis of a single oral arm is shown, starting from the volume rendering (d), the thickness-labeled skeleton of the three-winged portions, each characterized by a specific hue (red, green, and blue) is observed, and again with the color intensity proportional to the thickness of the structure at each point (e). Finally, in (f) the skeleton has been superimposed to a transparent volume rendering of the arm, with the addition of the oral openings viewed as small spheres of pure red, green, and blue, depending on the part that the specific oral opening belongs to. A complete analysis of the cast has been also carried out, addressing the differences of the oral arms vs. the scapulae systems. In Fig 8a., the frequency histogram of the branch lengths of the two systems is plotted. As expected, the number of the branches is much higher in the oral arms, being a larger structure, but other interesting features, not easily recognizable from the graphical outputs, can be found: the mode of the branch length in the two systems is different, being higher in the scapulae than in the oral arms.
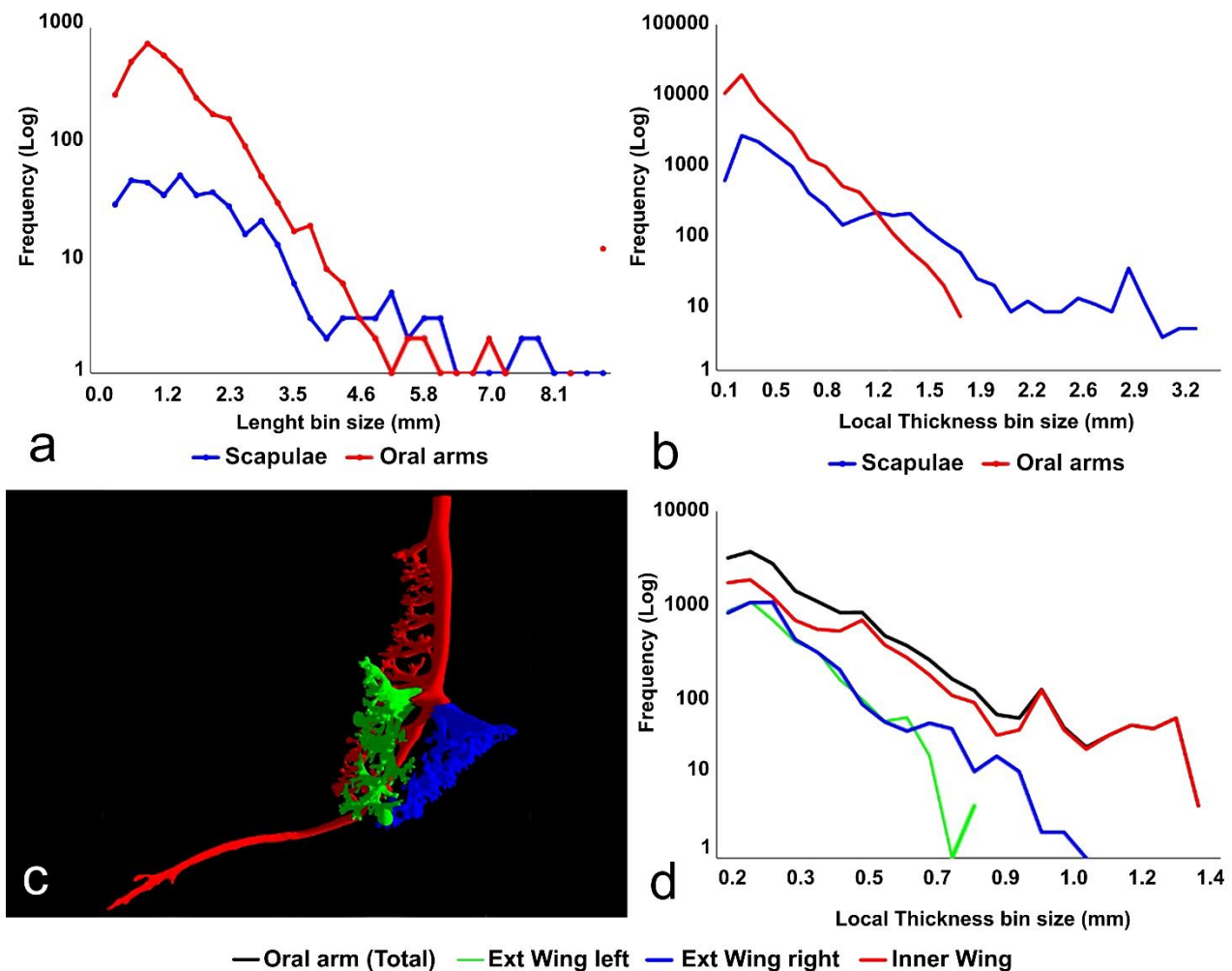
Fig 8. Morphometric analysis of the scapulae vs. the oral arms and thickness analysis of the three-winged portions in an oral arm. **(a)** Frequency plots of the branch lengths. **(b)** Thickness of the scapulae vs. the oral arms. **(c)** 3D isosurface rendering of a single oral arm. **(d)** Frequency histogram of the LT values within the three wings.

The distribution of the lengths in the scapulae is also significantly wider, with a less sharp peak and a less steep slope where the branch lengths increase (Fig 8b). The oral arms also show a small amount of very long branches, which are the canals in the terminal clubs.

Table 1 provides important morphological measurements about the length of the branches in the two different structures. Despite the long canals, the average branch length is noticeably smaller in the oral arms, with the more terminal portion of the canals being numerically the most important contributor of the gastrovascular structure (Fig 8a).

Table 1. Summary of the skeleton analysis [43].

	Scapulae	Oral Arms
Average Branch Length [mm]	3.54	2.36
Average Branch Euclidean Distance [mm]	2.87	1.93
ED/Length	0.812	0.820
Number of Total Branches	396	3304
Number of Total Junctions	192	1685
Number of Total Endpoints	205	2987

Results from the computed morphometric analysis of the tomographic data from the endocast of a specimen of 14.6 cm in diameter.

ED = Euclidean Distance.

The tortuosity of the branches is almost identical (and rather straight), as highlighted by the Euclidean Distance of the two endpoints vs. the length of the branch being slightly higher than 0.8. More, the number of endpoints (roughly equivalent to the number of openings) vs. the number of branches is higher in the oral arm structure, highlighting again the larger relative contribution of these canals to the system.

Concerning the thickness analysis of the two systems, the frequency histograms of the local thickness (LT) values of the cast have been plotted in Fig 8b. The oral arms frequency distribution highlights an almost perfect lognormal distribution of the thicknesses. In the scapulae, the section of the plot featuring the smaller size of the canals shows almost exactly the same lognormal trend. The contribution (at the higher LT values) of the central main canals connecting to the stomach, splitting first in 4 and later in 8 channels, is evidenced by the peek in the frequency plot.

The analysis on the single oral arm aims at highlighting the differences of the two outer winged portions compared to the inner one. The investigated oral arm has been separated in three sub-structures, independently analyzed, as shown in Fig 8c.

In the thickness analysis of the single arm (Fig 8d), the two outer wings (green and blue) show trends almost exactly overlapping, while the inner wing (red) presents a slightly different trend due mostly to the presence of the terminal club canal and the thickest canals where the smaller ones are connected to it (see also Fig 7e).

In addition to thickness analysis, on the same arm (the best accurate reproduction of an oral arm), the number of the openings has been calculated. The number of endpoints in the inner (red) and external (blue and green) parts of the three-winged portion accounted for 234 (internal), 129 and 128 openings (external), respectively.

Likewise, the number of the openings of the central canal (Fig 6) has been quantified, with its branching ending with 81 endpoints.

Considering the whole organism (8 oral arms), based on the numbers reported above for the single oral arm, the inner openings (central canals + internal wing of the oral arms) should account for about 1953 openings while the external ones (blue and green parts of the winged portion) should account for about 2048.

2.4 Functional anatomy

The injections experiments in living specimens show a clear and permanent two-way flow circulation within the two hemi-canals. After injecting the staining solutions in the center of the stomach, the stain initially flows only in two directions, down towards the manubrium and into the umbrellar canals.

In the umbrella, the stain flows outwards only in the adradial canals first (Fig 9a, c), reaching the proximal main ring canal. From this ring, the stain circulates via the inner ring canal either towards the interradial and perradial canals (Fig 9a-c), and towards the distal ring canal (Fig. 9d), starting to stain the inner anastomosed canals mesh (Fig. 9e). When the distal ring canal is reached, the stain flows towards the outer portion of the interradial and perradial canals, staining the rest of the canals mesh (Fig 9f; S5 Video). The stain into the interradial canals flows into the upper portion of the stomach again, while the stain into the perradial canals reaches the edges of the central stomach cruciform opening, driven towards the manubrium (Fig 9a-f; Fig 11a).
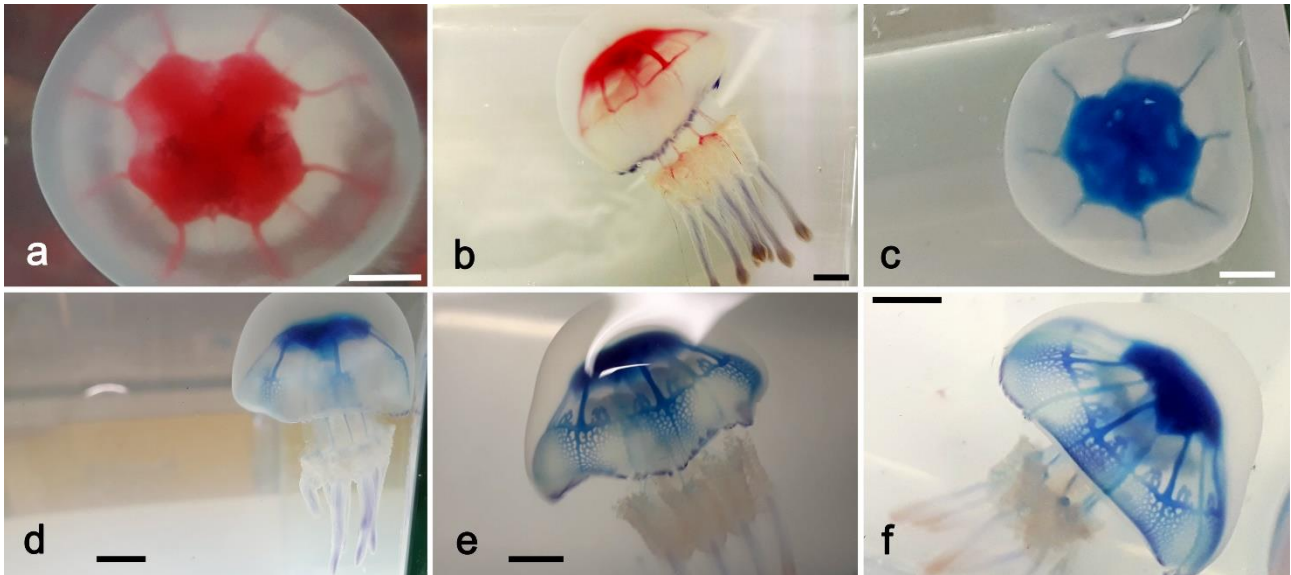
Fig. 9 Functional anatomy of the gastrovascular system. (**a**) Living specimen with stained stomach, with stain diffusion into the adradial canals after 1 min from the injection (scale bar = 1 cm). (**b**) Same specimen, lateral view, after 1 min from (a). Staining of the internal ring canal. Manubrium: the stain transits into the external hemi-canals, and the upper openings of the external oral arm wings (scale bar = 1 cm). (**c**) Similar to (a), but specimen injected with methylene blue stain (scale bar = 1 cm). Adradial canals stained. (**d**) Initial coloration of the inner ring canal and the outwards adjacent anastomosed canals mesh (scale bar = 1 cm). (**e**) Beginning of coloration of the per- and interradial canals inside the inner ring canal. Beginning of coloration of the distal ring canal (scale bar = 1 cm). (**f**) Umbrellar canal system now completely stained (scale bar = 1 cm).
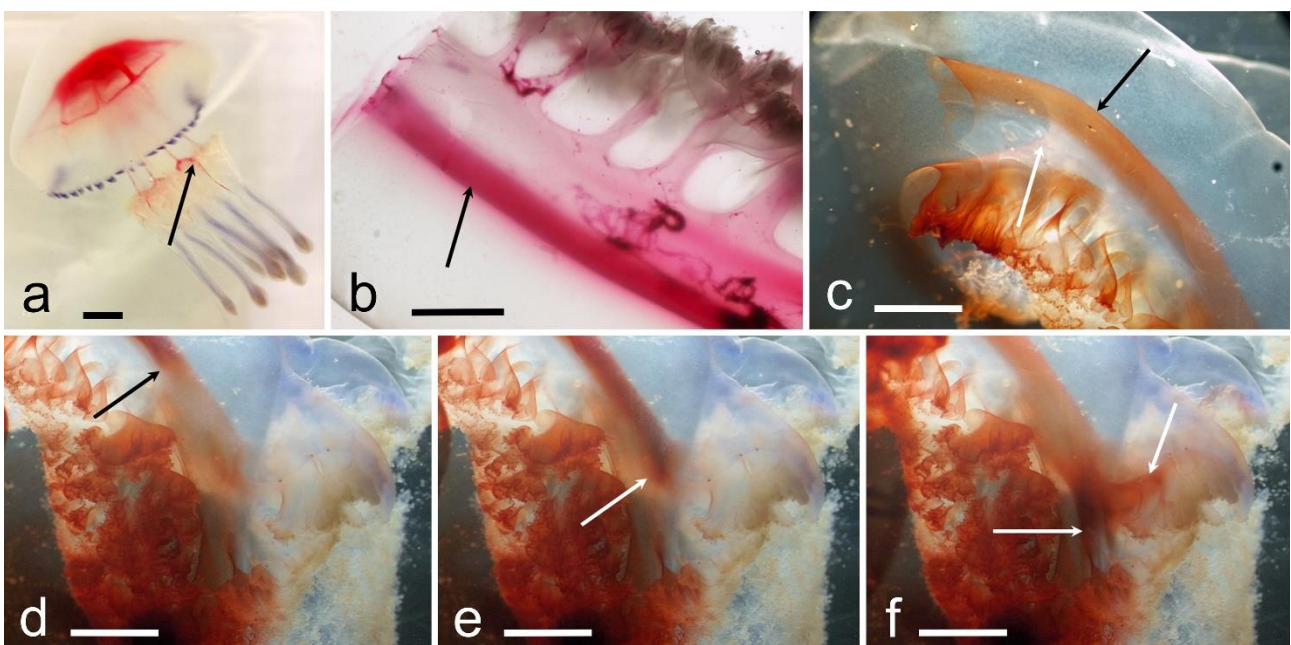
Fig. 10 Functional anatomy of the gastrovascular system. **(a)** Living specimen as in Fig 9 a-b, with mucous stained filament expelled from the upper openings of the external wings of the oral arms (scale bar = 1 cm). **(b)** Live excised scapula with red stain released just near the cutting surface (left). Stain mainly flowed in the lower hemi-canal (arrow) (scale bar = 0.5 cm). **(c)** Live oral arm cut under the scapulae, stained as above. Stain concentrated in the outer hemi-canal (black arrow), whilst the inner hemi-canal is unstained (white arrow). The frillings of the inner wing are stained by the stain droplets initially released in the proximity of the upper cutting surface, then externally diffused (bottom left) (scale bar = 0.5 cm). **(d-f)** Photographs from a clip following the stain diffusion into the outer hemi-canal. Arrows indicate three successive moments of the stain flux (scale bar = 0.5 cm).

At manubrium level, the stain solution evidenced a descending stream in the distal, outer hemi-canals (Fig 9b, Fig 10a) and an initial spill of a mucous colored filament is evicted mainly from the openings placed in the upper portion of the external oral arm wings (Fig. 10a).

A second experiment was performed on a living but excised oral arm at subscapular level of an adult specimen (diameter of 27 cm) where the stain was placed right on the cutting surface, showed an incoming flow only in the external, distal hemi-canal. This flow travelled up to the upper portion of the external wings (Fig 10c-f; S6 Video). An attempt to document the opposite flow by releasing the dye on the outer surface of the inner wing did not yield results, as the shock induced by the cut and related manipulation of the oral arm caused the release of mucus that quickly blocked the openings of all wings, internal wings included. Indeed, the experiment must be carried out in an extremely short time, in order not to lose an efficient flow induced by the ciliary beat, and therefore an "acclimatization" interval to reduce the phenomenon was not possible.

These data are supported by several *in vivo* observations, either in open water and in laboratory environment, where medusae, when physically stressed, quickly released a transparent semi-liquid stinging mucus from the outer wings of the oral arms and from the external portion of the scapulae. In contrast, in whole specimens, no mucus release from the inner wing of the oral arm has been recorded. It was also possible, during June-August, to observe some fully mature specimens releasing

the eggs. In that situation, filaments of more compact mucus (even longer than twenty centimeters and sandy colored due to phytoplankton and suspended particles agglutination) were observed dangling from the outer wings only.

However, the presence of particles in the water allowed us to document their transit into the two hemi-canals, centrifugal in the external one, centripetal in the internal one (S7 Video).

The scapulae (living but excised) show a slower speed of the flux, anyway it was possible to detect an outgoing flux into the lower canal (Fig 10b), originating from the distal hemi-canal of the oral arm, which is in line with the previous observations in the oral arms canals.

The test carried out using living stained zooplankton as food for a 10 cm jellyfish gave results congruent with previous experiments, even if the dispersion of the plankton in the body of water before its ingestion, the small size of individual organisms and their fast transit in the inner hemi-canals (approximately 1/2 - 1 cm/sec), did not allow us to properly document this experiment, except as a personal observation.

As a whole, summarizing all our observations, it seems that the centripetal flow starts from the openings placed on the internal "conoid" of the oral arms (inner wings plus the openings of the central canal) and on part of the scapular medial upper openings connected to the superior hemi-canals in the scapulae, while the centrifugal flow affects the openings on the two external wings and the more distal upper scapular openings connected to the lower hemi-canals of the scapulae (Fig. 11b).
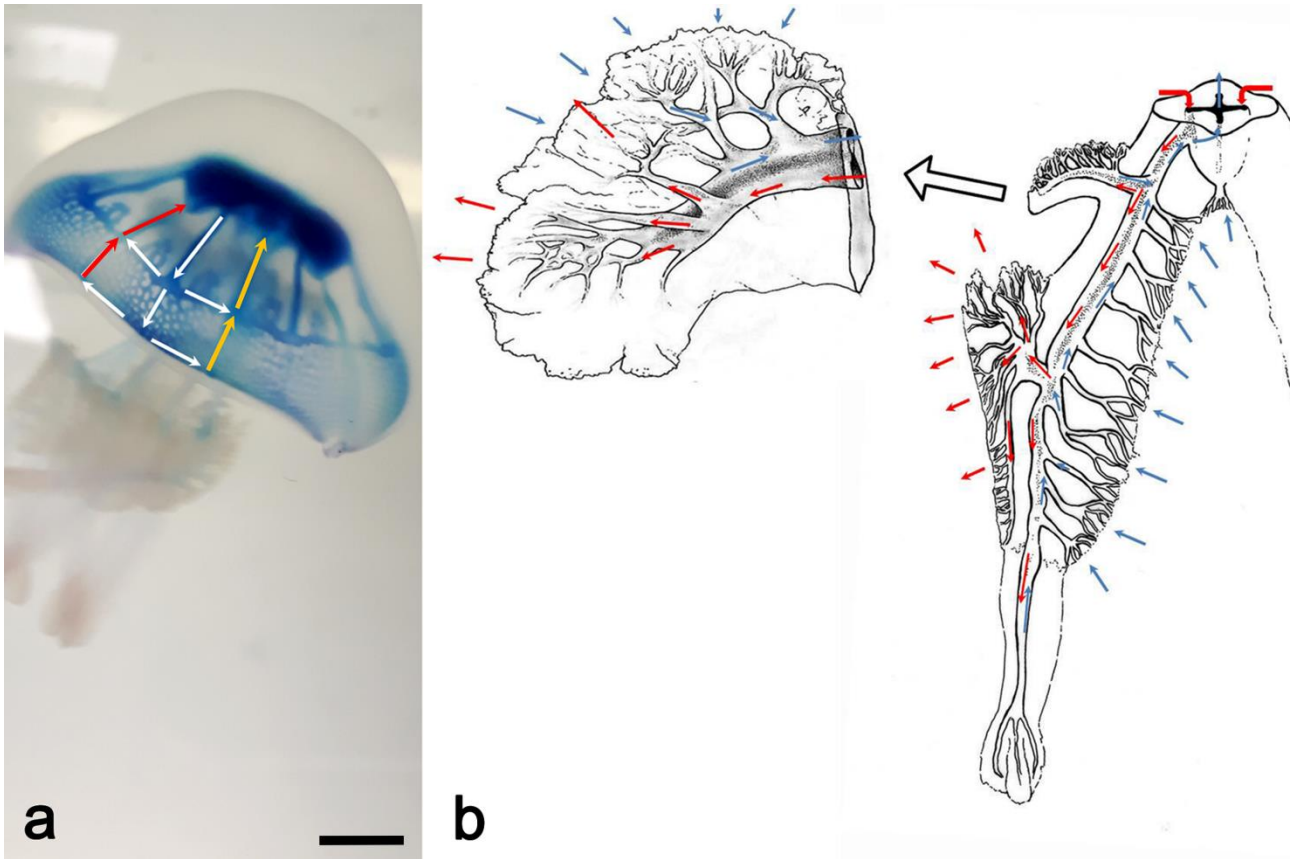
Fig 11. Functional anatomy of the gastrovascular system. **(a)** Living specimen as in Fig. 9 c-e, with superimposed arrows that outline the flow sequence; I, from stomach to the inner ring canal through the adradial canals (white arrows); II, through the inner ring canal towards the per/interradial canals and towards the distal ring canal; III, through the distal ring canal towards the per/interradial canals (yellow arrows) and relative anastomoses; simultaneously a perradial outgoing flux flows from the inner ring canal junction towards the manubrium (red arrows) (scale bar = 1 cm). **(b)** Drawing showing the bidirectional flux in the manubrium. Blue arrows, incoming flux, red arrows, outgoing flux. Top left, magnification at scapular level.

3. Discussion

Up to present day, the investigation of gastrovascular system in jellyfish mostly relied on the more traditional techniques: stain injection, dissections and external observations primarily on preserved specimens. Stain injections alone surely can highlight the path of canals trough the body of the jellyfish, but they can give few clues about the shape and the volume of the gastrovascular system. In addition, the traditional methods are significantly limited by the size and thickness of jellyfish. In large individuals, the remarkable opacity and thickness of the mesoglea layer highly affect the quality and precision of the observations. That is why, currently, the shapes and representations of Rhizostomeae gastrovascular systems, based on this kind of observations, are not highly detailed and lack tridimensional data.

The protocol described in this work, based on resin endocasts + 3D imaging by X-ray microtomography, solves most of these issues. The resin endocast is relatively cheap and easy to reproduce, providing tridimensional information about the gastrovascular systems of jellyfish, not accessible with traditional methods. Once scanned, it can be further analyzed with dedicated software tools in order to extract quantitative parameters such as volume, length, thickness and connectivity of canals. The spatial resolution of microtomographic images allows the investigation of fine details or inaccessible areas, such as the count of branching and openings of *Rhizostoma pulmo* gastrovascular system, impossible to study with traditional methods. Furthermore, the virtual volume reconstructed via 3D X-ray imaging becomes easily sharable in multiple copies all over the world, thus avoiding the issues related to samples dimension, number, processing, and delivery. We intend to share on request the raw data obtained. Clearly, data have to be used only for scientific, educational or divulgative purposes (no lucrative use).

Additionally, our unexpected findings on the double flux circulation and the openings functional specialization shed new light on the knowledge about the appearance and development of trough-gut during evolution.

The genus *Rhizostoma* Cuvier 1800 includes three species, *Rhizostoma pulmo* (Macri 1778), *Rhizostoma octopus* (Gmelin 1791) and *Rhizostoma luteum* (Quoy & Garmand, 1827). Their formal

descriptions, however, lack of data about their gastrovascular system in the manubrium. Anatomic observations of this structure are only available for *Rhizostoma octopus* [92,196–198].

In, literature, the unique description of a similar hemi-canals system in the manubrium, as the one evidenced in our study, belongs to Stiasny [196], which noted in *Lobonemoides robustus*, and other inscapulatae rhizostomeans, "two separate parallel tubes running inside the oral arm". Inside the genus *Rhizostoma*, he shortly reported in *Rhizostoma octopus* "The wider canals usually show double lumen" [196]. Russell [92] on the contrary, gave an accurate description of the canal system both in the umbrella and at manubrium level in *Rhizostoma octopus*, as a unique canal. In his detailed studies, there is no mention of any medial narrowing in the manubrium canals. Considering the correctness of Russell [92] description, the anatomies of the two species *Rhizostoma octopus* and *Rhizostoma pulmo* should differ [92].

Rhizostoma pulmo showed this unique and never previously described two hemi-canal structure that runs along all the manubrium, excluding the terminal clubs. Apart the distal appendages, all the centrifugal circulation is completely physically separated from the centripetal one. In addition, no flow reversal was ever observed in our experiments.

The experiments on living specimens showed therefore a permanent specialized two-way circulation within the two hemi-canals: an outgoing flow in the distal hemi-canals expelled mainly from the upper external mouths of the upper portion of the oral arm, and an incoming flow starting from the frilled internal (medial) part of the oral arms, continuing in the proximal hemi-canals (Fig 11b) with an opposite direction compared with the parallel outgoing one.

Generally, in jellyfish, the oral mouth is thought to carry out both the ingestion and the egestion of food [178]. This is accomplished by spatially or temporarily separated currents that move food particles in and out the stomach to the mouth for excretion [118].

Classic umbrellar flows, observed in various jellyfish, mainly Semaeostomeae [15,92,199–201], showed centrifugal flows exclusively into the adradial canals, with the interradial canals involved in a recirculation between the distal umbrella and stomach. Centripetal fluxes have been observed only in the perradial canals, flowing out at the four edges of the cruciform mouth in the Semaeostomeae (or

the central cruciform canal in the Rhizostomeae). In *Aurelia aurita* (Semaeostomeae), for example, the outward currents flow outside the gastrovascular system from the peripheral base of the gastro-oral groove while the inward currents flow in the proximal part of the groove [92,118,182].

Our observations of the umbrellar flow pattern in *Rhizostoma pulmo* correspond broadly to that described in *A. aurita* [92] (apart from the differences related to the presence in *Rhizostoma pulmo* of an internal ring canal and the numerous anastomoses present between the internal and external ring canals), with a centripetal flow exclusively in the perradial canals, physically isolated in their section between the internal ring canal and the central cruciform opening. Centrifugal flow occurs in the adradial canals, while the interradial canals appear to be involved in a recirculation from the periphery towards the stomach (Fig. 11a).

In *Cassiopea* sp., a drop in the pH in association with the secretion of proteinase has been measured after feeding. When the digestion is completed, the gut is "flushed out" and the pH rises [202]. Based on literature, this mechanism could fit species like *Rhizostoma octopus* since a single channel through the manubrium is described [92]. However, it has to be considered that few studies investigated gastrovascular circulation in jellyfish, with the exception of studies focusing on feeding physiology [181,185].

In *Rhizostoma pulmo*, we showed a complete physical separation of the currents by the development of a layer between the opposite fluxes. This double canal structure also implied a differentiation of the function of the openings on the oral arms, that we will not call mouths anymore. The openings with the excretory function, "anuses", are only the ones placed on the external wings of the oral arms and part of the scapular ones. At the same time, the openings (now proper mouths) placed on the frilled internal (medial) wings of the oral arms have the inhaling function, considering that none of these internal openings was recorded as excretory. Furthermore, these observations match with the typical stinging mucus release behavior that barrel jellyfish perform into the wild when disturbed. Mucus is typically observed right on the outer surface of the oral arms, and on the most distal portion of the scapulae. The release of mucous strips containing oocytes also corresponded with the aforementioned observations.

It could be hypothesized that these directions of flow could be reversible but, in all our observations, a reversal of flows has never been recorded.

It is also interesting to focus on the results about the computation of number and thickness of anuses and mouths. The number of openings in the manubrium is apparently similar (1953 in vs 2048 out), plus, the canals leading to the mouths are slightly thicker if compared to those leading to the anuses. Considering a continuous double flux where the net outflow should be zero, the slightly greater thickness of mouths could balance in terms of circulation the higher number of smaller anuses.

In addition, this is the first quantification (their number is incredible, completely unsuspected, until now) ever of the number of openings in scapulae and oral arms in Rhizostomeae. Up to now, in literature, they have been described just as "numerous", or "hundreds", or not reported at all [15,16,92,118,178].

It should be kept in mind that these values are not 100% accurate since the resin could have not filled all the canals (there are some indications that some of the canals of the outer wings, due to their limited thickness, are not always filled with resin up to all openings). This justifies the difference of the number of total openings based on the most complete single arm (4001) vs the number of total openings measured in the whole cast (2987, Table 1).

These observations are in contrast with the classic idea of Cnidaria anatomy and physiology where a single pore (or more openings, as in *Rhizostoma octopus*) accomplish both uptake and excretion due to an intermittent (all in/all out) ciliary flux [179–181,194,202–204].

Anatomically speaking, the umbrellar canal system corresponds to Russell's observations in *Rhizostoma octopus* [92], but it is not the case for the oral arm canals. There, the circulation pattern seems an adaptation towards a functional through-gut, since it has been shown to sustain a permanent continuous flow and to support a continuous feeding since different openings have different functions. This new arrangement may advantage *Rhizostoma pulmo* in predation, growth and overall fitness since it may sustain a higher metabolism rate compared to other jellyfish characterized by intermittent feeding [205]. This could also be at the basis of the dimensions of *Rhizostoma pulmo*, that is one of the biggest jelly species in the world in terms of biomass, which weigh even more than 25 kg [206].

From a broader perspective, our results may also give new clues about this adaptive development towards a sort of digestive apparatus analogous to the trough-gut common within bilaterians.

Generally, cnidarians are considered to possess a blind gut [178]. Our findings, together with Arai [185] who showed radial canals distal excretory pores and papillae in *Aequorea victoria*, demonstrate that this paradigm is not 100% safe from debate [185]. In our case, we cannot define our results on the circulation in *Rhizostoma pulmo* as a proper through-gut but, surely, we can partially refuse the bias of a single oral opening with both the uptake and excrete function.

We don't believe that the whole classic paradigm is wrong, but that, in our case, this is rather a further example of adaptive convergence (by modifying pre-existing structures) in the direction of an anatomically different apparatus, but functionally analogous to a through-gut, just like the independent event within the *Aequorea* complex, resulting in analogue function-based structures in Cnidaria [207,208]. Citing Dunn [209] in his work "The hidden biology of sponges and ctenophores", we totally agree with his reflection that "early animal evolution has been presented as a ladder, where 'primitive' living species are thought of as the ancestors of 'complex' living species [209]. It is more and more evident that we cannot array animals from simple to complex, because there is no single axis of complexity".

As a conclusion, evolutionary scenarios cannot be easily solved but their comprehension has to be gathered step by step. In this context, deeper knowledge about the through-gut is fundamental to reconstruct the history of body plan evolution and diversification. Thus, further research is needed to discover, describe, examine and distinguish the various functional and structural similarities in Cnidaria and the other metazoan phyla. Within Rhizostomeae, further analyses will be needed to see whether similar adaptations are exclusive to *Rhizostoma pulmo*, or are typical of the whole genus, and whether similar adaptations are present in other rhizostomeans, as Stiasny's [196] pioneering observations would seem to indicate [196].

4. Materials and Methods

4.1 Sampling area

Rhizostoma pulmo (Macri, 1778) samples (Table 2) were collected in the Gulf of Trieste (North Adriatic Sea, Italy), where two coastal sites were selected: Grado Lagoon and Duino-Sistiana (Gulf of Trieste) (Fig 12); in the south coastal area of France (Bages Sigean Lagoon and Thau Lagoon) and in the Gulf of Cadiz (specimens of *Rhizostoma luteum*, atlantic coast of Spain). Dates of samplings are reported in Table 2.
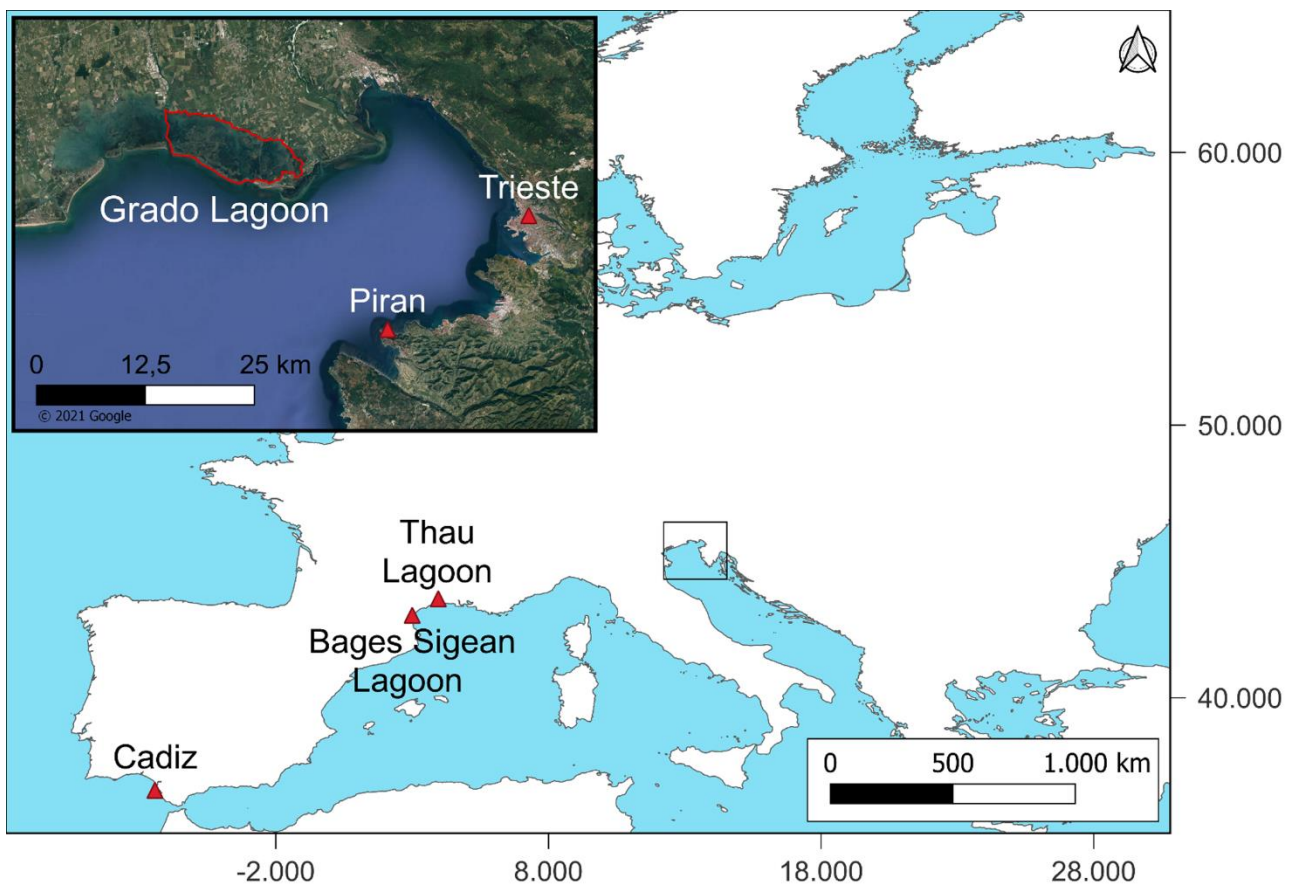

Fig 12. Sampling map. Square indicates the top left magnification of the Gulf of Trieste (Italy). Red triangles indicate the sampling areas. The red bordered area is part of the Grado Lagoon, where juvenile specimens were sampled. Map was made with QGIS v3.20.3 [210]. Map source from Natural Earth (Free vector and raster map data @ naturalearthdata.com), which material are in the public domain, no permission to use is needed.

4.2 Sampling design

The choice of the two Italian areas derived from past observations of the research team. During summer (end of July/early August), blooms of young *Rhizostoma pulmo* medusae were usually observed in the Grado Lagoon while blooms of adult medusae of *Rhizostoma pulmo* were commonly observed through the Gulf of Trieste from summer to winter, as also reported by Andreja Ramšak and Katja Stopar (Pers. Observation, 2007).

Taking advantage from these observations, it was possible to collect specimens of all sizes, from juveniles to adults. All the samples were collected through diving sessions using containers of adequate size to avoid damages to medusae.

It was not necessary to request any type of permit to sample the specimens used in this research, neither in the Gulf of Trieste, nor in the Bages Sigean and Thau Lagoon, France, nor along the coasts of Cadiz, Spain, as the jellyfish are not protected by any type of convention.

A total of 75 juveniles (diameter up to 15 cm) and 60 adult jellyfish (diameter greater than 15 cm) were locally sampled and brought to the lab. Here, half of the young specimens were reared in tanks (Aurelia-80, Reef-Eden), the remaining individuals were fixed in 4% formalin-saltwater solution and then stored in containers of adequate size. A total of six adult specimens came from France and a total of 30 lab-reared post-ephyrae while one young specimen of 4 cm diameter of *Rhizostoma luteum* came from Spain (Table 2). These last specimens allowed us to start some preliminary comparative observations, which will lead to future research to compare *Rhizostoma pulmo* with the other co-generic species.

Table 2. List of collected samples and locations for *Rhizostoma pulmo* and *Rhizostoma luteum*.

Species	Location	Geographical coordinates	Date of sampling	Collected by
Rhizostoma pulmo	Duino/Sistiana Gulf of Trieste (Italy)	45°45'42.2"N 13°37'18.3"E	08/03/2018 09/15/2019 07/09/2020 07/23/2020 08/26/2020 10/28/2020 07/28/2021	Avian M., Motta G., Macaluso V., Pillepich N.
	Grado Lagoon (Italy)	45°40'59.4"N 13°22'03.7"E	07/31/2019 08/13/2019 10/11/2019 08/11/2020 08/16/2020 07/29/2021 09/02/2021	Avian M., Motta G., Macaluso V., Pillepich N.
	Bay of Piran (Slovenia)	45°31'05.3"N 13°33'09.5"E	08/23/2018 09/06/2018	Ramšak A.
	Thau Lagoon (France)	43°23'26.1"N 3°36'12.0"E	09/2018	Bonnet D.
	Bages Sigean Lagoon (France)	43°05'51.6"N 2°59'59.7"E	06/27/2018	Bonnet D.
Rhizostoma luteum	ICMAN Inst. P.Real, Cadiz (Spain)	-	06/11/2019	Prieto L.
	Bay of Cadiz (Spain)	36°32'38.8"N 6°14'40.3"W	07/09/2019	Prieto L.

4.3 Morphological analyses

Different methods were tested to characterize the complex gastrovascular system of *Rhizostoma pulmo*.

4.3.1 Contrast experimental methods

First, different contrast media, such as Indian ink, neutral red 1.5%, carmine red 1.5%, 0.5% methylene blue and, in one case, 1% agar solution contrasted with 0.3% methylene blue have been injected to highlight the gastrovascular canals of both umbrella and manubrium. Injections have been made with an insulin syringe into the stomach from the exumbrellar apex. To maintain agar solution fluidity, samples, water and the containers were kept at a temperature of 60° C. For this analysis, formalin preserved individuals were employed. This type of experimental procedure has been used once only, as the endocast obtained is temporary (it lasts a maximum of a few days), and too fragile to be isolated from the surrounding tissues. All other experiments were performed with stained aqueous solutions.

Second, in order to evidence the gastrovascular circulation on living juvenile specimens of *Rhizostoma pulmo*, 2 ml of neutral red 1.5% in freshwater, or methylene blue 0.5%, were injected from the exumbrella apex with an insulin syringe into the stomach, letting the stain flow into the canals (12 experiments, performed between 2019 and 2020). Circulation was video recorded with a Canon G16 camera. Only living juveniles (collected at Grado Lagoon) were used due to their tissue transparency, adult tissues were too opaque to properly see through. After the staining phase, samples were quickly fixed in 4% formalin in seawater solution, then the scapulae and oral arms were excised and observed under a Leica Microsystems M205C Stereomicroscope equipped with a Canon G16 camera. The internal flux circulation of the seawater-stained solution in living specimens was video-recorded, and several pictures were taken.

Living zooplankton was also used to better understand the gastrovascular circulation. Living zooplankton was filtered through a 200 μm mesh zooplankton net, and stained with a vital seawater solution of methylene blue (0.3%) or neutral red (1%). Then, two medusae were separately fed with the stained zooplankton for a feeding time of 30 minutes; during this time interval samples were

continuously observed. After feeding time, samples were fixed in formalin 4% solution and they were dissected for zooplankton identification in the canals of the gastrovascular system.

Furthermore, to better document the circulation process and the ciliary movement role, single oral arms from living samples were cut and vital-stained seawater solution was released near the mouth and canals openings at the section level. The same protocol was applied to investigate scapular circulation, where the stain solution was released in proximity of the cut surface of the scapulae. Inwards and outwards flows were simultaneously observed and recorded under a binocular microscope (Leica Microsystems M205C Stereomicroscope equipped with a Canon G16 camera).

4.3.2 Internal cast of the gastrovascular system

The aim of this experiment was to set-up a protocol to produce a cast of the whole gastrovascular system in order to understand the pattern of the complex canals ramifications. Several endocasts were made, either on whole specimens and on partially sectioned manubrium portions. For the following experiments formalin fixed individuals were used.

Three different types of resins were used:

a) Acrylic resin Mercox Blu (Ladd Research). Producer instructions were strictly followed. Resins were injected into the stomach (inner umbrella) of a 10 cm-diameter whole young specimen, and directly in an excised manubrium.

b) Epoxy resin (Resin 4 Décor©). Native resin was too dense to be easily injected without damaging the small channels. After several tests we found that diluting the resin with acetone at different concentrations to reduce viscosity (5% in bigger individuals and 7.5% in smaller ones) facilitated the injection without compromising the polymerization reaction.

c) Epoxy resin (Liquidissima, Resin Pro©). This resin was less viscous compared to the previous one, and a 5% dilution with acetone was enough to provide optimal results.

In whole organisms, injections were made in the stomach (through the exumbrella apex) with a 50 ml syringe and a rubber cannula. During the injection the organisms were kept in water and lightly massaged to allow the resin to flow all over the gastrovascular canals. After a hardening time of 24

hours, jellyfish were digested in a 20% solution KOH with a sample/solution volume ratio of 1:5 for 24 hours at 40 °C.

After several trials we can assert that the third resin was the most versatile tool, its reduced viscosity avoided excessive canal dilation and has ensured lower efforts during the injections. The second resin was the most viscous and required a greater dilution with the solvent to be efficiently injected. Anyway, both resins produced high quality endocasts. The first acrylic resin, due to its extremely low viscosity, specifically formulated for casts of circulatory systems, in our case it was not useful, as it failed to form a compact cast by fragmenting into a large number of shards.

4.3.3 X-ray computed microtomography measurements

The most complete endocast (of a young specimen of 14.6 cm of diameter, Grado Lagoon) was investigated

by using the microfocus X-ray computed tomography (μCT) technique. The measurements were performed by using the FAITH instrument (manuscript in preparation) of the Elettra synchrotron light facility in Basovizza (Trieste, Italy). The FAITH station is a fully-customized cone-beam CT system equipped with a sealed microfocus X-ray source (Hamamatsu L12161, Japan) operating in an energy range from 40 to 150 kV at a maximum current of 500 μA. A 2192x1776 pixels flat panel detector (Hamamatsu C11701DK) featuring a pixel size of 120x120 μm^2 was used as detector. Exploiting the magnification effect offered by the cone-beam geometry [211], the source-object-detector distance can be varied to achieve a spatial resolution close to the minimum focal spot size of the source (5 μm) while imaging samples from a few millimeters up to about 20 centimeters in lateral size. The X-ray μCT scans were acquired using the following experimental conditions: tube voltage = 40 kV, tube current = 250 μA, number of projections = 1800, angular step = 0.2 degrees, total scan duration = 6 min. The effective pixel size was set to 62.0 to image the whole endocast or selected regions of interest (local area modality), respectively. From the radiographs (projection images) acquired by the flat panel detector during a 360 degrees rotation of the specimen, a set of 2D axial slices was reconstructed by the free software NRecon 1.7.0.4 (Brulker, USA). In order to visualize and inspect the structure

of the sample, the freeware software Fiji [124] and the commercial software VGStudio MAX 2.0 (Volume Graphics, Germany) were employed.

4.3.4 Morphometric analysis of the X-ray microtomographic data

To obtain a comprehensive description of the gastrovascular system, we analyzed two specific regions of the specimen, with a different focus: 1) the whole manubrium, to compare the structure of the oral arms vs. the scapulae. 2) A single oral arm, to characterize the topology of the three different structures (the wings) supporting the openings of the canals. For these analyses, the most whole and accurate casted and skeletonized oral arm has been chosen. This procedure ensured to avoid underestimation due to incomplete injection of the resin, cast fractures and, at the same time, to avoid under- or overestimation related with the skeletonization process.

The topological characterization of the systems features two main concepts: the local thickness (LT) analysis, and the "skeleton" (i.e., the medial axes of the structure, in this specific case) analysis. The LT of a segmented class in a tomographic dataset is described as the calculation for each voxel (vx) of the radius of the maximum inscribed sphere in the class that contains that vx [212]. The skeleton has been measured via the "thinning" algorithm [213], as we were interested in the calculation of the medial axis of the structures. The combination of the two analyses can provide a volume where the medial axes are labeled, vx by vx, with the LT values, to provide the local quantification of the thicknesses. A similar approach has been successfully applied to characterize the pore space topology in porous materials [214,215].

The analysis on both the manubrium and the single arm was carried out as follows: first, the grayscale 8-bit dataset was segmented using the Otsu thresholding algorithm [216] applied to the full dataset grayscale frequency histogram to generate a binary volume. The binarized volume was then used to calculate the LT of the segmented class (the gastrovascular system). In the dataset #1 (manubrium) two sub-datasets, the first featuring the scapulae and the second featuring the 8 (eight) oral arms, were separated and analyzed independently. In the dataset #2 (the single oral arm) the three-winged portions were manually separated under the scapulae and subsequently independently analyzed.

The binary volumes of the different systems were filtered using an isotropic Gaussian filter with a structuring element of 5 (five) vx and followed by a segmentation preserving the original dataset connectivity to generate a smoother structure. This filtering is necessary to reduce the noise of the data and suppress the generation of many spurious branches in the skeletonization process. The 3D-isotropic-Gaussian filter fully preserves the mediality of the original dataset, while suppressing the smallest branches generated by the structure roughness during the thinning process. After the skeletonization, two consecutive 4 (four) vx pruning cycles, to delete the remaining short ending branches, were applied. This combination of filtering and pruning operations provided the smallest number of spurious end branches (e.g., the ones radiating from the long oral arm structures, generated by changes in shape and not by the presence of canals), while preserving the short branches at the oral apertures. In order to provide a thickness-labeled skeleton, each vx in the resulting skeletons was labeled using the respective LT value. The analysis of the single oral arm was carried a step further, to also investigate the number of openings in the three-winged portions: the number of endpoints (ideally equivalent to the number of oral apertures) was then calculated, separately for each wing of one oral arm.

4.3.5 Morphometric analysis of jellyfish body (six from the Gulf of Trieste and six from the Bages Sigean and Thau Lagoon)

During this study several morphometric features of the jellyfish were measured, but given the focus of the present work the results were here omitted. The diameter of a jellyfish is normally measured by taking the maximum diameter of the umbrella (ideally lying on a flat surface), between opposite rhopalia or between opposite marginal lappets. In the case of *Rhizostoma pulmo* (and many other rhizostomean jellyfish), it is impossible to stretch out its umbrella, so in order to take the "real umbrella diameter" (between two opposite rhopalia, or marginal lappets) using a soft measuring tape stretched over the exumbrellar surface is useful; but since in this species the umbrellar shape is practically a hemisphere, the functional *apparent diameter* (AD) was measured as $AD=2RD/\pi$ where RD is the *real diameter* (inter-rhopaliar semicircle, without the marginal lappets length). In the present study, all diameters reported refer to the AD, not the RD (S1a Fig).

Conceptualization: Massimo Avian

Sampling and natural environment observations

Massimo Avian, Delphine Bonnet, Vanessa Macaluso, Nicole Pillepich, Laura Prieto, Andreja Ramšak, Gregorio Motta.

Lab experiments and in vivo observations

Massimo Avian, Vanessa Macaluso, Nicole Pillepich, Gregorio Motta.

X-ray computed microtomography measurements
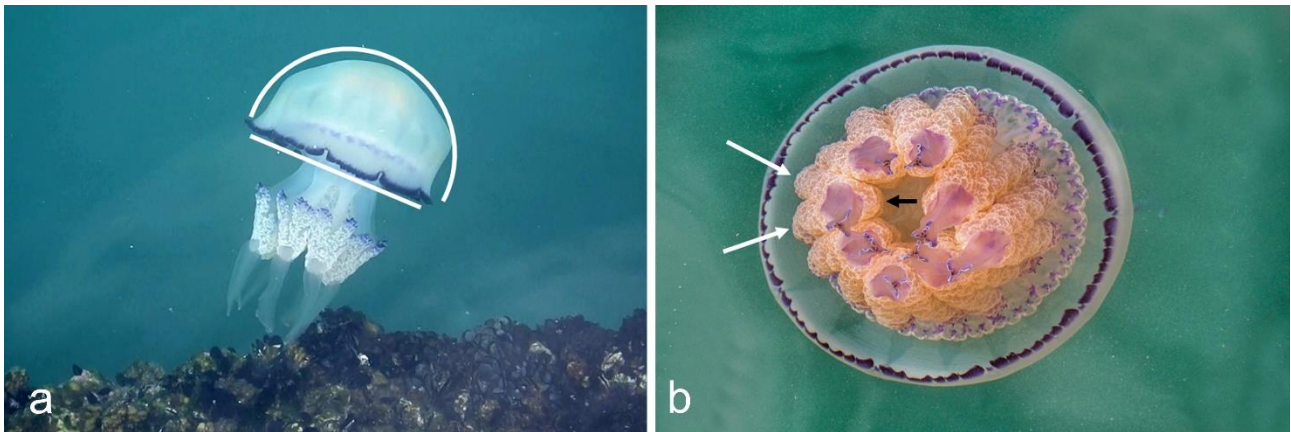
Diego Dreossi, Lucia Mancini.

**Morphometric analysis of the tomographic data**

Lucia Mancini, Marco Voltolini.

Writing – original draft

Massimo Avian, Lucia Mancini, Marco Voltolini, Delphine Bonnet, Vanessa Macaluso, Nicole Pillepich, Laura Prieto, Andreja Ramšak, Antonio Terlizzi, Gregorio Motta.

S1 Fig. *Rhizostoma pulmo*, **adult specimens, Gulf of Trieste, North Adriatic Sea**. **(a)** Semicircle indicates the real umbrellar diameter, straight line indicates the apparent diameter. **(b)** Upside-down specimen showing the three-winged pattern of the oral arms. White arrows indicate the two external wings, black arrow the internal one (Photo courtesy of Paolo Coretti). Both specimens have an apparent diameter of about 30 cm.
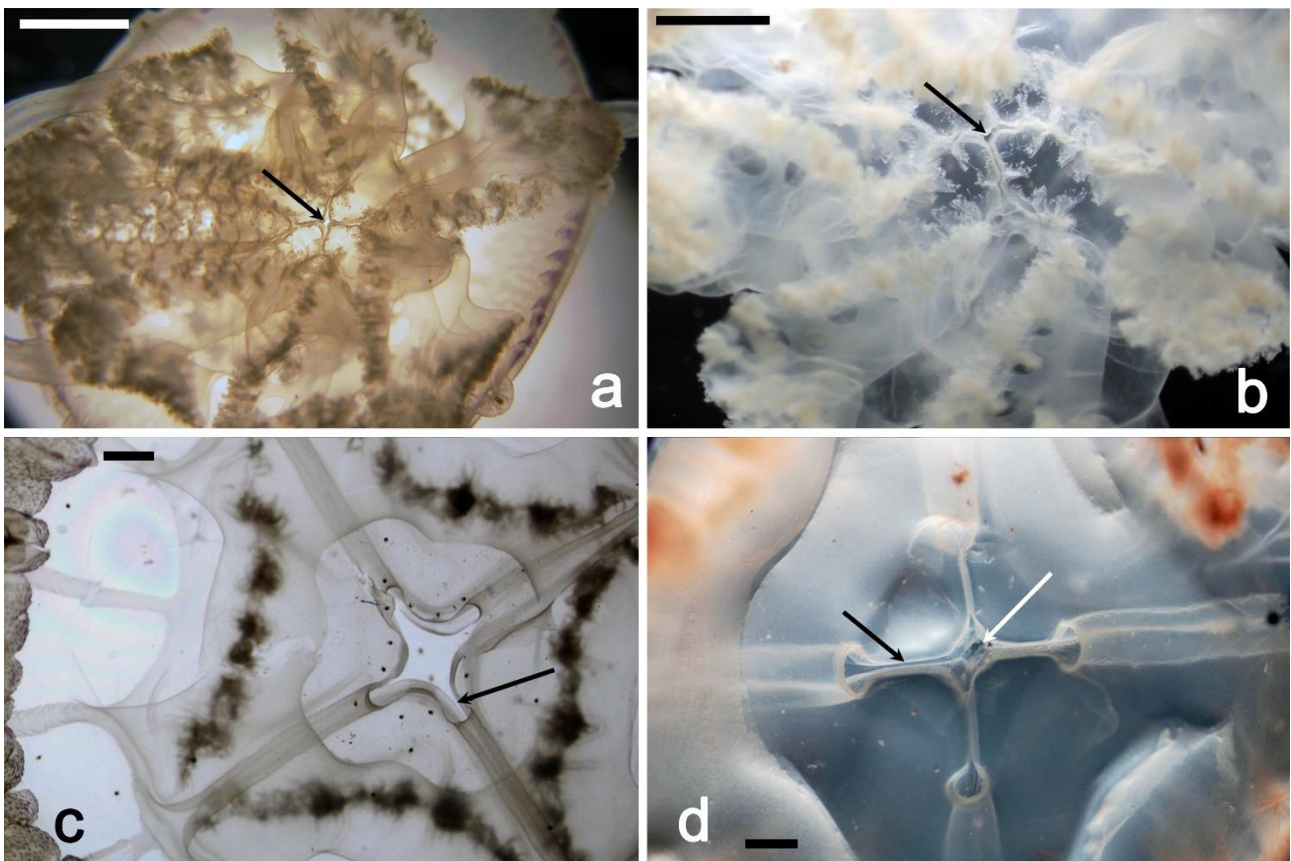
S2 Fig. Early development of the manubrium canal system. **(a)** Young specimen of 2.7 cm diam., subumbrellar view. Arrow indicates the residual of the central mouth opening still open (scale bar =

0.25 cm). **(b)** As in (a), specimen 3 cm diam. (scale bar = 0.25 cm). **(c)** Subumbrellar view of a 4 cm diam. specimen, manubrium excised under the genital sinuses. Visible the four perradial canals projecting into the still wide central canal (scale bar = 0.25 cm). **(d)** Same view in a specimen of 5 cm diam., with the same pattern as in (c), but with a noticeable size reduction of the central quadrangular canal (scale bar = 0.25 cm). Black arrows in (c) and (d)indicate the edges of the perradial canals, white arrows indicate the central quadrangular canal.
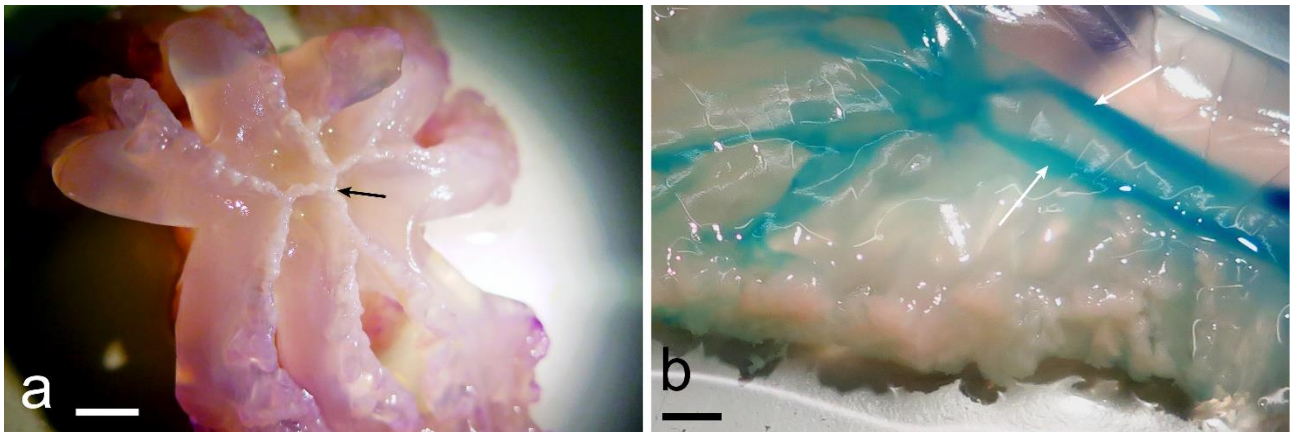
S3 Fig. Central area of the manubrium and hemi-canals. **(a)** Specimen of 12.4 cm diam. with the juvenile central mouth closed (arrow) (scale bar = 1 cm). **(b)** oral arm of a specimen of 23.5 cm diam., showing the stained hemi-canal system on the right (arrows) and on the left the anastomosis that gives rise to the canals that reach both the inner wing (bottom left) and the outer ones (top).

S1 Video. Micro CT-scan 3D rendering. 360° animation of the whole endocast evidencing the different structures: umbrella (green), scapulae (blue), central canal (yellow), oral arms (red).

https://doi.org/10.1371/journal.pone.0272023.s004

S2 Video. Micro CT-scan 3D rendering. 360° animation of the whole endocast evidencing transverse sections of the manubrium.

https://doi.org/10.1371/journal.pone.0272023.s005

S3 Video. Micro CT-scan 3D rendering. 360° animation of the whole endocast evidencing oblique, longitudinal, and transverse sections of the manubrium at supra-scapular and sub-scapular (at the distal portion of the central canal) level.

https://doi.org/10.1371/journal.pone.0272023.s006

S4 Video. Micro CT-scan 3D rendering. 360° animation of the whole endocast evidencing transverse sections of the umbrella, manubrium at supra-scapular and sub-scapular (at the distal portion of the central canal) level and finally longitudinal sections at central canal level.

https://doi.org/10.1371/journal.pone.0272023.s007

S5 Video. Methylene blue stain diffusion into the gastrovascular system. Specimen of 4.2 cm in diameter. The injection of the stain was carried out into the stomach, just in the middle of the exumbrella.

https://doi.org/10.1371/journal.pone.0272023.s008

S6 Video. Neutral red stain diffusion into the gastrovascular system of an excised oral arm. The stain was released on the cutting plan (top). Internal wing on the left, the external ones on the right.

https://doi.org/10.1371/journal.pone.0272023.s009

S7 Video. Bidirectional particle flux into the hemi-canals. The oral arm is the same sample of Video 6.

https://doi.org/10.1371/journal.pone.0272023.s010

Chapter 6.

Article

Asexual Reproduction and Strobilation of *Sanderia malayensis* (Scyphozoa, Pelagiidae) in Relation to Temperature: Experimental Evidence and Implications

Massimo Avian [1,†], Gregorio Motta [1], Mattia Prodan [1], Enrico Tordoni [1], Vanessa Macaluso [1], Alfred Beran [2], Alenka Goruppi [2], Giovanni Bacaro [1,*] and Valentina Tirelli [2,†]

[1] Department of Life Science, University of Trieste, Via L. Giorgieri 10, 34127 Trieste, Italy; avian@units.it (M.A.); GREGORIO.MOTTA@phd.units.it (G.M.); mattia.prodan@hotmail.it (M.P.); etordoni@units.it (E.T.); VANESSA.MACALUSO@studenti.units.it (V.M.)

[2] National Institute of Oceanography and Applied Geophysics—OGS, 34151 Trieste, Italy; aberan@inogs.it (A.B.); agoruppi@inogs.it (A.G.); vtirelli@inogs.it (V.T.)

[*] Correspondence: gbacaro@units.it

[†] Equal contribution as first author.

Abstract: *Sanderia malayensis* is a scyphozoan species present in the Indian and Pacific Oceans, ranging from the Suez Canal to Japan. Although this jellyfish is commonly kept in aquariums around the world, there is a knowledge gap regarding its biology and ecology, especially at the polyp stage. In this study, we tested the asexual reproductive activity of *S. malayensis* at three different temperatures: 10, 15 and 20 °C. Results showed significant increases of polyps at 15 and 20 °C, and a minimum at 10 °C, corresponding with daily budding rates of 6.61% ± 0.92%, 5.85% ± 2.36% and 0.66% ± 0.24%, respectively. Moreover, a second experiment was carried out to report about the ability of *S. malayensis* to prey on *Aurelia solida* at the ephyra stage. Unidirectional predation of *S. malayensis* ephyrae on *A. solida* and an absence of inverse predation was observed. These results could give new insights on the potential fitness and survival of this species if it will ever invade the Mediterranean Sea.

https://www.mdpi.com/1424-2818/13/2/37

References

1. Bush, A. O., Lafferty, K. D., Lotz, J. M. & Shostak, A. W. Parasitology Meets Ecology on Its Own Terms: Margolis et al. Revisited. *The Journal of Parasitology* **83**, 575 (1997).

2. Robison, B. H. Deep pelagic biology. *Journal of experimental marine biology and ecology* **300**, 253–272 (2004).

3. Condon, R. H. *et al.* Recurrent jellyfish blooms are a consequence of global oscillations. *Proceedings of the National Academy of Sciences* **110**, 1000–1005 (2013).

4. Madin, L., Purcell, J. & Miller, C. B. Abundance and grazing effects of Cyclosalpa bakeri in the subarctic Pacific. *Marine Ecology Progress Series* **157**, 175–183 (1997).

5. Mapstone, G. M. Global diversity and review of Siphonophorae (Cnidaria: Hydrozoa). *PLoS One* **9**, e87737 (2014).

6. Hamner, W., Madin, L., Alldredge, A., Gilmer, R. & Hamner, P. Underwater observations of gelatinous zooplankton: sampling problems, feeding biology, and behavior 1. *Limnology and Oceanography* **20**, 907–917 (1975).

7. Nogueira Júnior, M., da Costa, B. S. P., Martinez, T. A., Brandini, F. P. & Miyashita, L. K. Diversity of gelatinous zooplankton (Cnidaria, Ctenophora, Chaetognatha and Tunicata) from a subtropical estuarine system, southeast Brazil. *Marine Biodiversity* **49**, 1283–1298 (2019).

8. Graham, W. M. *et al.* Linking human well-being and jellyfish: ecosystem services, impacts, and societal responses. *Frontiers in Ecology and the Environment* **12**, 515–523 (2014).

9. Milisenda, G. *et al.* Reproductive and bloom patterns of Pelagia noctiluca in the Strait of Messina, Italy. *Estuarine, Coastal and Shelf Science* **201**, 29–39 (2018).

10. Gibbons, M. J. & Richardson, A. J. Beyond the jellyfish joyride and global oscillations: advancing jellyfish research. *Journal of Plankton Research* **35**, 929–938 (2013).

11. D'Ambra, I., Graham, W. M., Carmichael, R. H., Malej, A. & Onofri, V. Predation patterns and prey quality of medusae in a semi-enclosed marine lake: implications for food web energy transfer in coastal marine ecosystems. *Journal of plankton research* **35**, 1305–1312 (2013).

12. Horton, T. *et al.* World Register of Marine Species (WoRMS). (2022).

13. Schierwater, B. & DeSalle, R. *Invertebrate Zoology: A Tree of Life Approach*. (CRC Press, 2021).

14. Michael E. Huber, D. & Castro, P. *Marine Biology*. (McGraw-Hill Education, 2015).

15. Jarms, G., Morandini, A. C., Schmidt-Rhaesa, A., Giere, O. & Straehler-Pohl, I. World Atlas of Jellyfish: Scyphozoa Except Stauromedusae. *Abhandlungen und Verhandlungen des Naturwissenschaftlichen Vereins in Hamburg* (2019).

16. Avian, M. & Ramšak, A. Cnidaria: Classes Scyphozoa, Cubozoa, And Staurozoa. in *Invertebrate Zoology: A Tree of Life Approach*.

17. Shikina, S. & Chang, C.-F. Cnidaria. in *Encyclopedia of Reproduction (Second Edition)* (ed. Skinner, M. K.) 491–497 (Academic Press, 2018). doi:https://doi.org/10.1016/B978-0-12-809633-8.20597-9.

18. Piraino, S. *et al.* Pelagia benovici sp. nov.(Cnidaria, Scyphozoa): a new jellyfish in the Mediterranean Sea. *Zootaxa* **3794**, 455–468 (2014).

19. Kayal, E. *et al.* Phylogenomics provides a robust topology of the major cnidarian lineages and insights on the origins of key organismal traits. *BMC evolutionary biology* **18**, 1–18 (2018).

20. Liu, Y. *et al.* A new scyphozoan from the Cambrian Fortunian Stage of South China. *Palaeontology* **60**, 511–518 (2017).

21. Mariottini, G. L. & Pane, L. Cytotoxic and cytolytic cnidarian venoms. A review on health implications and possible therapeutic applications. *Toxins* **6**, 108–151 (2013).

22. Mariottini, G. L. & Pane, L. Mediterranean Jellyfish Venoms: A Review on Scyphomedusae. *Marine Drugs* **8**, 1122–1152 (2010).

23. Madin, L. & Harbison, G. Gelatinous Zooplankton. In. Steele J., Thorpe S., Turekian K.(eds.), Encyclopedia of Ocean Sciences. (2001).

24. Kienberger, K. *et al.* First description of the life cycle of the jellyfish Rhizostoma luteum (Scyphozoa: Rhizostomeae). *PloS one* **13**, e0202093 (2018).

25. Prieto, L., Armani, A. & Macías, D. Recent strandings of the giant jellyfish *Rhizostoma luteum* Quoy and Gaimard, 1827 (Cnidaria: Scyphozoa: Rhizostomeae) on the Atlantic and Mediterranean coasts. *Marine biology* **160**, 3241–3247 (2013).

26. Purcell, J. E., Baxter, E. J. & Fuentes, V. Jellyfish as products and problems of aquaculture. in *Advances in aquaculture hatchery technology* 404–430 (Elsevier, 2013).

27. Jankowski, T. The freshwater medusae of the world–a taxonomic and systematic literature study with some remarks on other inland water jellyfish. *Hydrobiologia* **462**, 91–113 (2001).

28. Kinsey, B. Barnes on Box Jellyfish. *Sir George Fisher Centre for Tropical Marine Studies. James Cook University of North Queensland, Townsville* (1986).

29. Shorten, M. *et al.* Kinematic analysis of swimming in Australian box jellyfish, Chiropsalmus sp. and Chironex fleckeri (Cubozoa, Cnidaria: Chirodropidae). *Journal of Zoology* **267**, 371–380 (2005).

30. Coates, M. M. Visual ecology and functional morphology of Cubozoa (Cnidaria). *Integrative and comparative biology* **43**, 542–548 (2003).

31. Bielecki, J., Zaharoff, A. K., Leung, N. Y., Garm, A. & Oakley, T. H. Ocular and extraocular expression of opsins in the rhopalium of Tripedalia cystophora (Cnidaria: Cubozoa). *PLoS One* **9**, e98870 (2014).

32. Malej, A. *et al.* Mnemiopsis leidyi in the northern Adriatic: here to stay? *Journal of Sea Research* **124**, 10–16 (2017).

33. Lal, S. Minor Phylum: Ctenophora. in (2007).

34. Shiganova, T. & Malej, A. Native and non-native ctenophores in the Gulf of Trieste, Northern Adriatic Sea. *Journal of Plankton Research* **31**, 61–71 (2009).

35. Shiganova, T. Invasion of the Black Sea by the ctenophore Mnemiopsis leidyi and recent changes in pelagic community structure. *Fisheries Oceanography* **7**, 305–310 (1998).

36. Carré, D. & Carré, C. Acquisition de cnidocystes et differenciation de pseudocolloblastes chez les larves et les adultes de deux ctenophores du genre Haeckelia Carus, 1863. *Canadian journal of zoology* **67**, 2169–2179 (1989).

37. Goodheart, J. A. & Bely, A. E. Sequestration of nematocysts by divergent cnidarian predators: mechanism, function, and evolution. *Invertebrate Biology* **136**, 75–91 (2017).

38. Organization, W. H. & others. *Opportunistic settlers and the problem of the ctenophore Mnemiopsis leidyi invasion in the Black Sea*. (London: IMO, 1997).

39. Hays, G. C., Doyle, T. K. & Houghton, J. D. R. A Paradigm Shift in the Trophic Importance of Jellyfish? *Trends in Ecology & Evolution* **33**, 874–884 (2018).

40. Kawahara, M., Uye, S., Ohtsu, K. & Iizumi, H. Unusual population explosion of the giant jellyfish Nemopilema nomurai (Scyphozoa: Rhizostomeae) in East Asian waters. *Marine Ecology Progress Series* **307**, 161–173 (2006).

41. Nishikawa, J., Thu, N. T., Ha, T. M., & others. Jellyfish fisheries in northern Vietnam. *Plankton and Benthos Research* **3**, 227–234 (2008).

42. Duarte, I. M., Marques, S. C., Leandro, S. M. & Calado, R. An overview of jellyfish aquaculture: for food, feed, pharma and fun. *Reviews in Aquaculture* **14**, 265–287 (2022).

43. Ohtsuka, S. *et al.* Symbionts of marine medusae and ctenophores. *Plankton Benthos Res* **4**, 1–13 (2009).

44. Moestafa, S. H. & McConnaughey, B. H. Catostylus ouwensi (Rhizostomae, Catosylidae), a new jellyfish from Irian (New Guinea) and Ouwensia catostyli n, gen., n, sp., Parasitic In C. Ouwensi. *Treubia* **27**, 1–9 (1966).

45. Phillips, P. J. & Levin, N. L. Cestode larvae from scyphomedusae of the Gulf of Mexico. *Bulletin of Marine Science* **23**, 574–584 (1973).

46. Stunkard, H. W. The Morphology and Life-History of Neopechona pyriforme (Linton, 1900) N. Gen., N. Comb.(Trematoda: Lepocreadiidae). *Biological Bulletin* **136**, 96–113 (1969).

47. Stunkard, H. W. Successive Hosts and Developmental Stages in the Life History of Neopechona cablei sp. n. (Trematoda: Lepocreadiidae). *The Journal of Parasitology* **66**, 636 (1980).

48. Child, C. A. & Harbison, G. R. A Parasitic Association Between a Pycnogonid and a Scyphomedusa in Midwater. *Journal of the Marine Biological Association of the United Kingdom* **66**, 113–117 (1986).

49. Pagès, F. Biological associations between barnacles and jellyfish with emphasis on the ectoparasitism of Alepas pacifica (Lepadomorpha) on Diplulmaris malayensis (Scyphozoa. *J Nat Hist* **34**, 2045–2056 (2000).

50. Moss, A. G., Estes, A. M., Muellner, L. A. & Morgan, D. D. Protistan epibionts of the ctenophore Mnemiopsis mccradyi Mayer. in *Jellyfish Blooms: Ecological and Societal Importance* 295–304 (Springer, 2001).

51. Bouillon, J. Considérations sur le développement des Narcoméduses et sur leur position phylogénétique. *Indo-Malayan Zoology* **4**, 189–278 (1987).

52. Bumann, D. & Puls, G. Infestation with larvae of the sea anemone Edwardsia lineata affects nutrition and growth of the ctenophore Mnemiopsis leidyi. *Parasitology* **113**, 123–128 (1996).

53. Busch, M. W., Kuhn, T., Münster, J. & Klimpel, S. Marine crustaceans as potential hosts and vectors for metazoan parasites. in *Arthropods as vectors of emerging diseases* 329–360 (Springer, 2012).

54. Okwa, O. O. Introductory Chapter: Helminthes Diversity-Focus on Nematodes. in *Helminthiasis* (IntechOpen, 2020).

55. Cribb, T. H. Digenea (endoparasitic flukes). (2005).

56. Cribb, T. H., Bray, R. A., Olson, P. D. & Littlewood, D. T. J. Life cycle evolution in the Digenea: a new perspective from phylogeny. *Advances in Parasitology* **54**, 197–254 (2003).

57. Køie, M. On the morphology and life-history of Opechona bacillaris (Molin, 1859) Looss, 1907 (Trematoda, Lepocreadiidae. *Ophelia* **13**, 63–86 (1974).

58. Martorelli, S. R. Digenea parasites of jellyfish and ctenophores of the southern Atlantic. in *Jellyfish Blooms: Ecological and Societal Importance* 305–310 (Springer Netherlands, 2001). doi:10.1007/978-94-010-0722-1_25.

59. Browne, J. G. Parasites of jellyfish in eastern Australia. (Griffith University, 2014).

60. Nogueira Júnior, M., Diaz Briz, L. M. & Haddad, M. A. Monthly and inter-annual variations of Opechona sp.(Digenea: Lepocreadiidae) parasitizing scyphomedusae off southern Brazil. *Marine Biology* **162**, 391–400 (2015).

61. Thiel, M. E. Wirbellose Meerestiere als Parasiten, Kommensalen oder Symbionten in oder an Scyphomedusen. *Helgoländer Wissenschaftliche Meeresuntersuchungen* **28**, 417–446 (1976).

62. Lauckner, G. Diseases of cnidaria. *Diseases of marine animals* **1**, 167–237 (1980).

63. Kondo, Y. *et al.* Seasonal changes in infection with trematode species utilizing jellyfish as hosts: Evidence of transmission to definitive host fish via medusivory. *Parasite* **23**, (2016).

64. Stunkard, H. LIFE-CYCLE AND DEVELOPMENTAL STAGES OF A DIGENETIC TREMATODE WHOSE UNENCYSTED METACERCARIAL STAGES OCCUR IN MEDUSAE. in *Biological Bulletin* vol. 133 488 (MARINE BIOLOGICAL LABORATORY 7 MBL ST, WOODS HOLE, MA 02543, 1967).

65. Stunkard, H. W. Observations on the morphology and life-history of the digenetic trematode, Lepocreadium setiferoides (Miller and Northup, 1926) Martin, 1938. *The Biological Bulletin* **142**, 326–334 (1972).

66. Stunkard, H. W. The marine cercariae of the Woods Hole, Massachusetts region, a review and a revision. *The Biological Bulletin* **164**, 143–162 (1983).

67. Diaz Briz, L. M., Martorelli, S. R., Genzano, G. N. & Mianzan, H. W. Parasitism (Trematoda, Digenea) in medusae from the southwestern Atlantic Ocean: medusa hosts, parasite prevalences, and ecological implications. *Hydrobiologia* **690**, 215–226 (2012).

68. Ohtsuka, S., Kondo, Y. & Sakai, Y. In-situ observations of symbionts on medusae occurring in Japan, Thailand, Indonesia and Malaysia. 広島大学総合博物館研究報告 9–18 (2010).

69. STUNKARD, H. W. THE MORPHOLOGY AND LIFE-HISTORY OFNEOPECHONA PYRIFORME(LINTON, 1900) N. GEN., N. COMB. (TREMATODA: LEPOCREADIIDAE). *The Biological Bulletin* **136**, 96–113 (1969).

70. Morandini, A. C., Martorelli, S. R., Marques, A. C. & Silveira, F. L. da. Digenean metacercaria (Trematoda, Digenea, Lepocreadiidae) parasitizing 'coelenterates' (Cnidaria, Scyphozoa and Ctenophora) from Southeastern Brazil. *Brazilian Journal of Oceanography* **53**, 39–45 (2005).

71. Bavay, A. Note sur un Distome parasite d'une Méduse. *Arch Parasit* **5**, 199–200 (1902).

72. Brotz, L., W, C. W., Kleisner, K., Pakhomov, E. & Pauly, D. Increasing jellyfish populations: trends in large marine ecosystems. in *Jellyfish Blooms IV* 3–20 (Springer, 2012).

73. Purcell, J. E. Jellyfish and Ctenophore Blooms Coincide with Human Proliferations and Environmental Perturbations. *Annual Review of Marine Science* **4**, 209–235 (2012).

74. Arai, M. N. Interactions of fish and pelagic coelenterates. *Canadian Journal of Zoology* **66**, 1913–1927 (1988).

75. Arai, M. N. Predation on pelagic coelenterates: a review. *Journal of the Marine Biological Association of the United Kingdom* **85**, 523–536 (2005).

76. Purcell, J. E. & Arai, M. N. Interactions of pelagic cnidarians and ctenophores with fish: a review. in *Jellyfish Blooms: Ecological and Societal Importance* 27–44 (Springer Netherlands, 2001). doi:10.1007/978-94-010-0722-1_4.

77. Ohtsuka, S. *et al.* Symbionts of marine medusae and ctenophores. *Plankton and Benthos Research* **4**, 1–13 (2009).

78. Marcogliese, D. J. The role of zooplankton in the transmission of helminth parasites to fish. *Reviews in Fish Biology and Fisheries* **5**, 336–371 (1995).

79. del Prado, M. del C. G., Puertas, L. S., Cadena, J. N. Á., Argumedo, R. L., & others. Opechona pyriforme metacercaria (Trematoda: Lepocreadiidae) in Eirene lactea (Cnidaria: Hydroidomedusae) from a reef lagoon in the Mexican Caribbean Sea. *Anales del Instituto de Biología. Serie Zoología* **71**, 1–6 (2000).

80. Macri, S. Nuove osservazioni intorno la storia naturale del polmone marino degli antichi. (1778).

81. Leoni, V., Bonnet, D., Ramírez-Romero, E. & Molinero, J. C. Biogeography and phenology of the jellyfish Rhizostoma pulmo (Cnidaria: Scyphozoa. *in southern European seas Global Ecol Biogeogr* **30**, 622–639 (2021).

82. Ramšak, A., Stopar, K. & Malej, A. Dispersal ecology of scyphomedusae Pelagia noctiluca and Rhizostoma pulmo in the European Southern Seas. (2007).

83. Bray, R. A. & Gibson, D. I. The Lepocreadiidae (Digenea) of fishes of the north-east Atlantic: review of the genera Opechona Looss, 1907 and Prodistomum Linton, 1910. *Systematic Parasitology* **15**, 159–202 (1990).

84. Bray, R. A., Cribb, T. H. & Cutmore, S. C. Lepocreadiidae Odhner, 1905 and Aephnidiogenidae Yamaguti, 1934 (Digenea: Lepocreadioidea) of fishes from Moreton Bay, Queensland, Australia, with the erection of a new family and genus. *Systematic Parasitology* **95**, 479–498 (2018).

85. Sokolov, S. G., Gordeev, I. I. & Atopkin, D. M. Phylogenetic affiliation of the lepocreadiid trematodes parasitizing some marine fishes in the North-western Pacific. *Marine Biology Research* **16**, 380–389 (2020).

86. Molin, R. Nuovi myzelmintha raccolti ed esaminati. Sitzungsberichte der Kaiserlichen Akademie der Wissenschaften. *Mathematisch-Naturwissenschaftliche Classe* **37**, 818–854 (1859).

87. Keser, R. *et al.* Helminth parasites of digestive tract of some teleost fish caught in the Dardanelles at Çanakkale, Turkey. *Helminthologia* **44**, 217–221 (2007).

88. Bray, R. A. Some helminth parasites of marine fishes of South Africa: Families Gorgoderidae, Zoogonidae, Cephaloporidae, Acanthocolpidae and Lepocreadiidae (Digenea). *Journal of Natural History* **19**, 377–405 (1985).

89. Bray, R. A. & Cribb, T. H. Lepocreadiidae (Digenea) of Australian coastal fishes: new species of Opechona Looss, 1907, Lepotrema Ozaki, 1932 and Bianium Stunkard, 1930 and comments on other species reported for the first time or poorly known in Australian waters. *Systematic Parasitology* **41**, 123–148 (1998).

90. Curran, S. S. *et al.* Opechona chloroscombri and Opechona corkumi n. sp. (Digenea: Lepocreadiidae) from the Northern Gulf of Mexico with Phylogenetic Analysis Based on 28S RDNA. *Journal of Parasitology* **107**, (2021).

91. Yip, S. Y. Parasites of Pleurobrachia pileus Müller, 1776 (Ctenophora), from Galway Bay, western Ireland. *Journal of Plankton Research* **6**, 107–121 (1984).

92. Russell, F. S. *The Medusae Of The British Isles Volume II: Pelagic Scyphozoa, With A Supplement To The First Volume Of Hydromedusae*. (Cambridge University Press, 1970).

93. Fuentes, V. *et al.* Life cycle of the jellyfish Rhizostoma pulmo (Scyphozoa: Rhizostomeae) and its distribution, seasonality and inter-annual variability along the Catalan coast and the Mar Menor. *Mediterranean). Mar Biol* **158**, 2247–2266 (2011).

94. Holst, S., Sötje, I., Tiemann, H. & Jarms, G. Life cycle of the rhizostome jellyfish Rhizostoma octopus (L.) (Scyphozoa, Rhizostomeae), with studies on cnidocysts and statoliths. *Marine Biology* **151**, 1695–1710 (2007).

95. Averbuj, A. & Cremonte, F. Parasitic castration of Buccinanops cochlidium (Gastropoda: Nassariidae) caused by a lepocreadiid digenean in San José Gulf, Argentina. *J Helminthol* **84**, 381–389 (2010).

96. Averbuj, A. & Cremonte, F. Parasitic castration of Buccinanops cochlidium (Gastropoda: Nassariidae) caused by a lepocreadiid digenean in San José Gulf, Argentina. *Journal of Helminthology* **84**, 381–389 (2010).

97. Barnett, L. J., Miller, T. L. & Cribb, T. H. Two new Stephanostomum-like cercariae (Digenea: Acanthocolpidae) from Nassarius dorsatus and N. olivaceus (Gastropoda: Nassariidae) in Central Queensland, Australia. *Zootaxa* **2445**, 35–52 (2010).

98. Grati, F., Polidori, P., Scarcella, G. & Fabi, G. Estimation of basket trap selectivity for changeable nassa (Nassarius mutabilis) in the Adriatic Sea. *Fisheries Research* **101**, 100–107 (2010).

99. Polidori, P. *et al.* Towards a better management of Nassarius mutabilis (Linnaeus, 1758): biometric and biological integrative study. *Acta Adriatica: International Journal of Marine Sciences* **56**, 233–243 (2015).

100. Fisher, W., L, B. M. & Schneider, M. Fiches FAO d'identification des espèces pour les besoins de la pêche (Révision 1). Mediterranee et mer Noire. *CEE, FAO* **37. Vertebres**, 2 (1987).

101. Diaz Briz, L., Sánchez, F., Marí, N., Mianzan, H. & Genzano, G. Gelatinous zooplankton (ctenophores, salps and medusae): an important food resource of fishes in the temperate SW Atlantic Ocean. *Marine Biology Research* **13**, 630–644 (2017).

102. Tilves, U., Sabatés, A., Blázquez, M., Raya, V. & Fuentes, V. L. Associations between fish and jellyfish in the NW Mediterranean. *Marine Biology* **165**, (2018).

103. Mir-Arguimbau, J., Sabatés, A. & Tilves, U. Trophic ecology of Trachurus mediterraneus juveniles associated with the jellyfish Rhizostoma pulmo and Cotylorhiza tuberculata. *Journal of Sea Research* **147**, 28–36 (2019).

104. Cribb, T. H. & Bray, R. A. Gut wash, body soak, blender and heat-fixation: approaches to the effective collection, fixation and preservation of trematodes of fishes. *Systematic Parasitology* **76**, 1–7 (2010).

105. Lockyer, A., Olson, P. & Littlewood, D. Utility of complete large and small subunit rRNA genes in resolving the phylogeny of the Neodermata (Platyhelminthes): implications and a review of the cercomer theory. *Biological Journal of the Linnean Society* **78**, 155–171 (2003).

106. Gustinelli, A. *et al.* First description of the adult stage of Clinostomum cutaneum Paperna, 1964 (Digenea: Clinostomidae) from grey herons Ardea cinerea L. and a redescription of the metacercaria from the Nile tilapia Oreochromis niloticus niloticus (L.) in Kenya. *Systematic Parasitology* **76**, 39–51 (2010).

107. Hall, T. BioEdit: a user-friendly biological sequence alignment editor and analysis program for Windows 95/98/NT. in *Nucleic Acids Symp. Ser.* vol. 41 95–98 (1999).

108. Kumar, S., Stecher, G., Li, M., Knyaz, C. & Tamura, K. MEGA X: Molecular Evolutionary Genetics Analysis across Computing Platforms. *Molecular Biology and Evolution* **35**, 1547–1549 (2018).

109. R Core Team. *R: A Language and Environment for Statistical Computing.* (R Foundation for Statistical Computing, 2021).

110. Wickham, H., Chang, W. & H, W. M. Package 'ggplot2'. Create Elegant Data Visualisations Using the Grammar of Graphics. *Version* **2**, 1–189 (2016).

111. Clarke, K. & Gorley, R. Getting started with PRIMER v7. *PRIMER-E: Plymouth, Plymouth Marine Laboratory* **20**, (2015).

112. Anderson, M. J. Permutational multivariate analysis of variance (PERMANOVA). *Wiley statsref: statistics reference online* 1–15 (2014).

113. Lebour, M. V. Medusae as hosts for larval trematodes. *Journal of the Marine Biological Association of the United Kingdom* **11**, 57–59 (1916).

114. Van Cleave, H. Ctenophores as the Host of a Cestode. *Transactions of the American Microscopical Society* **46**, 214–215 (1927).

115. Dollfus, R. P. Liste des coelentérés marins, palearctiques et indiens ouont été trouvés des trematodes digenetiques. *Bull. Inst. Peches. mar. Maroc* 9–10 (1963).

116. Martorelli, S. Primera cita de una cercaria tricocerca parásita de Dorsanum moniliferum (Mollusca: Buccinidae) para el Atlántico Sud-Occidental. *Aportes al conocimiento de su ciclo de vida. Neotropica* **37**, 57–65 (1991).

117. Rebecq, J. Considérations sur la place des trématodes dans le zooplancton marin. *Ann. Fac. Sci. Marseilles* **38**, 61–84 (1965).

118. Arai, M. A Functional Biology of the Scyphozoa Chapman & Hall. (1997).

119. Galil, B. S., Kress, N., Shiganova, T. A., & others. First record of Mnemiopsis leidyi A. Agassiz, 1865 (Ctenophora; Lobata; Mnemiidae) off the Mediterranean coast of Israel. *Aquatic Invasions* **4**, 357–360 (2009).

120. Fuentes, V. L., Atienza, D., Gili, J.-M., Purcell, J. E., & others. First records of Mnemiopsis leidyi A. Agassiz 1865 off the NW Mediterranean coast of Spain. *Aquatic Invasions* **4**, 671–674 (2009).

121. Covelli, S., Faganeli, J., Horvat, M. & Brambati, A. Mercury contamination of coastal sediments as the result of long-term cinnabar mining activity (Gulf of Trieste, northern Adriatic sea). *Applied Geochemistry* **16**, 541–558 (2001).

122. Purcell, J. E. Quantification of Mnemiopsis leidyi(Ctenophora, Lobata) from formalin-preserved plankton samples. *Marine ecology progress series. Oldendorf* **45**, 197–200 (1988).

123. Hosia, A. & Båmstedt, U. Seasonal changes in the gelatinous zooplankton community and hydromedusa abundances in Korsfjord and Fanafjord, western Norway. *Marine Ecology Progress Series* **351**, 113–127 (2007).

124. Schindelin, J. Fiji: an open-source platform for biological-image analysis. *Nature Methods* **9**, 676–682 (2012).

125. Hothorn, T., Bretz, F. & Westfall, P. Simultaneous Inference in General Parametric Models. *Biometrical Journal* **50**, 346–363 (2008).

126. Malačič, V., Celio, M., Čermelj, B., Bussani, A. & Comici, C. Interannual evolution of seasonal thermohaline properties in the Gulf of Trieste (northern Adriatic) 1991–2003. *Journal of Geophysical Research: Oceans* **111**, (2006).

127. Ginetsinskaya, T. Problems of trematode ecology. *Trematodes, their life cycles, biology and evolution, TA Ginetsinskaya (ed.). Amerind Publishing Co. Pvt. Ltd., New Delhi, India* 318–346 (1988).

128. Cocci, P., Troli, E., Angeletti, M. & Palermo, F. A. Field Monitoring of Tritia mutabilis (Linnaeus, 1758) Egg Capsule Deposition and Intracapsular Embryonic Patterns Using Artificial Substrates and Machine Learning-Based Approaches. *Frontiers in Marine Science* 755 (2021).

129. Mallet, A., Jouvenel, J.-Y., Broyon, M., Pirot, N. & Geffroy, B. Histology of Tritia mutabilis gonads: using reproductive biology to support sustainable fishery management. *Aquatic Living Resources* **34**, 6 (2021).

130. Abbate, D. & Cavallari, D. C. A new species of Nassarius (Gastropoda, Nassariidae) from Canopus bank, off Northeast Brazil. *Papéis Avulsos de Zoologia* **53**, 1–4 (2013).

131. Shiganova, T. A., Legendre, L., Kazmin, A. S. & Nival, P. Interactions between invasive ctenophores in the Black Sea: assessment of control mechanisms based on long-term observations. *Marine ecology progress series* **507**, 111–123 (2014).

132. Mianzan, H., Mari, N., Prenski, B. & Sanchez, F. Fish predation on neritic ctenophores from the Argentine continental shelf: a neglected food resource? *Fisheries Research* **27**, 69–79 (1996).

133. Milisenda, G. *et al.* Jellyfish as prey: frequency of predation and selective foraging of Boops boops (Vertebrata, Actinopterygii) on the mauve stinger Pelagia noctiluca (Cnidaria, Scyphozoa). *PLoS one* **9**, e94600 (2014).

134. Bos, A. R., Cruz-Rivera, E. & Sanad, A. M. Herbivorous fishes Siganus rivulatus (Siganidae) and Zebrasoma desjardinii (Acanthuridae) feed on Ctenophora and Scyphozoa in the Red Sea. *Marine Biodiversity* **47**, 243–246 (2017).

135. Alekseenko, E., Lidia, M., Paul, N., & others. Modelling assessment of interactions in the Black Sea of the invasive ctenophores Mnemiopsis leidyi and Beroe ovata. *Ecological Modelling* **376**, 1–14 (2018).

136. Swanberg, N. The feeding behavior of Beroe ovata. *Marine Biology* **24**, 69–76 (1974).

137. Lamb, P. D. *et al.* Jellyfish on the menu: mtDNA assay reveals scyphozoan predation in the Irish Sea. *Royal Society open science* **4**, 171421 (2017).

138. Pestorić, B. *et al.* Scyphomedusae and Ctenophora of the Eastern Adriatic: Historical Overview and New Data. *Diversity* **13**, 186 (2021).

139. BETTOSO, N. First record of Carybdea marsupialis (L., 1758)(Cnidaria, Cubozoa) in the Gulf of Trieste. *Periodicum biologorum* **104**, 233–233 (2002).

140. Del Negro, P., Kokelj, F., Tubaro, A. & Della Loggia, R. Chrysaora hysoscella in the Gulf of Trieste: presence, evolution and cutaneous toxicity in man. in *Marine Coastal Eutrophication* 427–430 (Elsevier, 1992).

141. Júnior, M. N., Diaz-Briz, L. & Haddad, M. A. New records of Opechona sp. metacercariae (Digenea: Trematoda) on hydromedusae from south Brazil. *Marine Biodiversity Records* **6**, (2013).

142. Lüdecke, M. D. Package ‘sjPlot’. (2021).

143. Polidori, P. *et al.* Towards a better management of Nassarius mutabilis (Linnaeus, 1758): biometric and biological integrative study. *Acta Adriat* **56**, 233–243 (2015).

144. Rottini, G., Gusmani, L., Parovel, E., Avian, M. & Patriarca, P. Purification and properties of a cytolytic toxin in venom of the jellyfish Carybdea marsupialis. *Toxicon* **33**, 315–326 (1995).

145. Brinkman, D. L. & Burnell, J. N. Biochemical and molecular characterisation of cubozoan protein toxins. *Toxicon* **54**, 1162–1173 (2009).

146. Woo, P. *Fish diseases and disorders: Vol. 1: Protozoan and metazoan infections*. (USA: CABI; ISBN 0-85199-015-0, 2006).

147. Bullard, S. A., Overstreet, R. M., & others. Digeneans as enemies of fishes. *Fish diseases* **2**, 817–976 (2008).

148. Littlewood, D. T. J. & Bray, R. A. *Interrelationships of the Platyhelminthes*. (CRC Press, 2000).

149. Cribb, T. The diversity of the Digenea of Australian animals. *International Journal for Parasitology* **28**, 899–911 (1998).

150. Manter, H. W. & others. Host specificity and other host relationships among the digenetic trematodes of marine fishes. in *SYMPOSIUM ON HOST SPECIFICITY AMONG PARASITES OF VERTEBRATES (1st), University of Neuchatel, April 15-18, 1957. Neuchatel: University of Neuchatel.* (1957).

151. Ogawa, K. Diseases of cultured marine fishes caused by Platyhelminthes (Monogenea, Digenea, Cestoda). *Parasitology* **142**, 178–195 (2015).

152. Hoffman, G., Fried, B. & Harvey, J. Sanguinicola fontinalis sp nov.(Digenea: Sanguinicolidae): a blood parasite of brook trout, Salvelinus fontinalis (Mitchill), and longnose dace, Rhinichthys cataractae (Valenciennes). *Journal of Fish Diseases* **8**, 529–538 (1985).

153. OGAWA, K., HATTORI, K., HATAI, K. & KUBOTA, S. Histopathology of cultured marine fish, Seriola purpurascens (Carangidae) infected with Paradeontacylix spp.(Trematoda: Sanguinicolidae) in its vascular system. *Fish Pathology* **24**, 75–81 (1989).

154. Paladini, G., Longshaw, M., Gustinelli, A. & Shinn, A. P. Parasitic diseases in aquaculture: their biology, diagnosis and control. *Diagnosis and control of diseases of fish and shellfish* 37–107 (2017).

155. Kvach, Y., Matvienko, N., Bryjová, A. & Ondračková, M. Aquaculture as a possible vector in the spread of Posthodiplostomum centrarchi (Hoffman, 1958)(Digenea: Diplostomidae) in Europe. *BioInvasions Record* **7**, (2018).

156. Kabunda, M. & Sommerville, C. Parasitic worms causing the rejection of tilapia (Oreochromis species) in Zaire. *British Veterinary Journal* **140**, 263–268 (1984).

157. Lorio, W. J. Experimental control of metacercariae of the yellow grub Clinostomum marginatum in channel catfish. *Journal of Aquatic Animal Health* **1**, 269–271 (1989).

158. Paperna, I. infections and diseases of fishes in Africa: an update (No. 31). *Food and Agriculture Organization of the United Nations (FAO). Rome: FAO Fisher Dept* 26–8 (1996).

159. Overstreet, R. M. *et al.* Bolbophorus damnificus n. sp.(Digenea: Bolbophoridae) from the channel catfish Ictalurus punctatus and American white pelican Pelecanus erythrorhynchos in the USA based on life-cycle and molecular data. *Systematic Parasitology* **52**, 81–96 (2002).

160. *The State of World Fisheries and Aquaculture 2020: Sustainability in action*. (FAO, 2020).

161. JARDAS, I. & HRISTOVSKI, N. A new contribution to the knowledge of helminth parasite fauna of fishes from the channels between the mid-Dalmatian islands Adriatic Sea. *Acta Adriatica* **26**, 145–164 (1985).

162. Paradižnik, V. & Radujković, B. Digenea trematodes in fish of the North Adriatic Sea. *Acta Adriat* **48**, 115–129 (2007).

163. Radujkovic, B. & Sundic, D. Parasitic flatworms (Platyhelminthes: Monogenea, Digenea, Cestoda) of fishes from the Adriatic Sea. *Natura Montenegrina* **13**, 7–280 (2014).

164. Bjørgen, H., Li, Y., Kortner, T. M., Krogdahl, Å. & Koppang, E. O. Anatomy, immunology, digestive physiology and microbiota of the salmonid intestine: Knowns and unknowns under the impact of an expanding industrialized production. *Fish & Shellfish Immunology* **107**, 172–186 (2020).

165. L⊘kka, G., Austb⊘, L., Falk, K., Bjerkås, I. & Koppang, E. O. Intestinal morphology of the wild Atlantic salmon (Salmo salar). *Journal of morphology* **274**, 859–876 (2013).

166. Sanden, M. & Olsvik, P. A. Intestinal cellular localization of PCNA protein and CYP1A mRNA in Atlantic salmon Salmo salar L. exposed to a model toxicant. *BMC physiology* **9**, 1–11 (2009).

167. Bartoli, P. & Bray, R. A. Contribution to the knowledge of species of the genus Stephanostomum Looss, 1899 (Digenea: Acanthocolpidae) from teleosts of the Western Mediterranean, with the description of S. gaidropsari n. sp. *Systematic Parasitology* **49**, 159–188 (2001).

168. Akmirza, A. Digenean trematodes of fish in the waters off Gökçeada, the Aegean Sea, Turkey. *Journal of Black Sea/Mediterranean Environment* **19**, 283–298 (2013).

169. O'Connor, B. & McGrath, D. On the occurrence of the scyphozoan Rhizostoma octopus (L.) around the Irish coast in 1976. *The Irish Naturalists' Journal* 261–263 (1978).

170. Cribb, T. H., Chisholm, L. A. & Bray, R. A. Diversity in the Monogenea and Digenea: does lifestyle matter? *International Journal for Parasitology* **32**, 321–328 (2002).

171. Quinteiro, P., Tojo, J., Núñez, A., Santamarina, M. & Sanmartin, M. Stephanostomum lophii sp. nov.(Digenea: Acanthocolpidae), intestinal parasite of Lophius piscatorius, with reference to seasonal fluctuations of metacercariae in intermediate second hosts (Gadidae). *Journal of fish biology* **42**, 421–433 (1993).

172. Bartoli, P. & Bray, R. A. Four species of Stephanostomum Looss, 1899 (Digenea: Acanthocolpidae) from Seriola dumerili (Risso)(Teleostei: Carangidae) in the western Mediterranean, including S. euzeti n. sp. *Systematic Parasitology* **58**, 41–62 (2004).

173. Lamouroux, J. V. F. *Histoire naturelle des zoophytes, ou animaux rayonnés: faisant suite à l'histoire naturelle des vers de Bruguière*. vol. 138 (chez Mme veuve Agasse, 1824).

174. Shotter, R. The distribution of some helminth and copepod parasites in tissues of whiting, Merlangius merlangus L., from Manx waters. *Journal of Fish Biology* **8**, 101–117 (1976).

175. Kogovšek, T., Bogunović, B. & Malej, A. Recurrence of bloom-forming scyphomedusae: wavelet analysis of a 200-year time series. in *Jellyfish Blooms: New Problems and Solutions* 81–96 (Springer, 2010).

176. Licandro, P. A blooming jellyfish in the northeast Atlantic and Mediterranean. *Biology letters* **6**, 688–691 (2010).

177. Pitt, K. A. & Lucas, H. L. *Jellyfish blooms*. (Springer, 2014).

178. Ruppert, E. E., Barnes, R. D. & Fox, R. S. Invertebrate Zoology: A Functional Evolutionary Approach. (2004).

179. Larson, R. J. Feeding in coronate medusae (class scyphoza, order coronatae. *Marine Behaviour and Physiology* **6**, 123–129 (1979).

180. Mackie, G. O., Nielsen, C. & Singla, C. L. The Tentacle Cilia of Aglantha digitale (Hydrozoa: Trachylina) and their Control. *Acta Zoologica* **70**, 133–141 (1989).

181. Nagata, R., Morandini, A. C., Colin, S. P., Migotto, A. E. & Costello, J. H. Transitions in morphologies, fluid regimes, and feeding mechanisms during development of the medusa Lychnorhiza lucerna. *Marine Ecology Progress Series* **557**, 145–159 (2016).

182. Southward, A. J. Observations on the ciliary currents of the jelly-fish Aurelia aurita L. *Journal of the Marine Biological Association of the United Kingdom* **34**, 201–216 (1955).

183. Han, J. *et al.* Divergent evolution of medusozoan symmetric patterns: Evidence from the microanatomy of Cambrian tetramerous cubozoans from South China. *Gondwana Research* **31**, 150–163 (2016).

184. Wang, X. *et al.* Anatomy and affinities of a new 535-million-year-old medusozoan from the Kuanchuanpu Formation, South China. *Palaeontology* **60**, 853–867 (2017).

185. Arai, M. N. & Chan, I. M. Two types of excretory pores in the hydrozoan medusa Aequorea victoria (Murbach and Shearer, 1902. *Journal of Plankton Research* **11**, 609–614 (1989).

186. Presnell, J. S. The Presence of a Functionally Tripartite Through-Gut in Ctenophora Has Implications for Metazoan Character Trait Evolution. *Current Biology* **26**, 2814–2820 (2016).

187. Tamm, S. L. No surprise that comb jellies poop. *Science* **352**, 1182–1182 (2016).

188. Moroz, L. L. The ctenophore genome and the evolutionary origins of neural systems. *Nature* **510**, 109–114 (2014).

189. Ryan, J. F. The genome of the ctenophore Mnemiopsis leidyi and its implications for cell type evolution. *Science* **342**, (2013).

190. Whelan, N. V., Kocot, K. M., Moroz, L. L. & Halanych, K. M. Error, signal, and the placement of Ctenophora sister to all other animals. *Proceedings of the National Academy of Sciences of the United States of America* **112**, 5773–5778 (2015).

191. Kapli, P. & Telford, M. J. Topology-dependent asymmetry in systematic errors affects phylogenetic placement of Ctenophora and Xenacoelomorpha. *Sci. Adv* **6, eabc5162**, (2020).

192. Hejnol, A. & Martindale, M. Q. Acoel development indicates the independent evolution of the bilaterian mouth and anus. *Nature* **456**, 382–386 (2008).

193. Hejnol, A. & Martín-Durán, J. M. Getting to the bottom of anal evolution. *Zoologischer Anzeiger* **256**, 61–74 (2015).

194. Fankboner, P. V. Digestive System of Invertebrates. in *Encyclopedia of Life Sciences* (John Wiley & Sons Ltd1–6, 2003).

195. Pierson, J. Mesozooplankton and gelatinous zooplankton in the face of environmental stressors. *Geophysical Monograph* **256**, 105-127, (2021).

196. Stiasny, G. Mittheilungen über Scyphomedusen I. *Zoologische Mededelingen* **6**, 109–114 (1921).

197. Stiasny, G. Das Gastrovascularsystem als Grundlage für ein neuse System in Rhizostomeen. *Zool. Anz* **17**, 241–247 (1923).

198. Stiasny, G. Mitteilungen über Scyphomedusen II. *Zoologische Mededelingen* **11**, 177–198 (1928).

199. Dular, M., Bajcar, T. & Širok, B. Numerical investigation of flow in the vicinity of a swimming jellyfish. *Engineering Applications of Computational Fluid Mechanics* **3**, 258–270 (2009).

200. Feitl, K. E., Millett, A. F., Colin, S. P., Dabiri, J. O. & Costello, J. H. Functional morphology and fluid interactions during early development of the scyphomedusa Aurelia aurita. *The Biological Bulletin* **217**, 283–291 (2009).

201. Rudolf, D. & Mould, D. An interactive fluid model of jellyfish for animation. in *International Conference on Computer Vision, Imaging and Computer Graphics. 59-72* (2009).

202. Smith, H. *Contribution to the Anatomy and Physiology of Cassiopea frondosa*. (Carnegie Institution of Washington, 1937).

203. Musgrave, E. M. Experimental Observations of the organs of Circulation and the power of Locomotion in Pennatulids. *Journal of Cell Science* **s2-54 (215**, 443–481 (1909).

204. Schmidt-Rhaesa, A. *The Evolution of Organ Systems*. (Oxford University Press, 2007).

205. Jennings, J. B. F. *Digestion and Assimilation in Animals*. (Macmillan International Higher Education, 1972).

206. Göthel, H. *Guide De La Faune Sous-Marine: La Méditerranée. Invertébrés Marins Et Poisons*. (Eygen Ulmer GmbH & Co, 1992).

207. Nielsen, C. Animal Evolution Interrelationships of the Living Phyla. *Oxford University Press on Demand* **53**, 1689–1699 (2013).

208. Steinmetz, P. R. H. Independent evolution of striated muscles in cnidarians and bilaterians. *Nature* **487**, 231–234 (2012).

209. Dunn, C. W., Leys, S. P. & Haddock, S. H. The hidden biology of sponges and ctenophores. *Trends in Ecology and Evolution* **30**, 282–291 (2015).

210. QGIS Development Team. *QGIS Geographic Information System*. (QGIS Association, 2022).

211. Kak, A. C. & Slaney, M. Principles of computerized tomographic imaging. *Society for Industrial and Applied Mathematics* (2001).

212. Dougherty, R. & Kunzelmann, K. H. Computing local thickness of 3D structures with ImageJ. *Microscopy and Microanalysis* **13**, 1678–1679 (2007).

213. Lee, T. C., Kashyap, R. L. & Chu, C. N. Building skeleton models via 3-D medial surface axis thinning algorithms. *CVGIP: Graphical Models and Image Processing* **56**, 462–478 (1994).

214. Voltolini, M., Taş, N., Wang, S., Brodie, E. L. & Ajo-Franklin, J. B. Quantitative characterization of soil micro-aggregates: new opportunities from sub-micron resolution synchrotron X-ray microtomography. *Geoderma* **305**, 382–393 (2017).

215. Voltolini, M., M., K., H., T. & Ajo-Franklin, J. Visualization and prediction of supercritical CO2 distribution in sandstones during drainage: An in situ synchrotron X-ray micro-computed tomography study. *International Journal of Greenhouse Gas Control* **66**, 230–245 (2017).

216. Otsu, N. A threshold selection method from gray-level histograms. *IEEE transactions on systems, man, and cybernetics* **9**, 62–66 (1979).